Oncogenic Control and Metabolic Outputs of the Lipogenic Transcription Factor SREBP

Oncogenic Control and Metabolic Outputs of the Lipogenic Transcription Factor SREBP

A dissertation presented

by

Stephane Jean Hermann Ricoult

to

The Division of Medical Sciences

in partial fulfillment of the requirements

for the degree of

Doctor of Philosophy

in the subject of

Biological and Biomedical Sciences

Harvard University

Cambridge, Massachusetts

April 2016

Dissertation Advisor: Professor Brendan D. Manning Stephane Jean Hermann Ricoult

Oncogenic Control and Metabolic Outputs of the Lipogenic Transcription Factor SREBP

Abstract

The sterol regulatory element binding protein (SREBP) transcription factors have emerged as central regulators of *de novo* lipogenesis in the liver. However, while it is known that lipid synthesis is elevated in many cancers, much less is known about the control of lipid metabolism in this context. The goals of this dissertation were to better understand the mechanisms through which commonly mutated oncogenes and tumor suppressors promote *de novo* lipid synthesis, and to further define the importance of this process in cancer.

Using isogenic oncogene-expressing breast epithelial cells and breast cancer cell lines, I have identified a major mechanism through which two of the most commonly activated oncogenes in cancer promote *de novo* lipogenesis. In particular, I found that the expression of oncogenic PI3K or K-Ras is sufficient to stimulate *de novo* lipid synthesis in breast epithelial cells through the activation of mechanistic target of rapamycin complex 1 (mTORC1) and SREBP. Consistent with these findings, increased mTORC1 signaling in breast cancer patient tumor samples is associated with elevated expression of canonical SREBP targets involved in *de novo* lipogenesis. I further demonstrate that SREBP depletion in breast cancer cells or in oncogene-expressing epithelial cells reduces growth-factor independent proliferation.

To better understand the role of SREBP in cancer metabolism, I sought to determine whether SREBP regulates isocitrate dehydrogenase 1 (IDH1), which is both a metabolic enzyme and an oncogene. Specifically, I show that SREBP activates the expression of IDH1 across a panel of cancer cell lines from different lineages, and that IDH1 expression facilitates the flux of glutamine-derived carbons towards *de novo* lipid synthesis. In addition, SREBP stimulates the expression of oncogenic $IDH1^{R132C}$, which is a

neomorphic enzyme that produces the oncometabolite 2-hydroxyglutarate, and can regulate 2-hydroxyglutarate production in mutant-IDH1 cells.

Collectively, these studies expand our understanding of lipid metabolism in cancer and identify important roles for SREBP in cancer cell metabolism and proliferation. Our results will help guide future studies on the regulation of SREBP, the role of SREBP targets, and the production of specific lipid species in cancer, which will hopefully identify novel therapeutic targets to treat cancer patients.

TABLE OF CONTENTS

LIST OF FIGURES

GLOSSARY OF TERMS

2-HG	2-hydroxyglutarate
25-HC	25-hydroxycholesterol
4E-BP	eIF4E binding proteins
α-KG	α-ketoglutarate
ACAT	acetyl-CoA acetyltransferase
ACC/ACACA	acetyl-CoA carboxylase
ACLY	ATP citrate lyase
ACSS2	acetyl-CoA synthetase
AMP	adenosine monophosphate
AMPK	AMP kinase
ATF4	activating transcription factor 4
ATG7	autophagy-related 7
ATGL	adipose triglyceride lipase
C/EBP	CCAAT/enhancer-binding protein
CAD	carbamoyl-phosphate synthetase 2, aspartate transcarbamoylase, dihydroorotase
CDK1	cyclin-dependent kinase 1
ChIP	chromatin immunoprecipitation
CHOP	C/EBP homologous protein
CPT1	carnitine palmitoyltransferase 1
CRTC2	CREB regulated transcription coactivator 2
D/L2HGDH	D/L-2-HG dehydrogenase
DAG	diacylglyceride
DGAT	diglyceride acyltransferase
DHAP	dihydroxyacetone phosphate

DNA-PK	DNA-dependent protein kinase
eEF2K	eukaryotic elongation factor 2 kinase
EGF	epidermal growth factor
EGLN	HIF prolyl hydroxylase 2
eIF4E	eukaryotic translation initiation factor 4E
ELOVL	elongation of very long chain fatty acids protein
ER	endoplasmic reticulum
Erk/MAPK	mitogen-activated protein kinase
$FADH_2$	flavin adenine dinucleotide
FASN	fatty acid synthase
FBS	fetal bovine serum
FH	fumarate hydratase
FKBP12	FK506 binding protein of 12kDa
FOXO	forkhead box O
G6PD	glucose-6-phosphate dehydrogenase
GAP	GTPase-activating protein
GLUT1/4	glucose transporter 1/4
GPAT	by glycerol-3P acyltransferase
GPDH	glycerol-3-phosphate dehydrogenase
GSK3	glycogen synthase kinase 3
HIF-1α	hypoxia-inducible factor
HMGCR	3-hydroxy-3-methylglutaryl-CoA reductase
HMGCS	3-hydroxy-3-methylglutaryl-CoA synthase
HSL	hormone-sensitice lipase
IDH	isocitrate dehydrogenase
IDL	intermediate density lipoprotein

IGF1	Insulin-like growth factor 1
INSIG	insulin-induced gene
LAM	lymphangioleiomyomatosis
LC-MS/MS	liquid chromatography–mass spectrometry/mass spectrometry
LDH	lactate dehydrogenase
LDL	low density lipoprotein
LDLR	LDL receptor
Lipin1	phosphatidic acid phosphatase LPIN1
LPL	lipoprotein lipase
LTsc1KO	liver-specific KO of *Tsc1*
MAG	monoacylglyceride
MDH	malate dehydrogenase
ME1	malic enzyme
MEK	MAPK kinase
mLST8	mTOR-associated protein, LST8 homologue
mRNA	messenger RNA
mTHF	mitochondrial tetrahydrofolate cycle
MTHFD2	methylenetetrahydrofolate dehydrogenase 2
mTOR	mechanistic target of rapamycin
mTORC1	mTOR complex 1
mTORC2	mTOR complex 2
MUFA	mono-unsaturated fatty acid
MVK	mevalonate kinase
NADH	nicotinamide adenine dinucleotide
NADPH	nicotinamide adenine dinucleotide phosphate
N-CoR1	nuclear receptor co-repressor 1

NF1	neurofibromin 1
Nrf1	nuclear factor, erythroid 2-like 1
PA	phosphatidic acid
PCSK9	proprotein convertase subtilisin/kexin type 9
PDK1	phosphoinositide-dependent kinase-1
PGD	phosphogluconate dehydrogenase
PHGDH	phosphoglycerate dehydrogenase
PI	propidium iodide
PI3K	phosphoinositide 3-kinase
PIP_2	phosphatidylinositol-4,5-bisphosphate
PIP_3	phosphatidylinositol-3,4,5-triphosphate
PKA/C	protein kinase A/C
PPAP	acylglycerol-3P acyltransferase
PPAR	peroxisome proliferator-activated receptor
PPP	pentose phosphate pathway
PRPP	5-phospho-α-D-ribosyl 1-pyrophosphate
PTEN	phosphatase and tensin homolog
qRT-PCR	quantitative reverse transcriptase polymerase chain reaction
Rag	RAS-related GTP-binding protein
Raptor	regulatory-associated protein of mTOR
REDD1	regulated in development and DNA damage responses 1
Rheb	Ras homolog enriched in brain
Rictor	Raptor-independent companion of mTOR
ROS	reactive oxygen species
rRNA	ribosomal RNA
Rsk	MAPK-activated protein kinase-1

RTK	receptor tyrosine kinases
S1P	site-1-protease
S2P	site-2-protease
S6	ribosomal protein S6
S6K1/2	ribosomal S6 kinase 1/2
SCAP	SREBP cleavage-activating protein
SCD	steroyl-CoA desaturase
SDH	succinate dehydrogenase
SGK	serum/glucocorticoid-regulated kinases
shRNA	small hairpin RNA
siRNA	small interfering RNA
SIN1	SAPK- interacting protein 1
SLC25A1	mitochondrial citrate transporter
SRE	sterol response element
SREBP	sterol regulatory element binding protein
SRM	selected reaction monitoring
TAG	triacylglyceride
TBC1D7	TBC1 domain family, member 7
TCA	tricarboxylic acid
TCGA	The Cancer Genome Atlas
TET	ten-eleven translocation
TSC1/2	tuberous sclerosis complex 1/2
ULK1	Unc-51 like autophagy activating kinase 1
UPR	unfolded protein response
VLDL	very low density lipoprotein

ACKNOWLEDGEMENTS

First, I would like to thank Dr. Brendan Manning for all his support and scientific guidance, which have helped me become a better scientist over the past six years. Brendan has created an amazing lab environment to conduct research, and I will be sad to leave it behind. I would also like to thank Jessica Yecies for initiating the work on SREBP and helping me get started on my project. I thank the present and past postdocs of the lab (Jess, Jim, Gerta, Sue, Alex, Marie, Yinan) for all their help and for having the answers to my many questions. In particular, I would like to thank Issam for always being available, regardless of whether it is to help with mouse work or to discuss the latest news from NASA. Thank you to the graduate students of the lab, especially Erika and Ilana, for helping me through the darker days of graduate school. I also thank the lab technicians of the lab (particularly George and Marc) who have kept the lab running smoothly.

Thank you to Karen Cichowski, John Blenis, Marcia Haigis, and Anders Näär for their scientific advice in my DAC meetings. Thank you to Sudha Biddinger, Marcia Haigis, Nada Kalaany, and Matthew Vander Heiden for taking the time to be on my defense committee. I would also like to thank John Asara, Min Yuan, and Susanne Breitkopf for their help with the mass spectrometry experiments. I also thank the National Science Foundation Graduate Research Fellowship Program for funding part of my graduate work.

Thank you to my BBS classmates for making graduate school an unforgettable experience.

I would like to thank my parents and Sébastien for always being a phone call away to celebrate my accomplishments, to help me overcome obstacles, and for always being so supportive. Thank you to my parents for making this entire journey to the Ph.D. possible.

Lastly, I would like to thank Laura Smith for putting up with me continuously underestimating how long things take in lab, for listening to my complaining, and for making me look forward to coming home every single day.

CHAPTER 1:

INTRODUCTION

Sections 1.1.1, 1.1.2, and 1.2 of this chapter are adapted from:

Ricoult SJH, Manning BD. The multifaceted role of mTORC1 in the control of lipid metabolism. *EMBO Rep* 2013; **14**: 242–251.

Section 1.1.3 of this chapter is adapted from:

Howell JJ, **Ricoult SJH**, Ben-Sahra I, Manning BD. A growing role for mTOR in promoting anabolic metabolism. *Biochem Soc Trans* 2013; **41**: 906–912.

1.1 mTORC1 AS A MAJOR REGULATOR OF CELL GROWTH AND PROLIFERATION

1.1.1 Overview

The mechanistic target of rapamycin (mTOR) is an evolutionarily conserved Ser/Thr kinase that exists within two functionally distinct protein complexes, mTOR complex 1 (mTORC1) and mTOR complex 2 (mTORC2). mTORC1 is composed of the core essential components mTOR, mLST8, and Raptor, while mTORC2 is composed of mTOR, mLST8, SIN1, and Rictor. Upon activation, mTORC1 directly phosphorylates ribosomal S6 kinases (S6K1 and S6K2), eukaryotic translation initiation factor 4E (eIF4E) binding proteins (4E-BP1 and 4E-BP2), and a growing number of other downstream targets[1]. While the overall effects of mTORC1 signaling can differ in various cells and tissues, its role in promoting anabolic cell growth and inhibiting the catabolic process of autophagy is evolutionarily conserved[2,3]. In contrast, mTORC2 appears to be primarily regulated by growth factor signaling, and phosphorylates a conserved hydrophobic motif in Akt, serum/glucocorticoid-regulated kinases (SGK), and some isoforms of protein kinase C (PKC), thereby increasing their kinase activity[4]. Through these targets, and likely others, mTORC2 signaling is believed to promote cell survival, proliferation, metabolism, and changes in the actin cytoskeleton. While these complexes are functionally distinct, they can influence each other's activity. For instance, mTORC2 stimulates an increase in Akt activity[5], which can lead to mTORC1 activation downstream of Akt. On the other hand, several negative feedback mechanisms are triggered by mTORC1 activation that can influence mTORC2 activity, including one leading to direct inhibitory phosphorylation of Rictor within mTORC2 by S6K1 downstream of mTORC1[6,7].

Rapamycin and its many analogs are widely used mTORC1 inhibitors that interact with the ubiquitous protein FKBP12 to bind to an allosteric site N-terminal to the mTOR kinase domain (i.e., the FKBP12-rapamycin binding domain). Although mTOR is present in both mTORC1 and mTORC2, rapalogs only have access to mTOR within mTORC1. However, it is now evident that prolonged

exposure to rapamycin can block the assembly of mTORC2 by sequestering uncomplexed mTOR in both cell culture and mice[8,9]. Therefore, one must consider that the observed effects of long-term rapamycin treatment might be due to loss of mTORC2 in some experimental systems, which can affect the many processes downstream of Akt. Also, the development of mTOR kinase domain inhibitors, which completely block mTOR within both complexes, has revealed that rapamycin only partially inhibits mTORC1 activity. Rapamycin strongly affects the phosphorylation of some mTORC1 targets (e.g., S6K1) but only modestly inhibits other targets (e.g., 4E-BP1)[10]. This differential sensitivity appears to be determined by the varying quality of mTORC1 substrates, which depends on how efficiently a given sequence is phosphorylated by mTORC1[11].

1.1.2 Upstream signaling

mTORC1 senses and integrates a diverse array of cellular signals. Within the complex, mTOR kinase activity is influenced by a variety of nutrients (e.g., amino acids, glucose, oxygen), cellular energy levels (i.e., ATP), and many secreted growth factors, cytokines, and hormones (e.g. insulin) (Figure 1.1). The Ras-related small G protein Rheb (Ras homolog enriched in brain), upon GTP loading, becomes an essential upstream activator of mTORC1[12]. Many of the signals that regulate mTORC1 do so by altering the GTP-binding status of Rheb through activation or inhibition of a GTPase-activating protein complex, comprised of tuberous sclerosis complex 1 (TSC1), TSC2, and TBC1D7 (the TSC complex)[13].

The PI3K-Akt and the Ras-Erk pathways are two distinct signaling pathways that respond to different signals and are capable of activating mTORC1 (Figure 1.1)[14]. Binding of growth-promoting molecules, such as insulin and insulin-like growth factor 1 (IGF1), to cell surface receptor tyrosine kinases (RTKs) activates phosphoinositide 3-kinase (PI3K)[15]. PI3K is a lipid kinase that phosphorylates phosphatidylinositol-4,5-bisphosphate (PIP_2) to produce phosphatidylinositol-3,4,5-triphosphate (PIP_3). Conversely, PIP_3 can be converted back to PIP_2 by phosphatase and tensin homolog (PTEN), a commonly

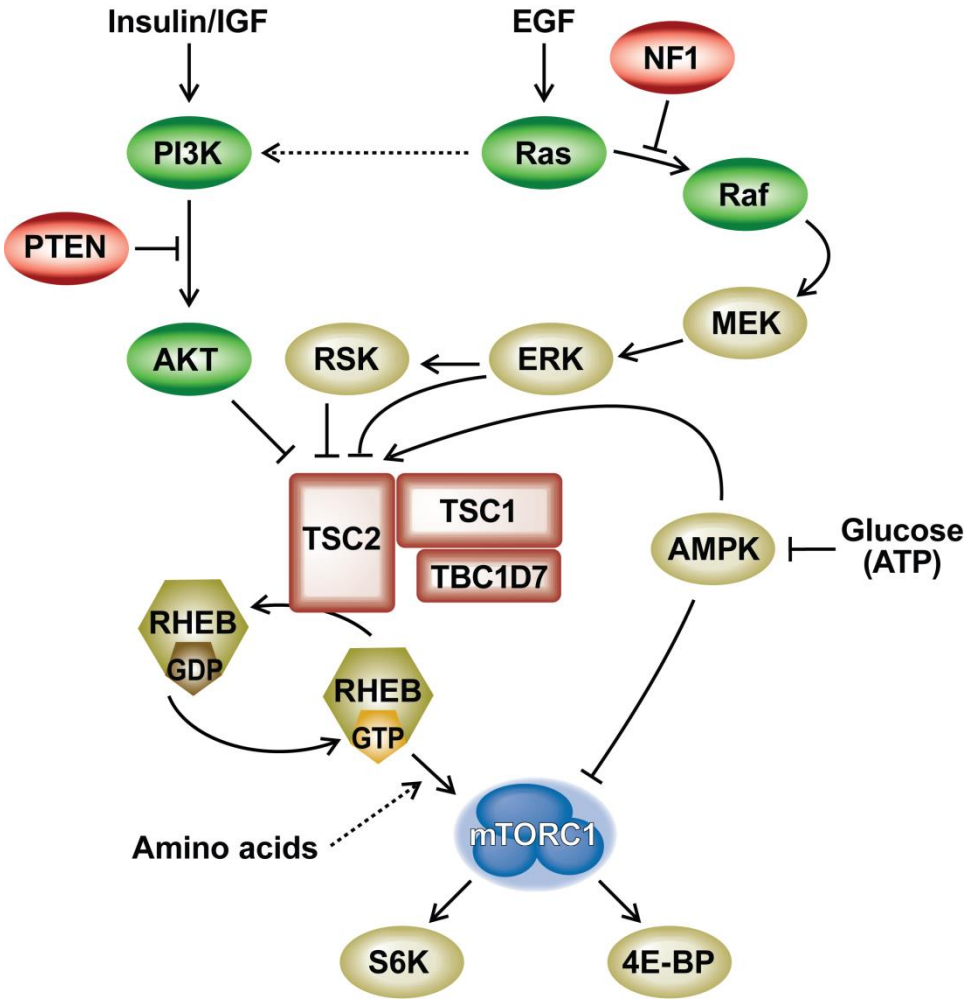

Figure 1.1. Regulation of mTORC1 by the PI3K-Akt and the Ras-Erk pathways.

The PI3K-Akt pathway (stimulated by insulin and IGF) and the Ras-Erk pathway (stimulated by EGF) converge on the TSC complex to regulate mTORC1 signaling. In part through AMPK, the TSC complex receives signals about systemic and local nutrient and energy availability. These signals either activate or inhibit the ability of the TSC complex to act as a GAP for Rheb, thereby inhibiting or activating mTORC1, respectively. The presence of amino acids is required for the activation of mTORC1 by GTP-bound Rheb. Two of the best characterized substrates of mTORC1 are S6K and 4E-BP. Many of the proteins upstream of mTORC1 are oncogenes (green) and tumor suppressors (red), and are frequently mutated in cancer and tumor syndromes.

disrupted tumor suppressor. PIP_3 recruits Akt to the plasma membrane, where membrane-bound phosphoinositide-dependent kinase-1 (PDK1) phosphorylates Akt at T308. This phosphorylation event partially activates Akt, whereas phosphorylation of Akt at S473 by mTORC2 or DNA-dependent protein kinase (DNA-PK) results in its full activation. Once activated, Akt regulates many cellular processes through its phosphorylation of proteins containing an RXXS/T motif. Akt phosphorylates TSC2 on multiple residues, which causes the TSC complex to dissociate from the lysosomal membrane, allowing Rheb to bind GTP and to activate mTORC1 at the lysosome[16–18].

Signaling through mTORC1 is also regulated by the Ras-Erk pathway, which is stimulated by growth factor (e.g., epidermal growth factor/EGF) binding to RTKs (Figure 1.1)[19]. Upon stimulation, the Ras GTPase activates Raf, which then phosphorylates MEK, a mitogen-activated protein kinase (MAPK) kinase, which in turn phosphorylates Erk (or MAPK). Erk is a major effector of the Ras pathway and phosphorylates many protein substrates involved in cell cycle progression and growth. Like Akt, Erk and its downstream target Rsk are protein kinases that phosphorylate and inhibit TSC2 to activate mTORC1 signaling. Ras-GTP can also activate the PI3K-Akt pathway independently of its downstream effectors by directly binding to PI3K[20]. Convergence of the PI3K-Akt and the Ras-Erk pathways on the TSC complex ensures that mTORC1 signaling is repressed in the absence of growth signals.

Nutrient availability is another important regulator of mTORC1 activity. Amino acids regulate mTORC1 activity independently of growth factors through the RAS-related GTP-binding protein (Rag) GTPases. In response to abundant amino acids, the Rag GTPases recruit mTORC1 to the lysosomal surface, where it can be activated by GTP-bound Rheb[21,22]. A decrease in cellular ATP, which can occur during glucose depletion or as a consequence of deficiencies in mitochondrial respiration, activates the TSC complex to inhibit Rheb and mTORC1. This response to cellular energy stress occurs, at least in part, through phosphorylation of TSC2 by AMP kinase (AMPK)[23–25]. Along with signals from these nutrients, mTORC1 signaling is also influenced by intracellular oxygen concentrations. In low oxygen conditions, levels of hypoxia-inducible factor (HIF-1α) increase due to the inhibition of oxygen-

dependent HIF prolyl hydroxylases, thus preventing HIF-1α hydroxylation and subsequent ubiquitination and degradation[26]. HIF-1α has been reported to inhibit mTORC1 through induced expression of REDD1, which appears to promote TSC complex function through a poorly defined mechanism[27,28]. Together, the Rheb and Rag GTPases integrate growth factor and nutrient availability to appropriately regulate mTORC1 activity and cell growth.

Although mTORC1 signaling is normally tightly regulated by these upstream pathways, aberrant mTORC1 signaling is associated with multiple diseases. Many of the regulatory proteins upstream of mTORC1 are frequently mutated in cancer, resulting in growth factor-independent mTORC1 activation in at least 50% of cancers, across nearly all lineages[29]. The PI3K-Akt and the Ras-Erk pathways are two of the most commonly activated pathways in cancer (Figure 1.1). Activating mutations in RTKs, PI3K, or Akt and loss of function mutations in the TSC genes or PTEN occur frequently in cancers and tumor syndromes (e.g., tuberous sclerosis complex and Cowden's syndrome). Similarly, mutations in the Ras-Erk pathway, including Raf and neurofibromin 1 (NF1), also occur in numerous cancers and tumor syndromes. The frequent mutation rate of these two pathways and their convergence on mTORC1 highlights the important role of mTORC1 as a major regulator of cell growth and proliferation.

1.1.3 Regulation of anabolic metabolism

Since mTORC1 can integrate both growth signals and nutrient availability, it is strategically well-positioned to decide whether or not a cell should grow. Under favorable growth conditions, mTORC1 inhibits autophagy, a process in which cells recycle cytosolic proteins and organelles into their nutrient components. This inhibition downstream of mTORC1 occurs partly through the phosphorylation of Unc-51 like autophagy activating kinase 1 (ULK1), a protein involved in initiating autophagy[30–32]. Additionally, mTORC1 promotes expression of genes encoding the primary glucose transporter (GLUT1) and the enzymes of glycolysis through its activation of the transcription factor HIF-1α, which mTORC1 activates through mRNA translation[33–35]. By increasing glucose supply and preventing autophagic

degradation of macromolecules, mTORC1 primes cells for growth. Concurrently, mTORC1 further stimulates cell growth by activating several distinct anabolic processes that produce macromolecules (Figure 1.2).

Protein synthesis is one of the best-established anabolic processes downstream of mTORC1. Phosphorylation of 4E-BP1 by mTORC1 causes 4E-BP1 to dissociate from eIF4E and to enhance cap-dependent translation through the eIF4F translation initiation complex[36]. This mechanism downstream of mTORC1 is particularly important for the translation of mRNAs containing 5'-terminal oligopyrimidine tracts, which encode most ribosomal proteins and translation elongation factors[37–39]. Although S6K1 and S6K2 phosphorylate several components of the translation machinery, such as S6, eIF4B, and eukaryotic elongation factor 2 kinase (eEF2K), it is still not known how these phosphorylation events affect translation[40,41]. The mechanism by which the transcription and maturation of ribosomal RNA (rRNA) are activated downstream of mTORC1 is also poorly defined , although it is postulated to involve the ribosome biogenesis transcriptional program[42,43]. Together, these processes downstream of mTORC1 lead to an initial increase in cap-dependent translation followed by ribosome synthesis and a global increase in mRNA translation.

mTORC1 also promotes the *de novo* synthesis of purine and pyrimidine nucleotides, both of which can be integrated into DNA and RNA. Through activation of the transcription factor sterol regulatory element binding protein (SREBP), mTORC1 promotes the expression of glucose-6-phosphate dehydrogenase (G6PD) and phosphogluconate dehydrogenase (PGD), two genes in the oxidative branch of the pentose phosphate pathway (PPP)[33,44,45]. This increase in gene expression is thought to facilitate the flux of carbons into ribose-5P and 5-phospho-α-D-ribosyl 1-pyrophosphate (PRPP), a key intermediate in *de novo* purine and pyrimidine synthesis. *De novo* purine synthesis is stimulated by mTORC1, in part, through its activation of activating transcription factor 4 (ATF4) and the associated transcription of methylenetetrahydrofolate dehydrogenase 2 (MTHFD2)[46]. MTHFD2 is a mitochondrial tetrahydrofolate

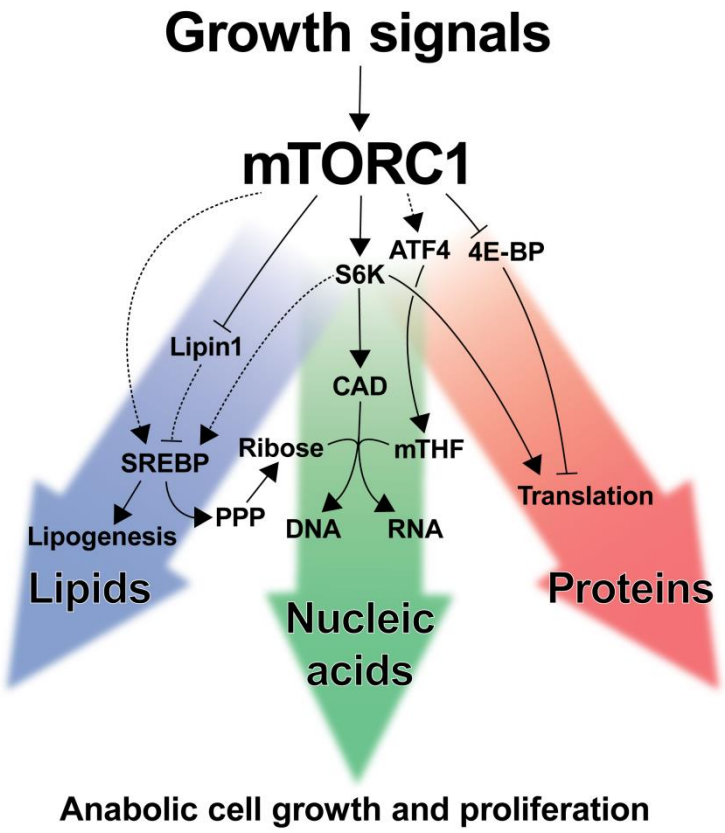

Figure 1.2. Stimulation of anabolic pathways by mTORC1 to promote the synthesis of proteins, lipids and nucleic acids required for cell growth and proliferation.

mTORC1 activates SREBP, a major transcriptional regulator of lipogenic genes, through the inhibition of Lipin1, the activation of S6K, and possibly additional mechanisms to promote *de novo* lipid synthesis. SREBP also stimulates the transcription of pentose phosphate pathway (PPP) enzymes to produce ribose, which is required for nucleic acid synthesis. *De novo* synthesis of pyrimidines is increased through the phosphorylation of CAD by S6K, while *de novo* synthesis of purines is increased through stimulation of the mitochondrial tetrahydrofolate cycle (mTHF) by the ATF4-mediated transcriptional activation of MTHFD2 downstream of mTORC1. Protein synthesis is enhanced through the activation of S6K and the inhibition of 4E-BP to stimulate cap-dependent translation initiation and ribosome biogenesis. These processes downstream of mTORC1 provide the building blocks for anabolic cell growth and proliferation.

cycle enzyme that provides one-carbon units for synthesis of the purine ring. Unlike the transcriptional effects of mTORC1 on the enzymes required for purine synthesis, mTORC1 acutely stimulates *de novo* pyrimidine synthesis through the phosphorylation of CAD (carbamoyl-phosphate synthetase 2, aspartate transcarbamoylase, dihydroorotase) by S6K1, downstream of mTORC1[47,48].

Along with proteins and nucleotides, proliferating cells have an increased demand for lipids, since they must double their lipid membrane content with each cell cycle. mTORC1 has emerged as a major promoter of *de novo* lipid synthesis in both growing cells and specialized lipid-producing cells, such as hepatocytes and adipocytes[49]. Although the exact molecular mechanism is currently unknown, mTORC1 stimulates lipogenesis through the activation of SREBP1 and 2[33,50]. The SREBPs are transcription factors that induce the expression of genes encoding most lipogenic enzymes involved in the synthesis of both fatty acids and sterols[51–53]. In addition, SREBPs provide reducing power for *de novo* lipid synthesis by activating the transcription of NADPH-producing enzymes, such as G6PD, PGD, and malic enzyme 1 (ME1)[33,44,45]. In response to mTORC1 activation, SREBPs promote the *de novo* synthesis of lipids through the transcription of their target genes.

The complex regulation of mTORC1 by nutrients and growth signals ensures that mTORC1 is only activated in settings that will foster cell growth. In favorable conditions, activation of mTORC1 coordinates the synthesis of the necessary cellular building blocks (i.e., proteins, nucleotides, lipids) to promote cell growth and proliferation (Figure 1.2). Given the central role of mTORC1 in promoting anabolic metabolism, it is not surprising that it is aberrantly activated in many cancers and other diseases[29,54].

1.2 THE MULTIFACETED ROLE OF mTOR IN THE CONTROL OF LIPID METABOLISM

1.2.1 Overview

Of the four major classes of biological macromolecules, our understanding of the molecular mechanisms by which cellular signaling pathways regulate lipid metabolism has lagged behind that of carbohydrates, proteins, and nucleic acids. However, lipids are critically important both structurally and functionally in all living organisms. An obvious reason for this dependence is the lipid makeup of the plasma membrane and many subcellular organelles. Moreover, lipids can act as signaling molecules on both a cellular (e.g., phosphatidylinositides) and organismal (e.g. steroid hormones) scale. Lipids are also used for energy storage, primarily as triacylglycerides (TAGs) in adipocytes, and as an alternative to glucose for catabolic metabolism. Despite the dependence of living organisms on lipids, we know very little about how lipid homeostasis is controlled by the intricate network of cellular signaling pathways that sense cellular growth conditions.

mTOR has emerged as a crucial link between cellular and systemic growth signals and the regulation of lipid metabolism. A large number of recent studies in cell and mouse models, combined with preclinical and clinical data on mTOR inhibitors, have revealed a pivotal role for mTOR, particularly within mTORC1, in controlling lipid homeostasis in multiple settings, both physiological and pathological. We review this evidence below, with a focus on the key aspects of lipid synthesis, storage, and mobilization. The emerging picture is that, through a variety of molecular mechanisms, mTORC1 signaling promotes processes to synthesize and store lipids, while inhibiting those leading to lipid consumption (Figure 1.3).

1.2.2 Lipogenesis

The regulation of *de novo* sterol and fatty acid synthesis by signaling pathways, especially insulin signaling, has garnered intense interest. Unlike most terminally differentiated cells, hepatocytes and

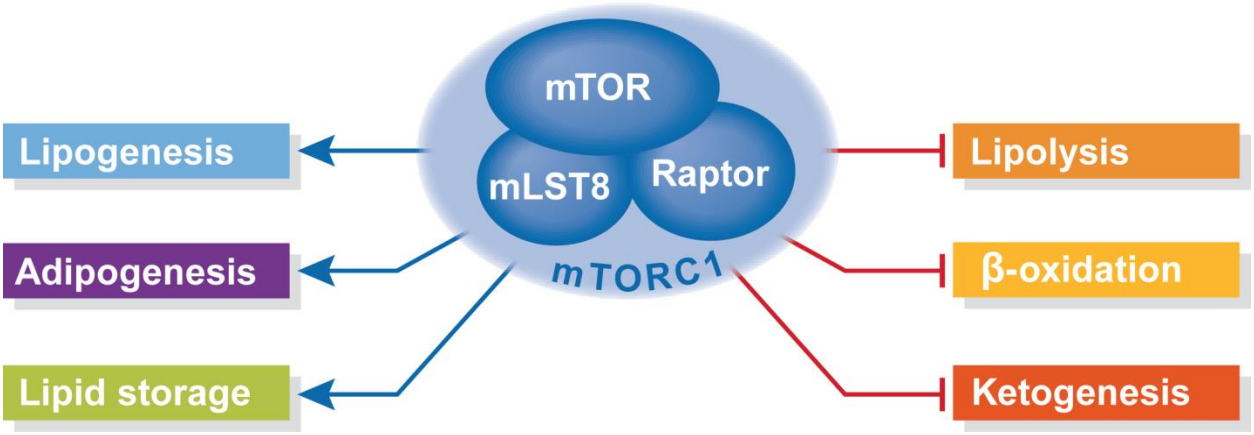

Figure 1.3. Regulation of lipid metabolism by mTORC1.

mTORC1 plays multiple roles in regulating lipid metabolism, including the promotion of lipid synthesis and storage and inhibition of lipid release and consumption.

adipocytes can synthesize significant amounts of lipid *de novo* through pathways in which cytosolic acetyl-CoA, derived from glucose or amino acid catabolism, is used to form the hydrophobic carbon backbone of lipids. Acetyl-CoA is either committed to sterol and isoprenoid biosynthesis through the action of acetyl-CoA acetyltransferase (ACAT) or to fatty acid biosynthesis through acetyl-CoA carboxylase (ACC) (Figure 1.4)[55]. For sterol synthesis, acetoacetyl-CoA produced by ACAT is converted into mevalonate by HMG-CoA synthase (HMGCS) and HMG-CoA reductase (HMGCR). Mevalonate is then used for the synthesis of farnesyl, geranyl, cholesterol, and steroid hormones. Farnesylation and geranylation are post-translational protein modifications that are required for proper membrane association and protein-protein interactions. Cholesterol is a major component of membranes in the cell, and the amount of cholesterol modulates membrane fluidity. For fatty acid synthesis, fatty acid synthase (FASN) extends malonyl-CoA produced by ACC by repeatedly attaching carbons from acetyl-CoA until palmitate (16:0) is produced. Palmitate can then be further extended by elongases and/or desaturated by steroyl-CoA desaturase (SCD), to make monounsaturated fatty acids. Once produced, fatty acids are incorporated into various complex lipids, each with different cellular functions. TAGs are the main form of lipid storage and are produced by glycerol-3P acyltransferase (GPAT), acylglycerol-3P acyltransferase (AGPAT), and diglyceride acyltransferase (DGAT), with each enzyme attaching a fatty acid to a glycerol backbone. Membrane phospholipids (e.g., phosphatidylcholines, phosphatidylserines, phosphatidylethanolamines) are produced by adding an active group to the glycerol backbone of diacylglyceride (DAG). Fatty acids can also be incorporated into signaling lipids such as phosphatidylinositides and sphingolipids. Given the important cellular roles of these different lipid classes, cells must carefully regulate *de novo* lipogenesis to maintain lipid homeostasis.

The multiple steps required for both the sterol and fatty acid synthesis branches are carried out by a large number of specific enzymes. Importantly, the SREBPs are transcription factors that stimulate the expression of genes encoding nearly all of these lipogenic enzymes[51]. The three SREBP isoforms,

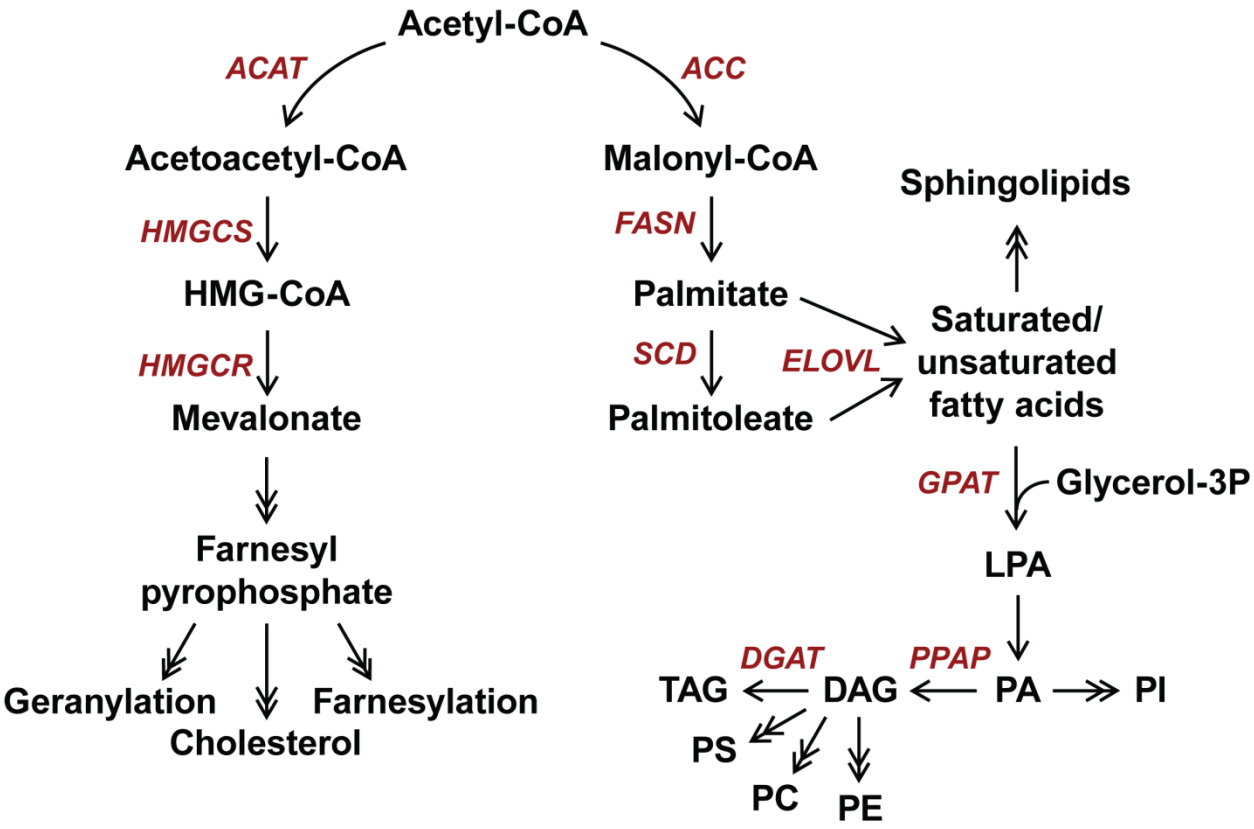

Figure 1.4. *De novo* synthesis of complex lipids.

Acetyl-CoA is the starting point of all *de novo* synthesized lipids. Sterol synthesis begins with the conversion of acetyl-CoA to HMG-CoA by ACAT and HMGCS. HMGCR, which catalyzes the conversion of HMG-CoA to mevalonate, is the target of statins. Mevalonate can then be used to produce membrane lipids (e.g., cholesterol) or signaling lipids (e.g., farnesyl, geranyl). Conversely, conversion of acetyl-CoA to malonyl-CoA is the first step of fatty acid synthesis. FASN then extends malonyl-CoA with the pairwise addition of carbons from acetyl-CoA to produce palmitate (16:0). Various fatty acids can be produced from palmitate with extension of the carbon chain by elongases (e.g., ELOVL) and/or desaturation by desaturases (e.g., SCD). Glycerophospholipids are produced by attaching these fatty acids to a glycerol backbone. Adapted from Baenke F, *et al*.[55].

encoded by two genes, are produced as inactive transmembrane proteins at the endoplasmic reticulum (ER) (Figure 1.5). Under conditions of abundant sterols, full length SREBP, through its sterol-sensing binding partner SREBP cleavage-activating protein (SCAP), is retained in the endoplasmic reticulum (ER) by the INSIG proteins[56]. Depletion of intracellular sterols results in release of the SREBP-SCAP complex from INSIG and their transport to the Golgi apparatus, where two proteolytic cleavage events by the site-specific proteases, S1P and S2P, liberate the active N-terminus of SREBP. This fragment then enters the nucleus and induces transcription from SREs within target genes. SREBP1a and 1c are products of alternative splicing of the *SREBF1* gene and have been primarily implicated in the control of genes involved in fatty acid synthesis, although SREBP1a is thought to activate most SRE-containing genes[53]. SREBP2 is encoded by *SREBF2* and is believed to play a more important role in the transcription of steroidogenic genes, including those involved in cholesterol synthesis in the liver [52,57]. While the SREBPs preferentially activate transcription of different sets of genes, there is substantial overlap between the targets of the SREBP isoforms and the tissue-specificity of these preferences has not been fully established. Importantly, independent studies have identified the SREBPs as major transcriptional effectors of mTORC1 signaling and have demonstrated that mTORC1 activation promotes lipogenesis through this family of transcription factors[33,50].

mTORC1 signaling promotes SREBP activation and lipogenesis in response to both physiological and genetic stimuli. In primary rodent hepatocytes and the intact liver, insulin or feeding has been shown to increase the expression of the major liver isoform of SREBP (SREBP1c) and its targets, and to promote *de novo* lipid synthesis, in a manner that is sensitive to rapamycin[58–60]. As described earlier, insulin activates mTORC1 through a pathway involving the Akt-mediated inhibition of the TSC complex[13,16,17]. Expression of constitutively active Akt or loss of either TSC1 or TSC2, both of which result in insulin-independent activation of mTORC1 signaling, stimulates the global expression of SREBP1 and 2 targets and drives lipogenesis through mTORC1[33,50]. These latter studies found that

Figure 1.5. The complex steps leading to SREBP activation and inputs from mTORC1 signaling. (**A**) SREBP processing and activation is regulated by mTORC1, through S6K and Lipin1, leading to the transcriptional induction of the *SREBF1* and *SREBF2* genes, encoding SREBP1 and SREBP2 respectively, and genes encoding a large number of lipogenic enzymes involved in both fatty acid and sterol synthesis. The mTORC1-mediated transcriptional activation of *SREBF1* could result from either autoregulation by SREBP1 or from an unknown parallel pathway downstream of mTORC1. (**B**) In the presence of sterols, SREBP resides in the ER bound to SCAP and the Insig proteins. When sterols become scarce, SCAP undergoes a conformational change, which releases the SCAP-SREBP complex from Insig, allowing its transport from the ER to the Golgi apparatus through COPII vesicles. Once in the Golgi, SREBP comes into contact with two site-specific proteases. S1P cleaves the luminal loop of SREBP and is followed by S2P cleavage of the N-terminal transmembrane region of SREBP, which releases the N-terminal region of SREBP containing the DNA-binding and trans-activating domains. The NLS-containing processed form of SREBP enters the nucleus to activate transcription of genes containing SREs in their promoters. Finally, the processed form of SREBP is unstable and subject to proteasome-mediated degradation. In some settings, SREBP processing has been found to require S6K1 downstream of mTORC1 and is therefore sensitive to rapamycin. However, the nuclear shuttling of SREBP has been found to require Lipin1 downstream of mTORC1, the phosphorylation of which is largely resistant to rapamycin, but sensitive to mTOR kinase domain inhibitors. The precise molecular mechanisms by which S6K1 and Lipin1 regulate SREBP activation are currently unknown.

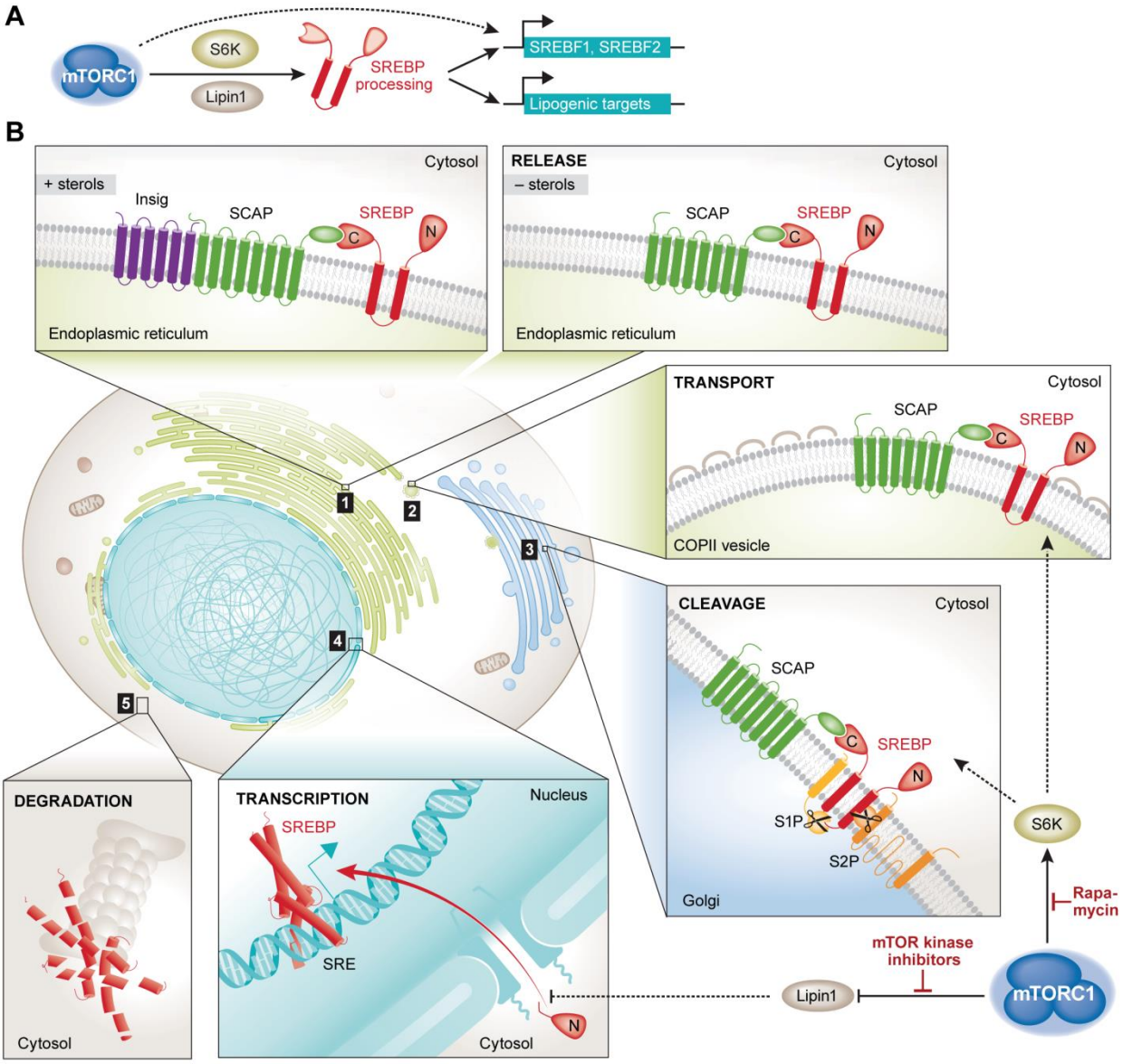

Figure 1.5 (Continued)

mTORC1 signaling promotes accumulation of the processed, mature form of SREBP1, which resides in the nucleus to induce its own expression and that of genes involved in both steroid and fatty acid biosynthesis. In exploring the molecular mechanism of this regulation, it was found that S6K1 is required downstream of mTORC1 to stimulate the increase in levels of active SREBP1, expression of SREBP1 and 2 targets, and *de novo* lipogenesis in TSC2-deficient cells[33]. SREBP1 regulation in this setting is independent of effects on the proteasomal degradation of its active form, suggesting that S6K1 somehow promotes the processing of SREBP1. Consistent with these findings, S6K1 has been found to promote the activation of hepatic SREBP1c through effects on its processing[61,62] and to affect the processing of SREBP2 in a hepatocellular carcinoma cell line[63]. mTORC1 signaling has also been suggested to increase SREBP1 activation in an S6K1-dependent manner in cultured myotubes[64].

Genetic mouse models have demonstrated that mTORC1 activation is essential, but not sufficient, to stimulate hepatic SREBP1c and its lipogenic targets in response to feeding[59,65]. Mice lacking mTORC1 in their liver, via liver-specific *Raptor* KO, fail to induce SREBP1c and lipogenesis[65] and have reduced levels of both liver triglycerides and circulating cholesterol on a "Western" diet[66]. However, characterization of mice with liver-specific KO of *Tsc1* (LTsc1KO), which exhibit constitutive activation of mTORC1 that is independent of insulin and feeding, revealed that mTORC1 signaling, while essential, is not capable of activating SREBP1c and hepatic lipid synthesis on its own[59]. In fact, these mice were found on two independent strain backgrounds to be resistant to the development of both age- and diet-induced hepatic steatosis due to decreased SREBP1c activation[59,67]. These seemingly paradoxical findings are the result of a strong feedback attenuation of Akt signaling that accompanies loss of function of the TSC complex in all settings[68]. A critical role for Akt signaling in the induction of SREBP1c and lipogenesis in the liver has been established through various rodent models[69–71], and this has recently been extended using mice with liver-specific *Rictor* KO, which results in the loss of mTORC2 activity and its activating phosphorylation of Akt[72]. Consistent with the essential nature of Akt signaling to hepatic SREBP1c, a restoration of Akt activity in LTsc1KO hepatocytes restores SREBP1c activation and

lipogenesis[59]. While multiple mTORC1-independent pathways might function in parallel downstream of Akt to help promote the activation of hepatic SREBP1c, including glycogen synthase kinase 3 (GSK3) inhibition[73], data from the LTsc1KO mice suggest that one pathway involves the repression of an isoform of the SREBP inhibitor Insig, Insig2a, which is only expressed in the liver[59]. A liver-specific mechanism is also consistent with the fact that mTORC1 activation alone is sufficient to promote SREBP activation and lipogenesis in other settings, even in the absence of Akt signaling[33].

The molecular mechanism by which S6K1 promotes SREBP processing is currently unknown, and it is clear from additional studies that S6K1 is not the only direct target downstream of mTORC1 involved in SREBP isoform regulation, which might vary by cellular context (Figure 1.5). Knockdown of the mRNA cap-binding protein eIF4E, which is normally activated by mTORC1 signaling through the phosphorylation and release of its inhibitory binding partner 4E-BP1, decreases overall levels of SREBP1 and its canonical target SCD in breast cancer cell lines[74]. The potential involvement of 4E-BP1 regulation by mTORC1 in some cells might explain the resistance of SREBP1 or 2 activation to rapamycin in specific settings[63,75]. The resistance of some mTORC1 targets to rapamycin is an important consideration when examining the role of mTORC1 signaling in any aspect of lipid metabolism. Another direct target of mTORC1 that, like 4E-BP1, is partially resistant to rapamycin for its regulation is the phosphatidic acid (PA) phosphatase lipin1, which has also been implicated in SREBP regulation[66,76]. Lipin1 appears to play a role in remodeling of the nuclear lamina, which is inhibited by mTORC1-mediated phosphorylation of multiple residues on this enzyme. Lipin1 phosphorylation also coincides with an increase in the levels of processed, nuclear SREBP1 and 2 and the expression of SREBP targets. Although the PA phosphatase activity of lipin1 was shown to be important for its inhibitory effect on nuclear SREBP levels[76], the molecular mechanism and tissue specificity of this regulation, as with S6K1 and 4E-BP1, remain unknown. Likewise, mTORC1-mediated phosphorylation of CREB regulated transcription coactivator 2 (CRTC2) was shown to be partially sensitive to rapamycin. This phosphorylation event has been suggested to increase SREBP1 transport to the Golgi by facilitating the

interaction of SEC23A and SEC31A, two subunits of the COPII complex involved in protein transport[77]. Finally, it is clear that mTORC1 signaling also increases the transcript levels of SREBP1 and 2 in cell culture models[33] and SREBP1c in both rodent hepatocytes and the intact liver in response to insulin or feeding[59–62]. This mTORC1-dependent transcriptional response leads to an increase in full-length SREBP isoforms that accompanies the increased processing and activation of SREBP. However, it remains unclear whether this transcriptional effect is simply a result of autoregulation by processed SREBPs at the *SREBF1* or *SREBF2* promoter or a parallel pathway independent from the effects of mTORC1 on SREBP processing (Figure 1.5A). Both *SREBF1* and *SREBF2* contain a characterized SRE in their promoters[78,79]. In cell culture models, exogenous expression of processed SREBP1a can stimulate the expression of endogenous SREBP1 and 2 transcripts in a manner that is no longer sensitive to rapamycin, suggesting that the transcriptional effects of mTORC1 signaling on SREBP expression are upstream of processed SREBP[33]. However, elegant studies with a transgenic version of SREBP1c in rat suggest that the role of mTORC1 in SREBP1c processing and gene expression are separable[62]. More such studies are needed to understand the multiple inputs of mTORC1 signaling into the regulation of SREBP isoforms, especially *in vivo*.

1.2.3 Adipogenesis

Adipocytes are specialized mesenchymal cells that either store lipids as energy reserves (white adipose tissue) or burn lipids through oxidation to generate heat (brown adipose tissue). Pharmacological and genetic studies have demonstrated that the differentiation of mesenchymal stem cells into mature adipocytes (i.e., adipogenesis) requires mTOR signaling (Figure 1.6). Rapamycin treatment has been reported to reduce adipogenesis in a variety of cell culture models. Rapamycin appears to block the early determination step in brown adipocyte differentiation, in which a mesenchymal stem cell commits to becoming a preadipocyte[80]. Similarly, rapamycin treatment or shRNA-mediated knockdown of *S6K1* in embryoid bodies hinders their commitment to preadipocytes[81]. However, much of our knowledge of

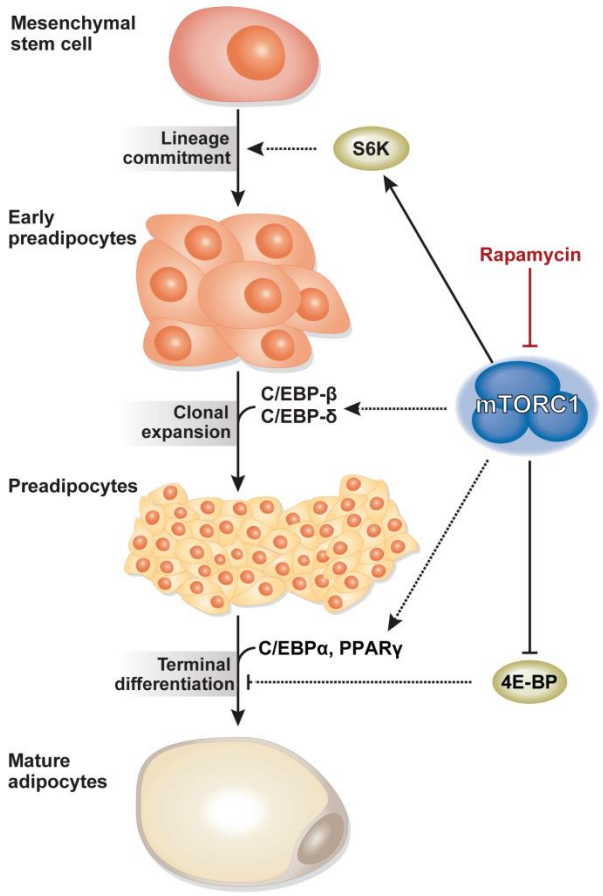

Figure 1.6. mTORC1 signaling has been implicated in promoting the three major steps of adipogenesis.

Adipogenesis consists of the differentiation of a mesenchymal stem cell to a mature adipocyte, which makes up a significant part of adipose tissue where energy is stored as lipids. The commitment of the mesenchymal stem cells to the adipocyte lineage is the first step of adipogenesis and has been found to be facilitated by S6K1 activity. C/EBP-β and –δ are the primary drivers of clonal expansion, which is critical for preadipocyte maturation, and the former has been suggested to be activated by mTORC1 signaling. The terminal differentiation of preadipocytes to mature adipocytes is mediated by PPARγ and C/EBP-α. mTORC1 promotes this final step through both its inhibition of 4E-BP and its activation of PPARγ through a poorly understood mechanism. While the precise molecular mechanisms have yet to be defined, rapamycin blocks adipogenesis.

adipogenesis comes from cell culture models of preadipocytes, following lineage commitment, and MEFs, and have therefore been focused on the later steps of white adipose differentiation. Treatment of preadipocytes with rapamycin leads to a marked decrease in adipocyte differentiation[82–86]. mTOR has been implicated in hormonal induction of clonal expansion, which is an initial step of differentiation that occurs through the action of two CCAAT/enhancer-binding proteins (C/EBP) family transcription factors, C/EBP-β and –δ. Overall levels of C/EBP-β have been found to decrease upon rapamycin treatment, which corresponds with a repression of clonal expansion of preadipocytes[83]. However, rapamycin has also been shown to inhibit pre-adipocyte differentiation after clonal expansion, thereby ruling out the anti-proliferative effects of rapamycin as its primary mode of inhibiting adipogenesis[84–86].

Several genetic models have further supported a critical role for mTORC1 activation in terminal adipocyte differentiation, where it appears to be both necessary and sufficient. For instance, MEFs lacking TSC1 or TSC2, which have sustained insulin-independent activation of mTORC1 signaling, exhibit an mTORC1-dependent enhanced capacity to differentiate into adipocytes, despite these cells being severely resistant to insulin, a major adipogenic factor[87]. Reciprocally, TSC2-deficient MEFs expressing a phosphorylation-site mutant of TSC2 that blocks the ability of mTORC1 to be activated by insulin and Akt signaling display reduced adipogenesis[87]. The enhanced adipogenesis in mesenchymal cells lacking the TSC tumor suppressors is likely to explain the common development of adipocyte-rich renal angiomyolipomas in patients with tuberous sclerosis complex[88]. Consistent with an essential role for mTORC1, RNAi knockdown of *Raptor* also blocks adipogenesis in preadipocytes[89]. Downstream of mTORC1, genetic evidence suggests a role for both S6K and 4EBP in the control of adipogenesis. The involvement of S6K in commitment of stem cells to preadipocytes was reinforced by the reduced size of this progenitor cell population in *S6K1* KO mice and a defect in the capacity of embryonic stem cells from these mice to commit to the adipocyte lineage[81]. Reciprocally, *4E-BP1/2* double-KO MEFs display enhanced differentiation toward adipocytes[90], suggesting that the ability of mTORC1 to both activate S6K and inhibit 4E-BP contributes to its role in promoting adipogenesis. Interestingly, the *S6K1* KO mice have

a lean phenotype on both normal and high-fat diets[81,91], while the *4E-BP1/2* double-KO mice are more sensitive to diet-induced obesity than their wild type counterparts[90]. However, the differences in adiposity in these systemic mouse models are likely to reflect multiple effects of mTORC1 signaling on lipid synthesis and mobilization, discussed in a later section, in addition to its role in promoting the development of adipose deposits.

The molecular mechanisms by which mTORC1 and its downstream targets stimulate adipocyte differentiation have yet to be fully defined. The temporal activation of two transcription factors, C/EBP-α followed by peroxisome proliferator-activated receptor γ (PPARγ), the master regulator of terminal adipocyte differentiation, is responsible for inducing the final stages of differentiation[92]. mTORC1 signaling has been shown to increase PPARγ transcript and protein levels, as well as its transactivating activity in various studies[87,89,93,94], albeit through unknown mechanisms. Cell culture experiments have suggested that regulation of the final differentiation steps are primarily independent of S6K and are likely to be dependent on 4E-BP inhibition downstream of mTORC1[82,90]. However, a recent study has indicated that PPARγ activation can also be suppressed by hyperactive mTORC1 signaling through its negative feedback effects on insulin signaling[95]. These findings indicate that there are likely to be mTORC1-dependent and independent inputs into PPARγ activation and adipocyte differentiation downstream of insulin signaling, with more *in vivo* experiments needed.

1.2.4 Lipolysis

In addition to its role in stimulating lipogenesis through SREBP, mTORC1 signaling is believed to promote the storage of fatty acids in lipid stores by inhibiting lipolysis. Neutral lipids, in the form of monoacylglyceride (MAG), DAG, and TAG inside the cell are subject to lipolysis in order to mobilize free fatty acids for energy production or remodeling into new lipid species, including specific membrane and signaling lipids. Patients treated with rapamycin frequently exhibit dyslipidemia, one facet of which is elevated levels of plasma free fatty acids, which could reflect an increase in lipolysis in adipose

tissue[96,97]. Mice treated with rapamycin exhibit a reduction in adipocyte size and overall adiposity, and rapamycin stimulates lipolysis in cultured adipocytes[98–100]. Genetic manipulations of mTORC1 signaling in several mouse models have reinforced the link between mTORC1 activation and an inhibition of lipolysis. The adipose tissue of *4E-BP1/2* double-KO mice exhibits decreased lipolysis[90], and *S6K1* KO mice are leaner with elevated rates of lipolysis[91]. However, mice with adipose-specific *Raptor* KO, while also lean with reduced adiposity, do not display an obvious increase in lipolysis[89]. This suggests that the lipolysis phenotypes observed in the whole-body *4E-BP* and *S6K1* KO models could be due to systemic effects, rather than those intrinsic to the adipocyte. Interestingly, adipose-specific *Atg7* (autophagy-related 7)-KO mice, which have a defect in autophagy, display decreased adipocyte lipolysis[101], suggesting that the inhibitory effects of mTORC1 on lipolysis could be, at least in part, through its attenuation of autophagy.

Although the molecular mechanisms of lipolytic regulation by mTOR are not fully understood, mTORC1 signaling has been found to influence three distinct lipases: adipose triglyceride lipase (ATGL), hormone-sensitice lipase (HSL) and lipoprotein lipase (LPL)[102]. In adipocytes, ATGL catalyzes the lipolysis of TAGs to DAGs within lipid droplets. HSL then converts the DAGs to MAGs. In 3T3-L1 adipocytes, mTORC1 suppression increases the transcription of ATGL, which parallels the enhanced lipolysis induced by rapamycin or siRNA knockdown of *Raptor*[99]. The phosphorylation of HSL at S563, an established PKA site, is associated with an increase in its lipase activity. A decrease in HSL phosphorylation correlates with mTORC1 activation and the diminished release of free fatty acids[100]. However, like ATGL transcriptional suppression, how mTORC1 signaling negatively affects HSL phosphorylation on this PKA site is currently unknown. Similar to mTORC1 inhibition, adipocyte-specific *Rictor* KO also leads to the phosphorylation of HSL at S563[103]. In addition to adipocyte lipolysis, mTORC1 has been implicated in the control of the extracellular lipase LPL. LPL is a water-soluble lipase present in plasma, as well as on the surface of endothelial cells, primarily in muscle and adipose tissue. It hydrolyzes TAG in circulating very low density lipoprotein (VLDL) to promote conversion to

intermediate density lipoprotein (IDL) and low density lipoprotein (LDL), which facilitates the uptake of lipoprotein into tissues[104]. Systemic rapamycin treatment has been found to decrease LPL activity in mouse adipose tissue and mouse and human plasma, albeit through an unknown mechanism[105,106]. The collective studies in patients treated with rapamycin and a variety of cell and mouse models suggest that mTORC1 activation, which occurs in metabolic tissues after feeding, promotes the synthesis and storage of lipids. In contrast, mTORC1 inhibition, such as during fasting, stimulates lipolysis and the release of free fatty acids into the circulation.

1.2.5 β-Oxidation and ketogenesis

Consistent with the inhibition of mTORC1 signaling promoting fatty acid release and consumption, there is growing evidence that mTORC1 suppresses the β-oxidation of fatty acids for energy or ketogenesis. Rapamycin has been found to increase β-oxidation in rat hepatocytes, and this has been attributed to increased expression of β-oxidation enzymes, including very long-chain acyl-CoA dehydrogenase and carnitine acyltransferase[58,107]. This effect of rapamycin could be due to the induction of autophagy, which appears to promote the β-oxidation of fatty acids from TAGs in hepatocytes[108]. However, genetic evidence suggests that autophagy has inhibitory effects on β-oxidation in adipose tissue[101,109]. Mice with whole-body KO of *S6K1* appear to have enhanced β-oxidation, as evidenced by increased levels of carnitine palmitoyltransferase 1(CPT1) transcript in isolated adipocytes[91]. Consistent with mTORC1 signaling attenuating β-oxidation, myoblasts isolated from *S6K1/S6K2* double-KO mice also display enhanced β-oxidation of fatty acids[110]. However, this phenotype was attributed to indirect effects from energy stress and AMPK activation in this setting. Like the *S6K1* KO and *S6K1/S6K2* double-KO mice, mice with adipose-specific *Raptor* KO are lean, with adipocytes displaying increased mitochondrial uncoupling, which could allow them to rapidly burn lipids without generating ATP[89,91,110]. Somewhat paradoxically, mTORC1 activation has also been linked to increased mitochondrial biogenesis in some settings[111]. This could explain the decrease in oxidative capacity of muscle[111–113] and Jurkat T cells[114] following the inhibition or complete loss of mTORC1 signaling. However, further studies are

needed to determine how the observed changes in mitochondrial gene expression and oxygen consumption in these settings influence the β-oxidation of fatty acids. The collective data suggest that mTORC1 signaling inhibits fatty acid oxidation, while also promoting mitochondrial biogenesis in some settings.

The acetyl-CoA released from β-oxidation can either enter the tricarboxylic acid (TCA) cycle or, under fasting conditions in the liver, be converted to ketone bodies. Genetic evidence suggests that mTORC1 signaling in the liver, which is respectively inhibited and activated by fasting and feeding, suppresses ketogenesis[115]. Mice with liver-specific *Tsc1* KO, which exhibit sustained mTORC1 signaling under fasting, have a defect in ketogenesis, while mice with liver-specific *Raptor* KO display an increase in fasting-induced ketogenesis. mTORC1 appears to suppress the expression of ketogenic enzymes through its regulation of nuclear receptor co-repressor 1 (N-CoR1) and PPARα[115], through a mechanism likely to be dependent on S6K2[116]. These inhibitory effects on PPARα and its transcriptional targets could also explain the negative regulation of fatty acid oxidation by mTORC1. The repression of β-oxidation and ketogenesis by mTORC1 is likely to act in concert with its stimulation of lipogenesis, further promoting the flux of acetyl-CoA towards lipid synthesis and storage.

1.2.6 Lipid transport

Several lines of evidence suggest a role for mTORC1 signaling in the control of lipid mobilization and transport. As stated above, patients treated with mTORC1 inhibitors frequently suffer from a dyslipidemia consisting of hypertriglyceridemia and hypercholesterolemia, as well as increased levels of plasma free fatty acids[97]. The source of the elevated circulating lipids in these patients is unknown. However, TAG and cholesterol transport out of the liver involves their packaging into apolipoprotein complexes, and plasma levels of both ApoB-100 and ApoC-III have been found to be increased in patients treated with rapamycin[96]. A study in guinea pigs revealed that the increase in circulating TAGs observed in response to rapamycin correlates with an increase in VLDL, the primary

mode of TAG export from the liver[117]. In cultured hepatocytes, the ability of insulin to repress the expression of both ApoB and ApoA5 is sensitive to rapamycin, suggesting that the increase in apolipoproteins observed upon rapamycin treatment *in vivo* might be due to direct effects on hepatocytes[118,119]. How mTORC1 negatively regulates the expression or protein levels of specific apolipoproteins is unknown and could be secondary to changes in apolipoprotein uptake or degradation. Conversely, mTORC1 signaling appears to upregulate the LDL receptor (LDLR), which facilitates the uptake of cholesterol-rich LDL from the plasma into the liver and peripheral tissues. *LDLR* gene expression is controlled by SREBP[120] and would, therefore, be predicted to be stimulated by insulin in an mTORC1-dependent manner. In addition, mTORC1 signaling downstream of the insulin receptor in the liver has been found to repress the expression of PCSK9 (proprotein convertase subtilisin/kexin type 9), a known negative regulator of LDLR protein levels[121]. Consequently, rapamycin treatment decreases LDLR levels in a PCSK9-dependent manner, thereby reducing LDL uptake and increasing its circulating levels. Combined with the rapamycin-stimulated increase in lipolysis and apolipoprotein levels, these effects on the LDLR suggest a mechanistic basis for the dyslipidemia observed in patients treated with mTORC1 inhibitors.

1.2.7 mTORC1 in physiology, obesity, and diabetes

The global effects of the mTORC1-mediated regulation of lipid metabolism detailed above would be predicted to promote the systemic flux of carbon into lipids and their storage as TAGs within adipose tissue (Figure 1.7). The postprandial increase in both glucose and insulin stimulates the acute activation of mTORC1 within metabolic tissues, where mTORC1 plays contextual roles in controlling lipid metabolism. In the liver, and likely in adipose tissue, mTORC1 activation induces lipogenesis. At the same time, mTORC1 is likely to block the β-oxidation of fatty acids in the liver, adipose, and perhaps muscle, instead promoting the utilization and storage of glucose in these tissues. TAGs and cholesterol produced in the liver facilitate the packaging and release of VLDL into circulation. mTORC1 signaling

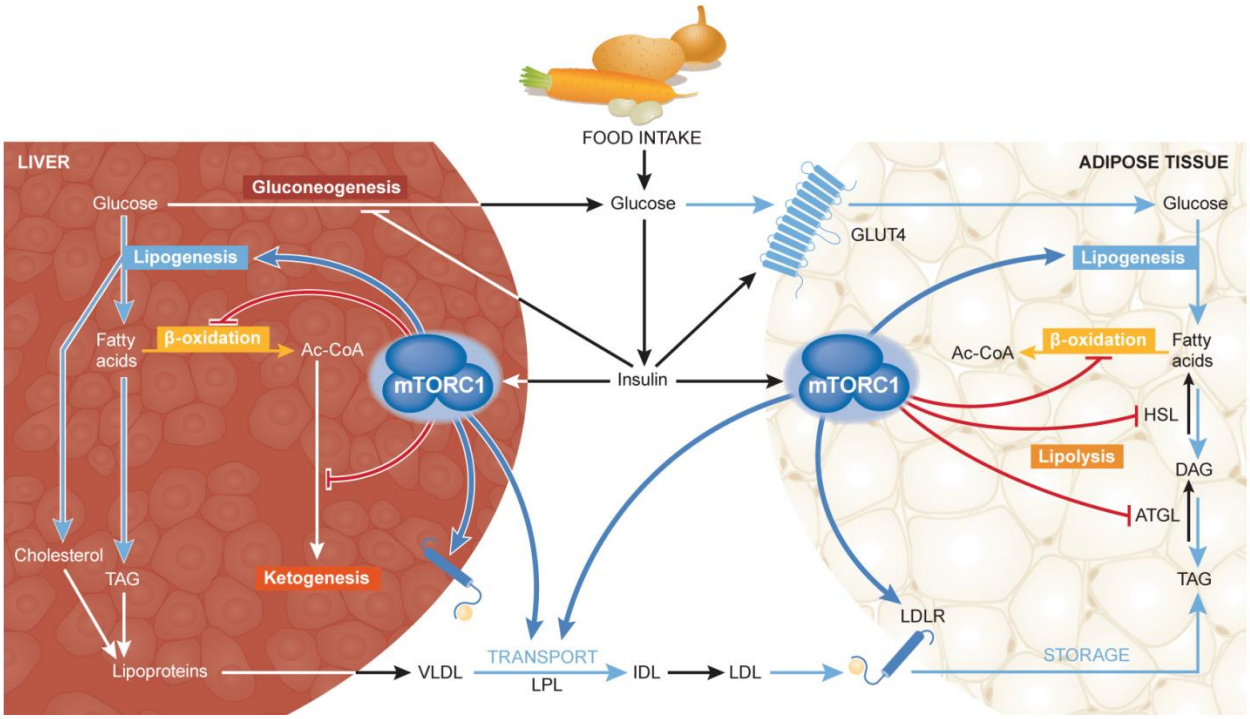

Figure 1.7. The increase in insulin levels following a meal alters hepatic and adipose lipid metabolism, at least in part, through mTORC1 signaling (a working model).

In the liver, mTORC1 promotes lipid synthesis through SREBP1c activation. In addition, mTORC1 signaling blocks lipid catabolism by blocking β-oxidation and ketogenesis in the liver. Consequently, mTORC1 activation in the liver promotes the synthesis of TAGs and, perhaps, cholesterol, which are incorporated into VLDL for transport to peripheral tissues. Evidence suggests that mTORC1 signaling can positively influence LPL activity, which promotes lipid delivery to peripheral tissues by hydrolyzing VLDL to IDL, which is then converted to LDL. Lipoprotein-bound TAGs are taken up by tissues, including adipocytes, through the LDLR. Both the expression and stability of LDLR, at least in the liver, are likely promoted by mTORC1 activation. In response to insulin, mTORC1 has been suggested to inhibit lipolysis in adipocytes by down-regulating ATGL and HSL. Therefore, the systemic effects of postprandial mTORC1 activation are to promote the flux of carbon from glucose to toward TAG storage in adipose tissue. See text for details regarding the evidence underlying this model.

might enhance uptake of lipids by peripheral tissues through the activation of LPL, which hydrolyzes VLDL to IDL, and an increase in the levels of LDLR. In adipose tissue, the insulin-stimulated activation of mTORC1 is predicted to contribute to the inhibition of lipolysis, further promoting the storage of TAGs, either mobilized from the liver or produced *de novo*, within the adipocytes.

While mTORC1 is activated transiently within metabolic tissues by normal feeding, conditions of nutrient overload and obesity can lead to chronically elevated mTORC1 signaling in these tissues[91,122]. The mechanism by which obesity leads to hyperactivation of mTORC1 is unknown but is likely through a combination of hyperglycemia and hyperinsulinemia under these conditions. Furthermore, evidence suggests that increased circulating levels of branch-chain amino acids, which are known to activate mTORC1, correlates with the development of obesity and insulin resistance[123]. In addition to potentially exacerbating obesity by further promoting lipid storage in adipose depots, chronic mTORC1 activation under such conditions is believed to contribute to the development of insulin resistance, which frequently accompanies obesity. Increased mTORC1 signaling can trigger a number of distinct feedback mechanisms, which in a cell autonomous manner, dampens the cellular response to insulin. The *in vivo* contribution of these feedback mechanisms to insulin resistance is well illustrated by loss and gain of function mouse models of mTORC1 signaling. For instance, *S6K1* KO mice have enhanced peripheral insulin sensitivity[91], whereas mice with liver-specific *Tsc1* KO display hepatic insulin resistance with greatly reduced Akt signaling[59]. Therefore, under conditions of obesity, mTORC1 activation in metabolic tissues is likely to both perpetuate obesity and promote insulin resistance, thereby expediting the progression to type-2 diabetes.

The fundamental role of mTORC1 in regulating whole-body lipid homeostasis, paired with its frequent upregulation in obesity and type-2 diabetes, suggests that mTOR inhibitors might offer some therapeutic benefit in metabolic diseases. In theory, mTORC1-specific inhibitors should suppress lipid synthesis and promote lipolysis and lipid catabolism, in addition to blocking mTORC1-dependent feedback mechanisms to resensitize tissues to insulin. However, important caveats arise from the use of

mTORC1 inhibitors to combat obesity and diabetes. First, prolonged treatment with rapamycin can disrupt mTORC2 and, therefore, Akt activation downstream of the insulin receptor, further exacerbating the insulin resistant phenotype[8]. Second, patients treated with rapamycin frequently exhibit increased levels of circulating TAGs, cholesterol and free fatty acids[97]. Therefore, while rapamycin treatment might help mobilize lipids and deplete fat stores, lipid clearance offers an additional pathological challenge. Targeting mTORC1 signaling indirectly might offer a more promising avenue. AMPK is a potent negative regulator of mTORC1, blocking its function through phosphorylation of both the TSC complex[13,23] and Raptor[24]. Therefore, mTORC1 signaling is blocked upon activation of AMPK, which is stimulated by a large variety of natural and synthetic compounds, including metformin, resveratrol, and aspirin[124]. Importantly, metformin is the most widely prescribed anti-diabetes drug in the world. Whether any of the beneficial metabolic effects of metformin are attributed to its inhibition of mTORC1 signaling is one of several important outstanding questions.

1.3 CANCER METABOLISM

1.3.1 Overview

Most cells in the human body are differentiated and are under tight regulation to ensure that they do not proliferate. However, cancer cells, as a result of unrepaired genetic alterations, bypass this regulation and gain the ability to proliferate uncontrollably. Unlike normal cells, rapidly proliferating cancer cells have a higher demand for cellular building blocks, because lipids, DNA, and many proteins need to be duplicated for every cell division. Moreover, solid tumors may not be able to obtain sufficient amounts of these macromolecules from the circulation, due to their limited diffusion in poorly vascularized regions. One of the hallmarks of cancer cells is an altered metabolic state, which is often reflected by an increase in anabolic metabolism[125]. It is perhaps not surprising that mTORC1 signaling is frequently activated in cancer, since it activates anabolic processes to promote cell growth. Our

understanding of cancer metabolism has grown drastically over the last few decades, and has revealed the complex rewiring of metabolic pathways in cancer.

1.3.2 Lipid synthesis

Lipid synthesis has been studied in great detail in the context of the liver and adipocytes, but much less is known about the role of lipid synthesis in cancer. Elevated rates of *de novo* lipid synthesis were first reported in tumor tissue more than 60 years ago[126]. Further work in Ehrlich ascites tumor cells estimated that 93% of tumor cell lipids were produced from glucose through the *de novo* synthesis pathway[127]. This result was particularly surprising given that most normal cells in the body acquire lipids from the circulation and not from *de novo* synthesis. The overexpression of FASN and other fatty acid synthesis enzymes in many types of cancer provided an initial clue as to how cancer cells upregulate lipid synthesis[128–130], but the complete mechanism connecting cancer-causing mutations to increased *de novo* lipid synthesis remained a mystery.

1.3.3 Glycolysis and the Warburg effect

Glycolysis is the metabolic process through which cells convert glucose to pyruvate in the cytosol. In addition to generating two ATP molecules, many of the intermediates of glycolysis can be used by anabolic processes (Figure 1.8)[131]. For example, glucose-6P can be diverted into the oxidative pentose phosphate pathway by G6PD, to generate NADPH (an important molecule in the *de novo* synthesis of lipids and nucleotides) and ribose-5P (a substrate for *de novo* nucleotide synthesis). Similarly, dihydroxyacetone phosphate (DHAP) can be converted by glycerol-3-phosphate dehydrogenase (GPDH) into glycerol-3P, which serves as a backbone for glycerophospholipid synthesis. Additionally, 3-phosphoglycerate can be used for the synthesis of serine, glycine, and cysteine, and contributes one-carbon units to the tetrahydrofolate cycle. Lastly, alanine can be produced from pyruvate by alanine transaminase. Lactate dehydrogenase (LDH), through its conversion of pyruvate to lactate, regenerates NAD^+ to maintain flux through glycolysis. No oxygen is required for glycolysis, which

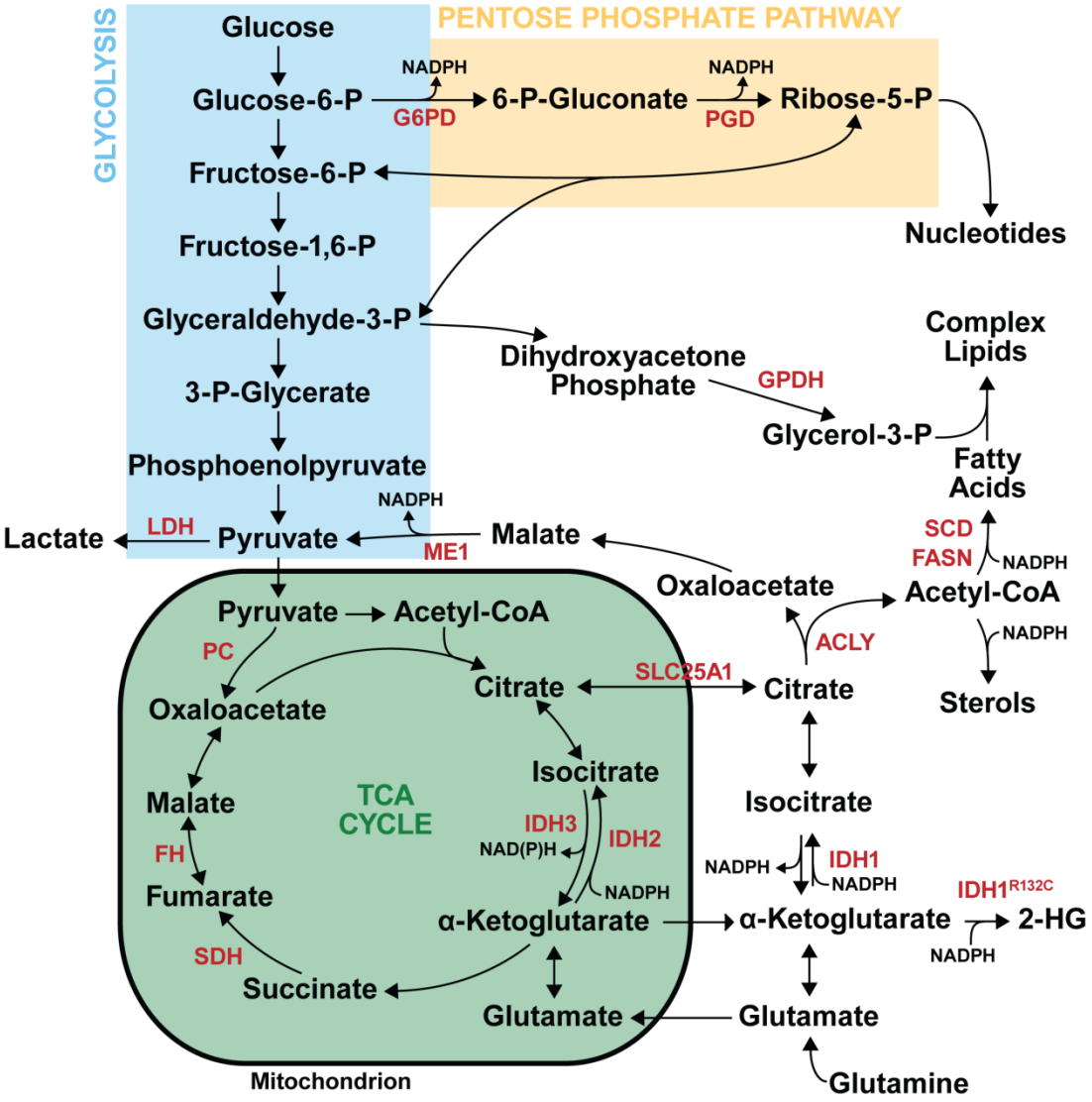

Figure 1.8. Metabolic pathways and their contributions to macromolecule synthesis.

Diagram showing the key intermediates of glycolysis, the pentose phosphate pathway, and the TCA cycle. These pathways provide carbons and reducing power, in the form of NADPH, to the *de novo* synthesis of lipids and nucleotides. The synthesis of amino acids other than glutamate and glutamine are not shown, but are described in the text. Metabolic enzymes mentioned in the text are shown in red. Adapted from Lunt, *et al.*[131]

differs from the oxygen-dependent oxidative phosphorylation. Consequently, glycolysis becomes an important source of ATP and metabolic intermediates when intracellular oxygen concentrations are low. In response to hypoxia and increased HIF-1α levels, flux through glycolysis is increased by the HIF-1α-mediated transcription of glucose transporters and many key glycolytic enzymes.

Early work by Otto Warburg on cancer metabolism demonstrated that cancer cells had an atypical upregulation of aerobic glycolysis regardless of oxygen levels, now referred to as the Warburg effect[132]. This finding conflicted with the work of Pasteur, who had found that fermentation, the bacterial equivalent of glycolysis, was inhibited by oxygen[133]. Cancer cells were initially believed to upregulate glycolysis to generate ATP and compensate for defects in mitochondrial oxidative phosphorylation. However, it has become clear that mitochondria and oxidative phosphorylation are functional in cancer cells[134,135]. The reason for the elevated glycolytic metabolism of cancer cells is still a matter of debate, but is believed to be for the production of key glycolytic intermediates involved in biosynthetic processes[131].

In cancer cells, elevated glycolytic flux is maintained through several mechanisms. Although HIF-1α is normally degraded under normoxic conditions, cancer cells have developed ways to bypass this regulation and create a pseudo-hypoxic state[136]. For example, mTORC1 increases the levels of HIF-1α through mRNA translation, which leads to increased transcription of its target genes in normoxia[33–35]. Other signaling pathways frequently activated in cancer can also increase flux through glycolysis. Akt can promote glucose uptake by increasing GLUT1 expression and activity, albeit through undefined mechanisms[137–139]. Alternatively, Akt can stimulate glycolytic flux through the phosphorylation of glycolytic enzymes[131,140]. By increasing flux through glycolysis, cancer cells increase the availability of key glycolytic intermediates that are used for biosynthetic processes.

1.3.4 TCA cycle

Through a series of oxidation reactions, the TCA cycle produces NADH and $FADH_2$, which donate electrons to oxidative phosphorylation. Unlike glycolysis, oxidative phosphorylation requires

oxygen as an electron acceptor to generate ATP. In addition to ATP production, the TCA cycle also provides key intermediates used for biosynthetic reactions (Figure 1.8)[141]. Citrate is an important TCA cycle intermediate, since ATP citrate lyase (ACLY) can convert cytosolic citrate to acetyl-CoA, a key substrate for the *de novo* synthesis of fatty acids and sterols. Likewise, oxaloacetate can be used to produce aspartate and arginine, while α-ketoglutarate can be used to produce glutamate and glutamine. These four amino acids can be incorporated into proteins, or, in the case of aspartate and glutamine, incorporated into the purine or pyrimidine ring during *de novo* nucleotide synthesis.

Several anaplerotic reactions exist to replenish the TCA cycle after intermediates are used up by biosynthetic processes. Carbons from glucose can be used to replenish the TCA cycle through the conversion of pyruvate into the TCA cycle intermediate oxaloacetate by pyruvate carboxylase. In certain cancer settings, glutamine has emerged as a major source of carbon and nitrogen, and can help maintain redox homeostasis[142]. After conversion of glutamine to glutamate in the cytosol, glutamate dehydrogenase produces α-ketoglutarate, which can enter the TCA cycle. Amino acids can be used in anaplerotic reactions to replenish the TCA cycle, which could contribute to their emerging role as an important source of biomass[143,144]. By refueling the TCA cycle through uptake of glucose, glutamine, and amino acids, cancer cells provide biosynthetic precursors that help support their rapid growth. Importantly, cancer cells can take up acetate[145–147], proteins[148], and lipids[149–152], although the cellular fate of these molecules is not fully understood.

1.3.5 Metabolic enzymes of the TCA cycle as tumor suppressors and oncogenes

Most of the work on cancer metabolism has identified broad metabolic changes driven by mutations in non-metabolic genes, like those that activate mTORC1. However, there are a few instances of cancer-causing mutations in metabolic enzymes, including fumarate hydratase (FH), succinate dehydrogenase (SDH), isocitrate dehydrogenase 1 (IDH1), and isocitrate dehydrogenase 2 (IDH2). Both FH and SDH are mitochondrial enzymes in the TCA cycle that catalyze the reversible conversion of

fumarate to malate and of succinate to fumarate, respectively. Mutations in FH have been identified in leiomyoma and renal cell carcinoma[153,154], whereas SDH mutations occur in paraganglioma or phaeochromocytoma[155]. These loss of function mutations cause a build-up in succinate and fumarate, which are thought to promote oncogenesis by inhibiting α-KG-dependent dioxigenases. In particular, they stabilize HIF-1α, through inhibition of HIF prolyl hydroxylases, and affect epigenetic gene regulation, through inhibition of DNA and histone demethylases[156–158]. However, the reasons for the tissue specificity of FH and SDH mutations have yet to be determined.

IDH1 and IDH2 catalyze the conversion of isocitrate to α-ketoglutarate, which generates NADPH (Figure 1.9A). Both enzymes function as homodimers, with IDH1 localized in the cytosol and IDH2 in the mitochondrial matrix. IDH3 is a tetrameric mitochondrial enzyme complex of the same function, but produces NADH instead of NADPH and is unrelated in structure to IDH1 and IDH2. Both IDH1 and IDH2 can also catalyze the reductive carboxylation of α-ketoglutarate to isocitrate in conditions of hypoxia or mitochondrial dysfunction (Figure 1.9B)[159–162]. The direction of the reversible isocitrate dehydrogenase reaction is determined by the ratio of citrate to α-ketoglutarate[163]. This substrate-level regulation of IDH1 allows it to respond to cellular needs by either producing NADPH or facilitating the flux of carbons from glutamine to citrate.

Unlike FH and SDH mutations which inhibit enzyme function, IDH mutations are neomorphic. IDH1 mutations occur in 70% of low grade gliomas and mutations in IDH1 or IDH2 occur in 20% of acute myeloid leukemias[164,165]. The vast majority of IDH1 mutations disrupt Arg132, whereas IDH2 mutations disrupt Arg140 or Arg172[165,166]. The neomorphic IDH mutations allow them to convert α-ketoglutarate to the oncometabolite D-2-hydroxyglutarate (D-2-HG) (Figure 1.9C)[167,168]. In normal cells, 2-HG is produced at low levels as a byproduct of metabolic reactions, and D/L-2-HG dehydrogenases (D2HGDH and L2HGDH) prevent a rise in 2-HG levels by converting D-2-HG or L-2-HG to α-ketoglutarate, respectively[169,170]. However, these two enzymes are unable to keep up with the rapid production of D-2-HG by the mutant IDH1 protein, resulting in very high levels of circulating and tumor

D-2-HG in patients with these mutations. The oncometabolite 2-HG was identified to be the driver of tumorigenesis, at least in part through its competitive binding to α-ketoglutarate-dependent enzymes[171,172]. D-2-HG increased cancer cell proliferation through its activation of α-ketoglutarate-dependent EGLN prolyl hydroxylases, which in turn destabilized HIF-1α[171]. Although most cancer cells benefit from HIF-1α activation, certain cell types including embryonic stem cells and brain tumor cells are actually inhibited by HIF-1α[171]. Similarly, D-2-HG produced by mutant IDH1 inhibits prolyl hydroxylases involved in collagen maturation, which leads to impaired basement membrane formation and ER stress[173]. Elevated 2-HG levels also promote dedifferentiation of cancer cells by reducing DNA methylation[174]. 2-HG inhibits TET methylcytosine dioxygenases, which convert 5-methylcytosine to 5-hydroxymethylcytosine, a required step for DNA demethylation. Analogously, elevated 2-HG levels inhibit the Jumanji family of histone demethylases[175,176]. These changes in DNA and histone methylation in response to 2-HG affect chromosome topology and cause the aberrant regulation of many genes[177]. With the identification of D-2-HG as a potent oncometabolite, pharmacological inhibitors of mutant IDH1 and 2 have been developed and are currently in clinical trials with promising results[178].

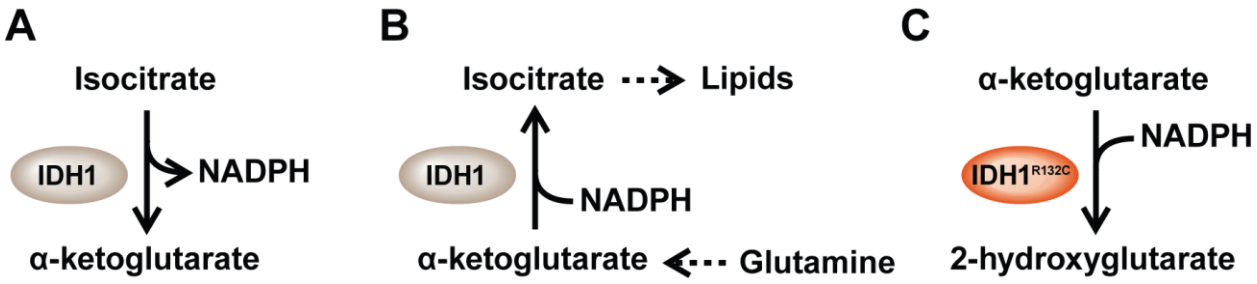

Figure 1.9. Metabolic functions of wild-type and mutant IDH1.

(**A**) Conversion of isocitrate to α-ketoglutarate by wild-type IDH1 produces cytosolic NADPH. (**B**) Certain conditions, including hypoxia and mitochondrial dysfunction, cause the wild-type IDH1 enzyme to catalyze the reductive carboxylation of α-ketoglutarate to isocitrate, which consumes NADPH. This reductive carboxylation reaction is thought to facilitate the flux of carbons from glutamine to *de novo* lipid synthesis. (**C**) Neomorphic mutations in IDH1, like the R132C mutation, cause the enzyme to produce the oncometabolite 2-hydroxyglutarate from α-ketoglutarate and NADPH.

1.4 SPECIFIC AIMS AND OVERVIEW OF THE DISSERTATION

Since the first observation of altered cellular metabolism in cancer cells in the 1920s, our understanding of tumor metabolism has greatly expanded. At the same time, a complex network of oncogenic signaling pathways has been uncovered. However, the intersection of cancer signaling pathways and cellular metabolism is still poorly understood. In particular, little is known about the regulation of lipid metabolism by oncogenic signaling pathways. In this dissertation, I uncover novel mechanisms through which mTORC1 and SREBP regulate cellular metabolism in cancer.

In Chapter 2, I establish a major mechanism through which two of the most commonly mutated oncogenes in cancer stimulate *de novo* lipid synthesis. Although lipid metabolism has been studied in great depth in the liver, much less is known about its regulation in cancer. I demonstrate that expression of oncogenic PI3K and K-Ras in isogenic breast epithelial cells or in a panel of genetically diverse breast cancer cell lines promotes lipid synthesis through mTORC1 and SREBP. Consistent with the regulation of SREBP by mTORC1, expression of these oncogenes activate both SREBP1 and SREBP2, which increase the expression of *de novo* lipogenesis enzymes. Elevated mTORC1 signaling in breast cancer patient tumor samples is also associated with high expression of SREBP targets *in vivo*. Importantly, depletion of SREBP proteins in breast cancer cells reduces the growth factor-independent proliferation of breast cancer cells and of oncogene-expressing epithelial cells. These data provide a mechanism through which oncogenic PI3K and K-Ras coordinate *de novo* lipid synthesis with the production of proteins and nucleotides by converging on mTORC1. In addition, I provide a mechanism to explain the increase in lipogenic enzymes and *de novo* lipogenesis observed in many cancers over the past 60 years.

In Chapter 3, I show that IDH1 transcription is activated by SREBP across a broad range of cancer lineages. Consistent with the role of SREBP targets in *de novo* lipogenesis, IDH1 facilitates *de novo* lipid synthesis from glutamine, but not from glucose or acetate. This regulation of IDH1 by SREBP provides a novel mechanism for the coordination of *de novo* lipid synthesis enzyme expression with

supporting processes that ensure sufficient carbon availability. Moreover, my data demonstrate that SREBP can activate expression of the oncogenic mutant-IDH1, and that it can regulate 2-HG production in IDH1-mutant cells. These results provide a novel regulatory mechanism for the production of 2-HG by mutant IDH1.

Together, my work highlights the important role of SREBP in different cancer settings through its control of canonical lipid synthesis genes as well as its new metabolic target, IDH1. I finish by discussing the therapeutic implications of these findings and by suggesting future experiments to address some of the unresolved aspects of my work.

1.5 REFERENCES

1 Laplante M, Sabatini DM. mTOR signaling in growth control and disease. *Cell* 2012; **149**: 274–293.

2 Dibble CC, Manning BD. Signal integration by mTORC1 coordinates nutrient input with biosynthetic output. *Nat Cell Biol* 2013; **15**: 555–564.

3 Howell JJ, Ricoult SJH, Ben-Sahra I, Manning BD. A growing role for mTOR in promoting anabolic metabolism. *Biochem Soc Trans* 2013; **41**: 906–912.

4 Sparks CA, Guertin DA. Targeting mTOR: prospects for mTOR complex 2 inhibitors in cancer therapy. *Oncogene* 2010; **29**: 3733–3744.

5 Sarbassov DD, Guertin DA, Ali SM, Sabatini DM. Phosphorylation and regulation of Akt/PKB by the rictor-mTOR complex. *Science* 2005; **307**: 1098–1101.

6 Dibble CC, Asara JM, Manning BD. Characterization of Rictor phosphorylation sites reveals direct regulation of mTOR complex 2 by S6K1. *Mol Cell Biol* 2009; **29**: 5657–5670.

7 Julien L-A, Carriere A, Moreau J, Roux PP. mTORC1-activated S6K1 phosphorylates Rictor on threonine 1135 and regulates mTORC2 signaling. *Mol Cell Biol* 2010; **30**: 908–921.

8 Lamming DW, Ye L, Katajisto P, Goncalves MD, Saitoh M, Stevens DM *et al.* Rapamycin-induced insulin resistance is mediated by mTORC2 loss and uncoupled from longevity. *Science* 2012; **335**: 1638–1643.

9 Sarbassov DD, Ali SM, Sengupta S, Sheen J-H, Hsu PP, Bagley AF *et al.* Prolonged rapamycin treatment inhibits mTORC2 assembly and Akt/PKB. *Mol Cell* 2006; **22**: 159–168.

10 Guertin DA, Sabatini DM. The pharmacology of mTOR inhibition. *Sci Signal* 2009; **2**: pe24.

11 Kang S a, Pacold ME, Cervantes CL, Lim D, Lou HJ, Ottina K *et al.* mTORC1 phosphorylation sites encode their sensitivity to starvation and rapamycin. *Science* 2013; **341**: 1236566.

12 Huang J, Manning BD. The TSC1–TSC2 complex: a molecular switchboard controlling cell growth. *Biochem J* 2008; **412**: 179–190.

13 Dibble CC, Elis W, Menon S, Qin W, Klekota J, Asara JM *et al.* TBC1D7 is a third subunit of the TSC1-TSC2 complex upstream of mTORC1. *Mol Cell* 2012; **47**: 535–546.

14 Mendoza MC, Er EE, Blenis J. The Ras-ERK and PI3K-mTOR pathways: cross-talk and compensation. *Trends Biochem Sci* 2011; **36**: 320–328.

15 Sengupta S, Peterson TR, Sabatini DM. Regulation of the mTOR Complex 1 Pathway by Nutrients, Growth Factors, and Stress. *Mol Cell* 2010; **40**: 310–322.

16 Inoki K, Li Y, Zhu T, Wu J, Guan K. TSC2 is phosphorylated and inhibited by Akt and suppresses mTOR signalling. *Nat Cell Bio* 2002; **4**: 648–657.

17 Manning BD, Tee AR, Logsdon MN, Blenis J, Cantley LC. Identification of the tuberous sclerosis

complex-2 tumor suppressor gene product tuberin as a target of the phosphoinositide 3-kinase/akt pathway. *Mol Cell* 2002; **10**: 151–162.

18 Menon S, Dibble CC, Talbott G, Hoxhaj G, Valvezan AJ, Takahashi H *et al.* Spatial control of the TSC complex integrates insulin and nutrient regulation of mTORC1 at the lysosome. *Cell* 2014; **156**: 771–785.

19 McKay MM, Morrison DK. Integrating signals from RTKs to ERK/MAPK. *Oncogene* 2007; **26**: 3113–3121.

20 Rodriguez-Viciana P, Warne PH, Dhand R, Vanhaesebroeck B, Gout I, Fry MJ *et al.* Phosphatidylinositol-3-OH kinase as a direct target of Ras. Nature. 1994; **370**: 527–532.

21 Kim E, Goraksha-Hicks P, Li L, Neufeld TP, Guan K-L. Regulation of TORC1 by Rag GTPases in nutrient response. *Nat Cell Biol* 2008; **10**: 935–945.

22 Sancak Y, Peterson TR, Shaul YD, Lindquist RA, Thoreen CC, Bar-Peled L *et al.* The Rag GTPases bind raptor and mediate amino acid signaling to mTORC1. *Science* 2008; **320**: 1496–1501.

23 Inoki K, Zhu T, Guan K-L. TSC2 mediates cellular energy response to control cell growth and survival. *Cell* 2003; **115**: 577–590.

24 Gwinn DM, Shackelford DB, Egan DF, Mihaylova MM, Mery A, Vasquez DS *et al.* AMPK phosphorylation of raptor mediates a metabolic checkpoint. *Mol Cell* 2008; **30**: 214–226.

25 Shaw RJ, Bardeesy N, Manning BD, Lopez L, Kosmatka M, DePinho R a *et al.* The LKB1 tumor suppressor negatively regulates mTOR signaling. *Cancer Cell* 2004; **6**: 91–99.

26 Semenza GL. Hydroxylation of HIF-1: oxygen sensing at the molecular level. *Physiology (Bethesda)* 2004; **19**: 176–82.

27 Brugarolas J, Lei K, Hurley RL, Manning BD, Reiling JH, Hafen E *et al.* Regulation of mTOR function in response to hypoxia by REDD1 and the TSC1/TSC2 tumor suppressor complex. *Genes Dev* 2004; **18**: 2893–2904.

28 DeYoung MP, Horak P, Sofer A, Sgroi D, Ellisen LW. Hypoxia regulates TSC1/2–mTOR signaling and tumor suppression through REDD1-mediated 14–3–3 shuttling. *Genes Dev* 2008; **22**: 239–251.

29 Menon S, Manning BD. Common corruption of the mTOR signaling network in human tumors. *Oncogene* 2008; **27**: S43–51.

30 Hosokawa N, Hara T, Kaizuka T, Kishi C, Takamura A, Miura Y *et al.* Nutrient-dependent mTORC1 association with the ULK1–Atg13–FIP200 complex required for autophagy. *Mol Biol Cell* 2009; **20**: 1981–1991.

31 Ganley IG, Lam DH, Wang J, Ding X, Chen S, Jiang X. ULK1·ATG13·FIP200 complex mediates mTOR signaling and is essential for autophagy. *J Biol Chem* 2009; **284**: 12297–12305.

32 Jung CH, Jun CB, Ro S-H, Kim Y-M, Otto NM, Cao J *et al.* ULK-Atg13-FIP200 complexes

mediate mTOR signaling to the autophagy machinery. *Mol Biol Cell* 2009; **20**: 1992–2003.

33 Düvel K, Yecies JL, Menon S, Raman P, Lipovsky AI, Souza AL *et al.* Activation of a metabolic gene regulatory network downstream of mTOR complex 1. *Mol Cell* 2010; **39**: 171–183.

34 Hudson CC, Liu M, Chiang GG, Otterness DM, Loomis DC, Kaper F *et al.* Regulation of Hypoxia-Inducible Factor 1 α Expression and Function by the Mammalian Target of Rapamycin. *Mol Cell Biol* 2002; **22**: 7004–7014.

35 Laughner E, Taghavi P, Chiles K, Patrick C, Semenza GL. HER2 (neu) Signaling Increases the Rate of Hypoxia-Inducible Factor 1 a (HIF-1 a) Synthesis : Novel Mechanism for HIF-1-Mediated Vascular Endothelial Growth Factor Expression. *Mol Cell Biol* 2001; **2**: 3995–4004.

36 Ma XM, Blenis J. Molecular mechanisms of mTOR-mediated translational control. *Nat Rev Mol Cell Biol* 2009; **10**: 307–318.

37 Jefferies HB, Reinhard C, Kozma SC, Thomas G. Rapamycin selectively represses translation of the 'polypyrimidine tract' mRNA family. *Proc Natl Acad Sci U S A* 1994; **91**: 4441–4445.

38 Meyuhas O. Synthesis of the translational apparatus is regulated at the translational level. *Eur J Biochem* 2000; **267**: 6321–6330.

39 Thoreen CC, Chantranupong L, Keys HR, Wang T, Gray NS, Sabatini DM. A unifying model for mTORC1-mediated regulation of mRNA translation. *Nature* 2012; **485**: 109–113.

40 Wang X, Li W, Williams M, Terada N, Alessi DR, Proud CG. Regulation of elongation factor 2 kinase by p90RSK1 and p70 S6 kinase. *EMBO J* 2001; **20**: 4370–4379.

41 Raught B, Peiretti F, Gingras A-C, Livingstone M, Shahbazian D, Mayeur GL *et al.* Phosphorylation of eucaryotic translation initiation factor 4B Ser422 is modulated by S6 kinases. *EMBO J* 2004; **23**: 1761–1769.

42 Chauvin C, Koka V, Nouschi A, Mieulet V, Hoareau-Aveilla C, Dreazen A *et al.* Ribosomal protein S6 kinase activity controls the ribosome biogenesis transcriptional program. *Oncogene* 2014; **33**: 474–483.

43 Mayer C, Grummt I. Ribosome biogenesis and cell growth: mTOR coordinates transcription by all three classes of nuclear RNA polymerases. *Oncogene* 2006; **25**: 6384–6391.

44 Amemiya-kudo M, Shimano H, Hasty AH, Yahagi N, Yoshikawa T, Matsuzaka T *et al.* Transcriptional activities of nuclear SREBP-1a , -1c , and -2 to different target promoters of lipogenic and cholesterogenic genes. *J Lipid Res* 2002; **43**: 1220–1235.

45 Shimomura I, Shimano H, Korn BS, Bashmakov Y, Horton JD. Nuclear sterol regulatory element-binding proteins activate genes responsible for the entire program of unsaturated fatty acid biosynthesis in transgenic mouse liver. *J Biol Chem* 1998; **273**: 35299–35306.

46 Ben-Sahra I, Hoxhaj G, Ricoult SJH, Asara JM, Manning BD. mTORC1 induces purine synthesis through control of the mitochondrial tetrahydrofolate cycle. *Science* 2016; **351**: 728–733.

47 Ben-Sahra I, Howell JJ, Asara JM, Manning BD. Stimulation of de novo pyrimidine synthesis by

growth signaling through mTOR and S6K1. *Science* 2013; **339**: 1323–1328.

48 Robitaille AM, Christen S, Shimobayashi M, Cornu M, Fava LL, Moes S *et al.* Quantitative phosphoproteomics reveal mTORC1 activates de novo pyrimidine synthesis. *Science* 2013; **339**: 1320–1323.

49 Ricoult SJH, Manning BD. The multifaceted role of mTORC1 in the control of lipid metabolism. *EMBO Rep* 2013; **14**: 242–251.

50 Porstmann T, Santos CR, Griffiths B, Cully M, Wu M, Leevers S *et al.* SREBP activity is regulated by mTORC1 and contributes to Akt-dependent cell growth. *Cell Metab* 2008; **8**: 224–236.

51 Horton JD, Goldstein JL, Brown MS. SREBPs: activators of the complete program of cholesterol and fatty acid synthesis in the liver. *J Clin Invest* 2002; **109**: 1125–1131.

52 Horton JD, Shah NA, Warrington JA, Anderson NN, Park SW, Brown MS *et al.* Combined analysis of oligonucleotide microarray data from transgenic and knockout mice identifies direct SREBP target genes. *Proc Natl Acad Sci USA* 2003; **100**: 12027–12032.

53 Shimano H, Horton JD, Shimomura I, Hammer RE, Brown MS, Goldstein JL. Isoform 1c of sterol regulatory element binding protein is less active than isoform 1a in livers of transgenic mice and in cultured cells. *J Clin Invest* 1997; **99**: 846–854.

54 Efeyan A, Zoncu R, Sabatini DM. Amino acids and mTORC1: From lysosomes to disease. *Trends Mol Med* 2012; **18**: 524–533.

55 Baenke F, Peck B, Miess H, Schulze A. Hooked on fat: the role of lipid synthesis in cancer metabolism and tumour development. *Dis Model Mech* 2013; **6**: 1353–1563.

56 Jeon T, Osborne TF. SREBPs: metabolic integrators in physiology and metabolism. *Trends Endocrinol Metab* 2011; **23**: 65–72.

57 Horton JD, Shimomura I, Brown MS, Hammer RE, Goldstein JL, Shimano H. Activation of cholesterol synthesis in preference to fatty acid synthesis in liver and adipose tissue of transgenic mice overproducing sterol regulatory element-binding protein-2. *J Clin Invest* 1998; **101**: 2331–2339.

58 Brown NF, Stefanovic-Racic M, Sipula IJ, Perdomo G. The mammalian target of rapamycin regulates lipid metabolism in primary cultures of rat hepatocytes. *Metabolism* 2007; **56**: 1500–1507.

59 Yecies JL, Zhang HH, Menon S, Liu S, Yecies D, Lipovsky AI *et al.* Akt stimulates hepatic SREBP1c and lipogenesis through parallel mTORC1-dependent and independent pathways. *Cell Metab* 2011; **14**: 21–32.

60 Li S, Brown MS, Goldstein JL. Bifurcation of insulin signaling pathway in rat liver: mTORC1 required for stimulation of lipogenesis, but not inhibition of gluconeogenesis. *Proc Natl Acad Sci USA* 2010; **107**: 3441–3446.

61 Li S, Ogawa W, Emi A, Hayashi K, Senga Y, Nomura K *et al.* Role of S6K1 in regulation of

SREBP1c expression in the liver. *Biochem Biophys Res Commun* 2011; **412**: 197–202.

62 Owen JL, Zhang Y, Bae S-H, Farooqi MS, Liang G, Hammer RE *et al.* Insulin stimulation of SREBP-1c processing in transgenic rat hepatocytes requires p70 S6-kinase. *Proc Natl Acad Sci USA* 2012; **109**: 16184–16189.

63 Wang BT, Ducker GS, Barczak AJ, Barbeau R, Erle DJ, Shokat KM. The mammalian target of rapamycin regulates cholesterol biosynthetic gene expression and exhibits a rapamycin-resistant transcriptional profile. *Proc Natl Acad Sci USA* 2011; **108**: 15201–15206.

64 Liu X, Yuan H, Niu Y, Niu W, Fu L. The role of AMPK/mTOR/S6K1 signaling axis in mediating the physiological process of exercise-induced insulin sensitization in skeletal muscle of C57BL/6 mice. *Biochim Biophys Acta* 2012; **1822**: 1716–1726.

65 Wan M, Leavens KF, Saleh D, Easton RM, Guertin DA, Peterson TR *et al.* Postprandial hepatic lipid metabolism requires signaling through Akt2 independent of the transcription factors FoxA2, FoxO1, and SREBP1c. *Cell Metab* 2011; **14**: 516–527.

66 Peterson TR, Sengupta SS, Harris TE, Carmack AE, Kang SA, Balderas E *et al.* mTOR complex 1 regulates lipin 1 localization to control the SREBP pathway. *Cell* 2011; **146**: 408–420.

67 Kenerson HL, Yeh MM, Yeung RS. Tuberous sclerosis complex-1 deficiency attenuates diet-induced hepatic lipid accumulation. *PLoS One* 2011; **6**: e18075.

68 Huang J, Manning BD. A complex interplay between Akt, TSC2 and the two mTOR complexes. *Biochem Soc Trans* 2009; **37**: 217–222.

69 Fleischmann M, Iynedjian PB. Regulation of sterol regulatory-element binding protein 1 gene expression in liver: role of insulin and protein kinase B/cAkt. *Biochem J* 2000; **349**: 13–17.

70 Leavens KF, Easton RM, Shulman GI, Previs SF, Birnbaum MJ. Akt2 is required for hepatic lipid accumulation in models of insulin resistance. *Cell Metab* 2009; **10**: 405–418.

71 Ono H, Shimano H, Katagiri H, Yahagi N, Sakoda H, Onishi Y *et al.* Hepatic Akt activation induces marked hypoglycemia, hepatomegaly, and hypertriglyceridemia with sterol regulatory element binding protein involvement. *Diabetes* 2003; **52**: 2905–2913.

72 Hagiwara A, Cornu M, Cybulski N, Polak P, Betz C, Trapani F *et al.* Hepatic mTORC2 activates glycolysis and lipogenesis through Akt, glucokinase, and SREBP1c. *Cell Metab* 2012; **15**: 725–738.

73 Bengoechea-Alonso MT, Ericsson J. A phosphorylation cascade controls the degradation of active SREBP1. *J Biol Chem* 2009; **284**: 5885–5895.

74 Luyimbazi D, Akcakanat A, McAuliffe PF, Zhang L, Singh G, Gonzalez-Angulo AM *et al.* Rapamycin regulates stearoyl CoA desaturase 1 expression in breast cancer. *Mol Cancer Ther* 2010; **9**: 2770–2784.

75 Guo D, Prins RRM, Dang J, Kuga D, Iwanami A, Soto H *et al.* EGFR signaling through an Akt-SREBP-1-dependent, rapamycin-resistant pathway sensitizes glioblastomas to antilipogenic therapy. *Sci Signal* 2009; **2**: ra82.

76 Huffman TA, Mothe-Satney I, Lawrence JC. Insulin-stimulated phosphorylation of lipin mediated by the mammalian target of rapamycin. *Proc Natl Acad Sci U S A* 2002; **99**: 1047–1052.

77 Han J, Li E, Chen L, Zhang Y, Wei F, Liu J *et al.* The CREB coactivator CRTC2 controls hepatic lipid metabolism by regulating SREBP1. *Nature* 2015; **524**: 243–246.

78 Sato R, Inoue J, Kawabe Y, Kodama T, Takano T, Maeda M. Sterol-dependent transcriptional regulation of sterol regulatory element-binding protein-2. *J Biol Chem* 1996; **271**: 26461–26464.

79 Amemiya-Kudo M, Shimano H, Yoshikawa T, Yahagi N, Hasty AH, Okazaki H *et al.* Promoter analysis of the mouse sterol regulatory element-binding protein-1c gene. *J Biol Chem* 2000; **275**: 31078–31085.

80 Vila-Bedmar R, Lorenzo M, Fernández-Veledo S. Adenosine 5'-monophosphate-activated protein kinase-mammalian target of rapamycin cross talk regulates brown adipocyte differentiation. *Endocrinology* 2010; **151**: 980–992.

81 Carnevalli LS, Masuda K, Frigerio F, Le Bacquer O, Um SH, Gandin V *et al.* S6K1 plays a critical role in early adipocyte differentiation. *Dev Cell* 2010; **18**: 763–774.

82 El-Chaâr D, Gagnon A, Sorisky A. Inhibition of insulin signaling and adipogenesis by rapamycin: effect on phosphorylation of p70 S6 kinase vs eIF4E-BP1. *Int J Obes Relat Metab Disord* 2004; **28**: 191–198.

83 Yeh WC, Bierer BE, McKnight SL. Rapamycin inhibits clonal expansion and adipogenic differentiation of 3T3-L1 cells. *Proc Natl Acad Sci U S A* 1995; **92**: 11086–11090.

84 Bell A, Grunder L, Sorisky A. Rapamycin inhibits human adipocyte differentiation in primary culture. *Obes Res* 2000; **8**: 249–254.

85 Gagnon A, Lau S, Sorisky A. Rapamycin-sensitive phase of 3T3-L1 preadipocyte differentiation after clonal expansion. *J Cell Physiol* 2001; **189**: 14–22.

86 Cho HJ, Park J, Lee HW, Lee YS, Kim JB. Regulation of adipocyte differentiation and insulin action with rapamycin. *Biochem Biophys Res Commun* 2004; **321**: 942–948.

87 Zhang HH, Huang J, Düvel K, Boback B, Wu S, Squillace RM *et al.* Insulin stimulates adipogenesis through the Akt-TSC2-mTORC1 pathway. *PLoS One* 2009; **4**: e6189.

88 Crino PB, Nathanson KL, Henske EP. The tuberous sclerosis complex. *N Engl J Med* 2006; **355**: 1345–1356.

89 Polak P, Cybulski N, Feige JN, Auwerx J, Rüegg MA, Hall MN. Adipose-specific knockout of raptor results in lean mice with enhanced mitochondrial respiration. *Cell Metab* 2008; **8**: 399–410.

90 Le Bacquer O, Petroulakis E, Paglialunga S, Poulin F, Richard D, Cianflone K *et al.* Elevated sensitivity to diet-induced obesity and insulin resistance in mice lacking 4E-BP1 and 4E-BP2. *J Clin Invest* 2007; **117**: 387–396.

91 Um SH, Frigerio F, Watanabe M, Picard F, Joaquin M, Sticker M *et al.* Absence of S6K1 protects against age- and diet-induced obesity while enhancing insulin sensitivity. *Nature* 2004; **431**: 200–

205.

92 Rosen ED, Hsu C-H, Wang X, Sakai S, Freeman MW, Gonzalez FJ *et al.* C/EBPalpha induces adipogenesis through PPARgamma: a unified pathway. *Genes Dev* 2002; **16**: 22–26.

93 Kim JE, Chen J. Regulation of peroxisome proliferator-activated receptor-gamma activity by mammalian target of rapamycin and amino acids in adipogenesis. *Diabetes* 2004; **53**: 2748–2756.

94 Yu W, Chen Z, Zhang J, Zhang L, Ke H, Huang L *et al.* Critical role of phosphoinositide 3-kinase cascade in adipogenesis of human mesenchymal stem cells. *Mol Cell Biochem* 2008; **310**: 11–18.

95 Laplante M, Horvat S, Festuccia WT, Birsoy K, Prevorsek Z, Efeyan A *et al.* DEPTOR cell-autonomously promotes adipogenesis, and its expression is associated with obesity. *Cell Metab* 2012; **16**: 202–212.

96 Morrisett JD, Abdel-Fattah G, Hoogeveen R, Mitchell E, Ballantyne CM, Pownall HJ *et al.* Effects of sirolimus on plasma lipids, lipoprotein levels, and fatty acid metabolism in renal transplant patients. *J Lipid Res* 2002; **43**: 1170–1180.

97 Kasiske BL, de Mattos A, Flechner SM, Gallon L, Meier-Kriesche HU, Weir MR *et al.* Mammalian target of rapamycin inhibitor dyslipidemia in kidney transplant recipients. *Am J Transpl* 2008; **8**: 1384–1392.

98 Zhang C, Yoon M-S, Chen J. Amino acid-sensing mTOR signaling is involved in modulation of lipolysis by chronic insulin treatment in adipocytes. *Am J Physiol Endocrinol Metab* 2009; **296**: E862–868.

99 Chakrabarti P, English T, Shi J, Smas CM, Kandror K V. Mammalian target of rapamycin complex 1 suppresses lipolysis, stimulates lipogenesis, and promotes fat storage. *Diabetes* 2010; **59**: 775–781.

100 Soliman GA, Acosta-Jaquez HA, Fingar DC. mTORC1 inhibition via rapamycin promotes triacylglycerol lipolysis and release of free fatty acids in 3T3-L1 adipocytes. *Lipids* 2010; **45**: 1089–1100.

101 Zhang Y, Goldman S, Baerga R, Zhao Y, Komatsu M, Jin S. Adipose-specific deletion of autophagy-related gene 7 (atg7) in mice reveals a role in adipogenesis. *Proc Natl Acad Sci U S A* 2009; **106**: 19860–19865.

102 Zechner R, Zimmermann R, Eichmann TO, Kohlwein SD, Haemmerle G, Lass A *et al.* FAT SIGNALS--lipases and lipolysis in lipid metabolism and signaling. *Cell Metab* 2012; **15**: 279–291.

103 Kumar A, Lawrence JCJ, Jung DY, Ko HJ, Keller SR, Kim JK *et al.* Fat cell-specific ablation of rictor in mice impairs insulin-regulated fat cell and whole-body glucose and lipid metabolism. *Diabetes* 2010; **59**: 1397–1406.

104 Wang H, Eckel RH. Lipoprotein lipase: from gene to obesity. *Am J Physiol Endocrinol Metab* 2009; **297**: E271–288.

105 Tory R, Sachs-Barrable K, Hill JS, Wasan KM. Cyclosporine A and Rapamycin induce in vitro cholesteryl ester transfer protein activity, and suppress lipoprotein lipase activity in human plasma.

Int J Pharm 2008; **358**: 219–223.

106 Blanchard P-G, Festuccia WT, Houde VP, St-Pierre P, Brûlé S, Turcotte V *et al.* Major involvement of mTOR in the PPARγ-induced stimulation of adipose tissue lipid uptake and fat accretion. *J Lipid Res* 2012; **53**: 1117–1125.

107 Peng T, Golub TR, Sabatini DM. The immunosuppressant rapamycin mimics a starvation-like signal distinct from amino acid and glucose deprivation. *Mol Cell Biol* 2002; **22**: 5575–5584.

108 Singh R, Kaushik S, Wang Y, Xiang Y, Novak I, Komatsu M *et al.* Autophagy regulates lipid metabolism. *Nature* 2009; **458**: 1131–1135.

109 Singh R, Xiang Y, Wang Y, Baikati K, Cuervo AM, Luu YK *et al.* Autophagy regulates adipose mass and differentiation in mice. *J Clin Invest* 2009; **119**: 3329–3339.

110 Aguilar V, Alliouachene S, Sotiropoulos A, Sobering A, Athea Y, Djouadi F *et al.* S6 kinase deletion suppresses muscle growth adaptations to nutrient availability by activating AMP kinase. *Cell Metab* 2007; **5**: 476–487.

111 Cunningham JT, Rodgers JT, Arlow DH, Vazquez F, Mootha VK, Puigserver P. mTOR controls mitochondrial oxidative function through a YY1-PGC-1alpha transcriptional complex. *Nature* 2007; **450**: 736–740.

112 Risson V, Mazelin L, Roceri M, Sanchez H, Moncollin V, Corneloup C *et al.* Muscle inactivation of mTOR causes metabolic and dystrophin defects leading to severe myopathy. *J Cell Biol* 2009; **187**: 859–874.

113 Bentzinger CF, Romanino K, Cloëtta D, Lin S, Mascarenhas JB, Oliveri F *et al.* Skeletal muscle-specific ablation of raptor, but not of rictor, causes metabolic changes and results in muscle dystrophy. *Cell Metab* 2008; **8**: 411–424.

114 Schieke SM, Phillips D, McCoy JP, Aponte AM, Shen R-F, Balaban RS *et al.* The mammalian target of rapamycin (mTOR) pathway regulates mitochondrial oxygen consumption and oxidative capacity. *J Biol Chem* 2006; **281**: 27643–27652.

115 Sengupta S, Peterson TR, Laplante M, Oh S, Sabatini DM. mTORC1 controls fasting-induced ketogenesis and its modulation by ageing. *Nature* 2010; **468**: 1100–1104.

116 Kim KK, Pyo S, Um SSH. S6 kinase 2 deficiency enhances ketone body production and increases peroxisome proliferator-activated receptor alpha activity in the liver. *Hepatology* 2012; **55**: 1727–1737.

117 Aggarwal D, Fernandez ML, Soliman GA. Rapamycin, an mTOR inhibitor, disrupts triglyceride metabolism in guinea pigs. *Metabolism* 2006; **55**: 794–802.

118 Sidiropoulos KG, Meshkani R, Avramoglu-Kohen R, Adeli K. Insulin inhibition of apolipoprotein B mRNA translation is mediated via the PI-3 kinase/mTOR signaling cascade but does not involve internal ribosomal entry site (IRES) initiation. *Arch Biochem Biophys* 2007; **465**: 380–388.

119 Nowak M, Helleboid-Chapman A, Jakel H, Martin G, Duran-Sandoval D, Staels B *et al.* Insulin-mediated down-regulation of apolipoprotein A5 gene expression through the phosphatidylinositol

3-kinase pathway: role of upstream stimulatory factor. *Mol Cell Biol* 2005; **25**: 1537–1548.

120 Streicher R, Kotzka J, Müller-Wieland D, Siemeister G, Munck M, Avci H *et al.* SREBP-1 mediates activation of the low density lipoprotein receptor promoter by insulin and insulin-like growth factor-I. *J Biol Chem* 1996; **271**: 7128–7133.

121 Ai D, Chen C, Han S, Ganda A, Murphy AJ, Haeusler R *et al.* Regulation of hepatic LDL receptors by mTORC1 and PCSK9 in mice. *J Clin Invest* 2012; **122**: 1262–1270.

122 Khamzina L, Veilleux A, Bergeron S, Marette A. Increased activation of the mammalian target of rapamycin pathway in liver and skeletal muscle of obese rats: possible involvement in obesity-linked insulin resistance. *Endocrinology* 2005; **146**: 1473–1481.

123 Newgard CB, An J, Bain JR, Muehlbauer MJ, Stevens RD, Lien LF *et al.* A branched-chain amino acid-related metabolic signature that differentiates obese and lean humans and contributes to insulin resistance. *Cell Metab* 2009; **9**: 311–326.

124 Hardie DG, Ross FA, Hawley SA. AMP-activated protein kinase: a target for drugs both ancient and modern. *Chem Biol* 2012; **19**: 1222–1236.

125 Hanahan D, Weinberg RA. Hallmarks of cancer: The next generation. *Cell* 2011; **144**: 646–674.

126 Medes G, Thomas A, Weinhouse S. Metabolism of neoplastic tissue. IV. A study of lipid synthesis in neoplastic tissue slices in vitro. *Cancer Res* 1953; **13**: 27–29.

127 Ookhtens M, Kannan R, Lyon I, Baker N. Liver and adipose tissue contributions to newly formed fatty acids in an ascites tumor. *Am J Physiol* 1984; **247**: R146–153.

128 Kuhajda FP. Fatty-acid synthase and human cancer: new perspectives on its role in tumor biology. *Nutrition* 2000; **16**: 202–208.

129 Kuhajda FP, Jennert K, Wood FD, Hennigart RA, Jacobs LB, Dick JD *et al.* Fatty acid synthesis : A potential selective target for antineoplastic therapy. *Proc Natl Acad Sci USA* 1994; **91**: 6379–6383.

130 Kuhajda FP, Piantadosi S, Pasternack G. Haptoglobin-related protein (Hpr) epitopes in breast cancer as a predictor of recurrence of the disease. *N Engl J Med* 1989; **636**: 636–641.

131 Lunt SY, Vander Heiden MG. Aerobic glycolysis: meeting the metabolic requirements of cell proliferation. *Annu Rev Cell Dev Biol* 2011; **27**: 441–464.

132 Warburg O. On respiratory impairment in cancer cells. *Science* 1956; **124**: 267–272.

133 Pasteur L. Expériences et vues nouvelles sur la nature des fermentations. *C R Acad Sci* 1861; **52**: 1260–1264.

134 Zu XL, Guppy M. Cancer metabolism: Facts, fantasy, and fiction. *Biochem Biophys Res Commun* 2004; **313**: 459–465.

135 Fantin VR, St-Pierre J, Leder P. Attenuation of LDH-A expression uncovers a link between glycolysis, mitochondrial physiology, and tumor maintenance. *Cancer Cell* 2006; **9**: 425–434.

136 Semenza GL. HIF-1: upstream and downstream of cancer metabolism. *Curr Opin Genet Dev* 2010; **20**: 51–56.

137 Barthel A, Okino ST, Liao J, Nakatani K, Li J, Whitlock JP *et al.* Regulation of GLUT1 gene transcription by the serine/threonine kinase Akt1. *J Biol Chem* 1999; **274**: 20281–20286.

138 Vander Heiden MG, Plas DR, Rathmell JC, Fox CJ, Harris MH, Thompson CB. Growth factors can influence cell growth and survival through effects on glucose metabolism. *Mol Cell Biol* 2001; **21**: 5899–5912.

139 Wieman HL, Wofford JA, Rathmell JC. Cytokine Stimulation Promotes Glucose Uptake via Phosphatidylinositol-3 Kinase/Akt Regulation of Glut1 Activity and Traffickin. *Mol Biol Cell* 2007; **18**: 1437–1446.

140 Elstrom RL, Bauer DE, Buzzai M, Karnauskas R, Harris MH, Plas DR *et al.* Akt stimultes aerobic glycolysis in cancer cells. . *Cancer Res* 2004; **64**: 3892–3899.

141 DeBerardinis RJ, Lum JJ, Hatzivassiliou G, Thompson CB. The biology of cancer: metabolic reprogramming fuels cell growth and proliferation. *Cell Metab* 2008; **7**: 11–20.

142 Daye D, Wellen KE. Metabolic reprogramming in cancer: Unraveling the role of glutamine in tumorigenesis. *Semin Cell Dev Biol* 2012; **23**: 362–369.

143 Hosios AM, Hecht VC, Danai L V., Johnson MO, Rathmell JC, Steinhauser ML *et al.* Amino acids rather than glucose account for the majority of cell mass in proliferating mammalian cells. *Dev Cell* 2016; **36**: 540–549.

144 Owen OE, Kalhan SC, Hanson RW. The key role of anaplerosis and cataplerosis for citric acid cycle function. *J Biol Chem* 2002; **277**: 30409–30412.

145 Comerford SA, Huang Z, Du X, Wang Y, Cai L, Witkiewicz AK *et al.* Acetate Dependence of Tumors. *Cell* 2014; **159**: 1591–1602.

146 Mashimo T, Pichumani K, Vemireddy V, Hatanpaa KJ, Singh DK, Sirasanagandla S *et al.* Acetate Is a Bioenergetic Substrate for Human Glioblastoma and Brain Metastases. *Cell* 2014; **159**: 1603–1614.

147 Schug ZT, Peck B, Jones DT, Zhang Q, Grosskurth S, Alam IS *et al.* Acetyl-CoA Synthetase 2 Promotes Acetate Utilization and Maintains Cancer Cell Growth under Metabolic Stress. *Cancer Cell* 2015; **27**: 57–71.

148 Commisso C, Davidson SM, Soydaner-Azeloglu RG, Parker SJ, Kamphorst JJ, Hackett S *et al.* Macropinocytosis of protein is an amino acid supply route in Ras-transformed cells. *Nature* 2013; **497**: 633–637.

149 Kamphorst JJ, Cross JR, Fan J, de Stanchina E, Mathew R, White EP *et al.* Hypoxic and Ras-transformed cells support growth by scavenging unsaturated fatty acids from lysophospholipids. *Proc Natl Acad Sci USA* 2013; **110**: 8882–8887.

150 Young RM, Ackerman D, Quinn ZL, Mancuso A, Gruber M, Liu L *et al.* Dysregulated mTORC1 renders cells critically dependent on desaturated lipids for survival under tumor-like stress. *Genes*

Dev 2013; **27**: 1115–1131.

151 Schoors S, Bruning U, Missiaen R, Queiroz KCS, Borgers G, Elia I *et al.* Fatty acid carbon is essential for dNTP synthesis in endothelial cells. *Nature* 2015; **520**: 192–197.

152 Nieman KM, Kenny H a, Penicka C V, Ladanyi A, Buell-Gutbrod R, Zillhardt MR *et al.* Adipocytes promote ovarian cancer metastasis and provide energy for rapid tumor growth. *Nat Med* 2011; **17**: 1498–503.

153 Toro JR, Nickerson ML, Wei M-H, Warren MB, Glenn GM, Turner ML *et al.* Mutations in the fumarate hydratase gene cause hereditary leiomyomatosis and renal cell cancer in families in North America. *Am J Hum Genet* 2003; **73**: 95–106.

154 Tomlinson IPM, Alam NA, Rowan AJ, Barclay E, Jaeger EEM, Kelsell D *et al.* Germline mutations in FH predispose to dominantly inherited uterine fibroids, skin leiomyomata and papillary renal cell cancer. *Nat Genet* 2002; **30**: 406–410.

155 Astuti D, Latif F, Dallol A, Dahia PLM, Douglas F, George E *et al.* Gene mutations in the succinate dehydrogenase subunit SDHB cause susceptibility to familial pheochromocytoma and to familial paraganglioma. *Am J Hum Genet* 2001; **69**: 49–54.

156 King A, Selak MA, Gottlieb E. Succinate dehydrogenase and fumarate hydratase: linking mitochondrial dysfunction and cancer. *Oncogene* 2006; **25**: 4675–4682.

157 Killian JK, Kim SY, Miettinen M, Smith C, Merino M, Tsokos M *et al.* Succinate dehydrogenase mutation underlies global epigenomic divergence in gastrointestinal stromal tumor. *Cancer Discov* 2013; **3**: 648–657.

158 Letouzé E, Martinelli C, Loriot C, Burnichon N, Abermil N, Ottolenghi C *et al.* SDH mutations establish a hypermethylator phenotype in paraganglioma. *Cancer Cell* 2013; **23**: 739–752.

159 Mullen AR, Hu Z, Shi X, Jiang L, Boroughs LK, Kovacs Z *et al.* Oxidation of alpha-ketoglutarate is required for reductive carboxylation in cancer cells with mitochondrial defects. *Cell Rep* 2014; **7**: 1679–1690.

160 Leonardi R, Subramanian C, Jackowski S, Rock CO. Cancer-associated isocitrate dehydrogenase mutations inactivate NADPH-dependent reductive carboxylation. *J Biol Chem* 2012; **287**: 14615–14620.

161 Wise DR, Ward PS, Shay JES, Cross JR, Gruber JJ, Sachdeva UM *et al.* Hypoxia promotes isocitrate dehydrogenase-dependent carboxylation of α-ketoglutarate to citrate to support cell growth and viability. *Proc Natl Acad Sci USA* 2011; **108**: 19611–19616.

162 Filipp F V, Scott DA, Ronai ZA, Osterman AL, Smith JW. Reverse TCA cycle flux through isocitrate dehydrogenases 1 and 2 is required for lipogenesis in hypoxic melanoma cells. *Pigment Cell Melanoma Res* 2012; **25**: 375–383.

163 Fendt S-M, Bell EL, Keibler MA, Olenchock BA, Mayers JR, Wasylenko TM *et al.* Reductive glutamine metabolism is a function of the α-ketoglutarate to citrate ratio in cells. *Nat Com* 2013; **4**: 2236.

164 The Cancer Genome Atlas Network -. Genomic and epigenomic landscapes of adult de novo acute myeloid leukemia. *N Engl J Med* 2013; **368**: 2059–2074.

165 Yan H, Parsons W, Jin G, McLendon R, Rasheed A, Yuan W *et al.* IDH1 and IDH2 mutations in gliomas. *N Engl J Med* 2009; **360**: 765–773.

166 Parsons DW, Jones S, Zhang X, Lin JC, Leary RJ, Angenendt P *et al.* An integrated genomic analysis of human glioblastoma multiforme. *Science* 2008; **321**: 1807–1812.

167 Dang L, White DW, Gross S, Bennett BD, Bittinger MA, Driggers EM *et al.* Cancer-associated IDH1 mutations produce 2-hydroxyglutarate. *Nature* 2009; **465**: 739–744.

168 Ward PS, Patel J, Wise DR, Abdel-Wahab O, Bennett BD, Coller HA *et al.* The common feature of leukemia-associated IDH1 and IDH2 mutations is a neomorphic enzyme activity converting a-ketoglutarate to 2-hydroxyglutarate. *Cancer Cell* 2010; **17**: 225–234.

169 Steenweg ME, Jakobs C, Errami A, van Dooren SJM, Adeva Bartolomé MT, Aerssens P *et al.* An overview of L-2-hydroxyglutarate dehydrogenase gene (L2HGDH) variants: a genotype-phenotype study. *Hum Mutat* 2010; **31**: 380–390.

170 Struys EA, Salomons GS, Achouri Y, Van Schaftingen E, Grosso S, Craigen WJ *et al.* Mutations in the D-2-hydroxyglutarate dehydrogenase gene cause D-2-hydroxyglutaric aciduria. *Am J Hum Genet* 2005; **76**: 358–360.

171 Koivunen P, Lee S, Duncan CG, Lopez G, Lu G, Ramkissoon S *et al.* Transformation by the (R)-enantiomer of 2-hydroxyglutarate linked to EGLN activation. *Nature* 2012; **483**: 484–488.

172 Losman J-A, Looper R, Koivunen P, Lee S, Schneider RK, McMahon C *et al.* (R)-2-Hydroxyglutarate is sufficient to promote leukemogenesis and its effects are reversible. *Science* 2013; **339**: 1621–1625.

173 Sasaki M, Knobbe CB, Itsumi M, Elia AJ, Harris IS, Chio IIC *et al.* D-2-hydroxyglutarate produced by mutant Idh1 perturbs collagen maturation and basement membrane function. *Genes Dev* 2012; **26**: 2038–2049.

174 Ito S, Shen L, Dai Q, Wu SC, Collins LB, Swenberg JA *et al.* Tet proteins can convert 5-methylcytosine to 5-formylcytosine and 5-carboxylcytosine. *Science* 2011; **333**: 1300–1303.

175 Lu C, Ward PS, Kapoor GS, Rohle D, Turcan S, Abdel-Wahab O *et al.* IDH mutation impairs histone demethylation and results in a block to cell differentiation. *Nature* 2012; **483**: 474–478.

176 Xu W, Yang H, Liu Y, Yang Y, Wang PP, Kim S-H *et al.* Oncometabolite 2-hydroxyglutarate is a competitive inhibitor of α-ketoglutarate-dependent dioxygenases. *Cancer Cell* 2011; **19**: 17–30.

177 Flavahan WA, Drier Y, Liau BB, Gillespie SM, Venteicher AS, Stemmer-Rachamimov AO *et al.* Insulator dysfunction and oncogene activation in IDH mutant gliomas. *Nature* 2015; **529**: 110–114.

178 Rohle D, Popovici-Muller J, Palaskas N, Turcan S, Grommes C, Campos C *et al.* An inhibitor of mutant IDH1 delays growth and promotes differentiation of glioma cells. *Science* 2013; **340**: 626–630.

CHAPTER 2:

ONCOGENIC PI3K AND K-RAS STIMULATE *DE NOVO* LIPID SYNTHESIS THROUGH mTORC1 AND SREBP

This chapter is adapted from:

Ricoult SJH, Yecies JL, Ben-Sahra I, Manning BD. Oncogenic PI3K and K-Ras stimulate *de novo* lipid synthesis through mTORC1 and SREBP. *Oncogene* 2016; **35**:1250-1260.

2.1 ABSTRACT

An enhanced capacity for *de novo* lipid synthesis is a metabolic feature of most cancer cells that distinguishes them from their cells of origin. However, the mechanisms through which oncogenes alter lipid metabolism are poorly understood. We find that expression of oncogenic $PI3K^{H1047R}$ or $K\text{-}Ras^{G12V}$ in breast epithelial cells is sufficient to induce *de novo* lipogenesis, and this occurs through the convergent activation of the mechanistic target of rapamycin complex 1 (mTORC1) downstream of these common oncogenes. Oncogenic stimulation of mTORC1 signaling in this isogenic setting or a panel of eight breast cancer cell lines leads to activation of the sterol regulatory element binding proteins (SREBP1 and SREBP2), which are required for oncogene-induced lipid synthesis. The SREBPs are also required for the growth factor-independent growth and proliferation of oncogene-expressing cells. Finally, we find that elevated mTORC1 signaling is associated with increased mRNA and protein levels of canonical SREBP targets in primary human breast cancer samples. These data suggest that the mTORC1-SREBP pathway is a major mechanism through which common oncogenic signaling events induce *de novo* lipid synthesis to promote aberrant growth and proliferation of cancer cells.

2.2 INTRODUCTION

The genetic events underlying cancer development are accompanied by the induction of a metabolic program, distinct from most normal cells, that facilitates the uncontrolled growth of cancer cells. However, the key molecular connections between the most commonly activated oncogenic pathways in human cancers and this metabolic reprogramming are poorly defined. One long-known, but poorly understood, alteration in cellular metabolism frequently observed in cancer is the activation of *de novo* lipid synthesis[1], a process that only minimally contributes to the lipid content of normal non-proliferating cells. While normal cells generally rely on the uptake of lipids from the circulation, cancer

cells often acquire the ability to make their own, which is believed to be required to meet an increased demand for membrane biogenesis during cell proliferation[2,3].

The expression of genes encoding lipogenic enzymes, including acetyl-CoA carboxylase (*ACACA*), fatty acid synthase (*FASN*) and steroyl-CoA desaturase (*SCD*), has been found to be elevated in a variety of cancers[2,4,5]. In normal, lipid-producing tissues, such as the liver, these and most other enzymes involved in *de novo* sterol and fatty acid synthesis are induced by the SREBP family of transcription factors, SREBP1 and 2[6]. The SREBPs are produced as inactive precursors, which reside as transmembrane proteins in the endoplasmic reticulum (ER)[7–11]. When sterols or unsaturated fatty acids become depleted, the membrane-bound SREBP traffics to the Golgi, where it is sequentially cleaved by two site-specific proteases. The N-terminal fragment of SREBP, representing the active transcription factor (referred to as the mature form), is released and can enter the nucleus to activate target genes with SREs in their promoters. Through transcriptional activation of its lipogenic target genes, SREBP is able to induce the *de novo* synthesis of sterols, fatty acids, and their neutral lipid derivatives.

In addition to its regulation by lipids, SREBP isoform processing and activation have been found to be stimulated by insulin and growth factor signaling through mTORC1[12]. Activation of mTORC1 signaling induces SREBP activation in cell culture models and in the liver, leading to the accumulation of mature processed SREBP, expression of SREBP target genes, and increased *de novo* lipid synthesis[13–16]. The molecular mechanism by which mTORC1 activates SREBP remains unknown but likely involves multiple direct downstream targets. Independent groups have shown that mTORC1 can promote SREBP processing through the mTORC1-regulated protein kinase S6K1 in various settings[13,17–20]. 4E-BP1, an inhibitor of cap-dependent translation that is blocked by mTORC1 signaling, has also been implicated in the regulation of SREBP downstream of mTORC1[18,21]. In addition, phosphorylation of the phosphatidic acid phosphatase Lipin1 by mTORC1 has been shown to promote accumulation of mature SREBP in the nucleus through an unknown mechanism[22]. An important feature of mTORC1 signaling that influences studies on its regulation of SREBP is that the downstream targets of mTORC1 are differentially sensitive

to mTOR inhibitors. S6K1 phosphorylation and activation is completely inhibited by rapamycin, while 4E-BP1 and Lipin1 phosphorylation and inhibition are only partially sensitive to rapamycin[22–24]. As such, it is useful to use both rapamycin, an allosteric inhibitor of mTORC1, and mTOR kinase inhibitors, which completely inhibit both mTORC1 and mTORC2, in such studies.

In normal cells and tissues, mTORC1 activity is tightly controlled by growth factors through the convergence of multiple upstream signaling pathways on a protein complex comprised of the tuberous sclerosis complex (TSC) tumor suppressors, TSC1 and TSC2, and the TBC1D7 protein (the TSC complex)[25,26]. The TSC complex acts as a GTPase-activating protein (GAP) for Rheb, a Ras-related small G-protein that potently activates mTORC1 when it is GTP-bound[27]. While loss of function mutations affecting the TSC complex lead to growth factor-independent activation of mTORC1 and are the genetic cause of the tumor syndromes TSC and lymphangioleiomyomatosis (LAM)[28], mutations in the complex components are more rare in sporadic cancers. Nonetheless, aberrant activation of mTORC1 is a frequent event in human cancers, across nearly all lineages[29]. Two of the most commonly activated pathways in cancer, the PI3K-Akt and the Ras-Erk pathways, converge on the TSC complex to activate mTORC1[30–34].

Here, we find that expression of oncogenic PI3K or K-Ras in normal cells induces *de novo* lipogenesis and that inhibition of mTORC1 or depletion of the SREBPs blocks this induction. We also find that this is a primary mechanism driving lipid synthesis in a panel of genetically-defined breast cancer lines. We find that depletion of the SREBPs hinders the viability and growth of cells with oncogenic activation of mTORC1 signaling. Lastly, we show an association between mTORC1 activation and expression of lipogenic targets of SREBP in primary human breast cancer samples. These findings identify the mTORC1-SREBP pathway as a major molecular link between oncogenic signaling events and the common increase in *de novo* lipid synthesis observed in human cancers.

2.3 MATERIALS AND METHODS

Cell culture

All cell lines were obtained from ATCC and maintained in RPMI-1640 with 10% fetal bovine serum (FBS) at 37°C and 5% CO_2. Lipid-reduced FBS was made by mixing with fumed silica (20 mg/ml) (S5130, Sigma) for 3 hours. Pools of MCF10A cells stably expressing pBabe-Puro-vector, -PI3KCA^{H1047R} (Addgene #12524)[35], or K-Ras^{G12V} (Addgene #9052), via retroviral transduction, were selected and cultured in DMEM-F12 with 5% horse serum, EGF (20 ng/ml), hydrocortisone (0.5 mg/ml), cholera toxin (100 ng/ml), Insulin (10 μg/ml), and puromycin (1 μg/ml) at 37°C and 5% CO_2. Rapamycin (553210, Calbiochem), PP242 (4257, Tocris), and Torin1 (4247, R&D Systems) were used to inhibit mTOR.

Plasmids and siRNAs

The pLKO mouse SREBP2 plasmid (Addgene #32018,) was a gift from David Sabatini[22]. SREBP2 shRNAs from the RNAi consortium were used: shSREBP2#1 (TRCN0000020665), shSREBP2#2 (TRCN0000020667), shSREBP2#3 (TRCN0000020666), shSREBP2#4 (TRCN0000020668). All siRNA experiments used ON-TARGET-plus SMARTpool siRNAs (30 nM; Dharmacon/GE) transfected using Lipofectamine RNAiMAX (Invitrogen), according to the manufacturer's instructions for reverse transfection. For Raptor and Rictor knockdowns, siRNAs were transfected on two consecutive days to achieve efficient knockdown. Each siRNA and shRNA targeting SREBP2 recognized a unique sequence in *SREBF2*, with at least 5 mismatches toward any sequence in *SREBF1*, and vice versa.

Immunoblotting

Cells were lysed in NP-40 buffer (40 mM HEPES, pH 7.4; 400 mM NaCl; 1 mM EDTA, pH 8.0; 1% NP-40 (CA-630, Sigma); 5% glycerol; 10 mM pyrophosphate; 10 mM β-glycerophosphate; 50 mM NaF; 0.5 mM orthovanadate) containing Protease Inhibitor Cocktail (Sigma) and 1 mM DTT. Nuclear

isolation was performed with a Nuclear Extract Kit (40010, Active Motif), with 10 μg/ml ALLN (208719, Millipore) treatment 20 min prior to isolation, and ALLN added to the hypotonic and lysis buffers. The nuclear fraction was washed with hypotonic buffer prior to lysis.

Antibodies used for immunoblots recognized SREBP1 (sc-8984, Santa Cruz), SREBP2 precursor and processed C-terminus (557037, BD), SREBP2 mature N-terminus (30682, Abcam), Actin (A5316, Sigma), and from Cell Signaling Technologies: ACC1 (3676), FASN (3180), SCD (2438), HA (2367), P-Akt-T308 (9275), P-Akt-S473 (4051), Total-Akt (4691), P-S6K1-T389 (9234), Total-S6K1 (2708), P-S6-S240/S244 (2215), Total-S6 (2217), 4E-BP1 (9644), Ras (3965), P-Erk1/2-T202/Y204 (9106), Total-Erk1/2 (9102), Lamin A/C (2032), Histone H3 (4499).

De novo lipid synthesis

Cells grown in 6-well plates were serum starved 16-18 h, with 5 μCi/mL 1-^{14}C-acetate (NEC084H001MC, Perkin Elmer) added to the media for the final 4 h. Cells were washed twice with PBS prior to lysis in 0.5% Triton X-100. Lipids were extracted with 2:1 (v/v) chloroform/methanol (500 μl) followed by low-speed centrifugation (1000 rpm, 20 min). ^{14}C-labeled lipid in the denser fraction was quantified in duplicate samples using a LS6500 scintillation counter (Beckman Coulter), and normalized to protein concentration for MCF10a and cell number for breast cancer cells.

mRNA expression analysis

RNA was isolated using the RNeasy Mini Kit (Qiagen). cDNA was synthesized using the Superscript III First Strand Synthesis System (Invitrogen) and quantified using SYBR-Green for qRT-PCR (Applied Biosystems 7300 Real Time PCR System). Each condition was run in triplicate and normalized to *RPLP0* (F-cagattggctacccaactgtt, R-gggaaggtgtaatccgtctcc) mRNA levels. Primer sequences: *SREBF1* (F-tgcattttctgacacgcttc; R-ccaagctgtacaggctctcc), *SREBF2* (F-tggcttctctccctactcca, R-gagaggcacaggaaggtgag), *ACACA* (F-atgtctggcttgcacctagta, R-ccccaaagcgagtaacaaattct), *FASN* (F-

aaggacctgtctaggtttgatgc, R-tggcttcataggtgacttcca), *SCD* (F-cccagctgtcaaagagaagg, R-caagaaagtggcaacgaaca).

Cell proliferation, size and death

Cell number and size were measured in solution, following trypsinization, using a Z2 Coulter Counter (Beckman Coulter). Medium was replaced every 24 h. For cell death, adherent and non-adherent cells were combined, washed in PBS, and resuspended in annexin buffer (10 mM HEPES; 140 mM NaCl; 2.5 mM $CaCl_2$, pH 7.4) prior to incubation with Annexin-V/FITC conjugate (A13199, Invitrogen) for 15 min. Cells for each sample were resuspended in annexin buffer containing propidium iodide (PI; P4170, Sigma) before analyzing by flow cytometry (FACS Calibur, BD). Percent cell death was calculated by dividing the sum of the cells positive for PI, Annexin-V, or both by the total number of cells.

Analysis of TCGA data

Reverse-phase protein array and gene expression data were downloaded from cBioPortal[36–38]. Samples with P-S6-S240 levels greater than one standard deviation above average were classified as "High Phospho-S6", whereas those greater than one standard deviation below average were classified as "Low Phospho-S6".

Breast cancer patient lysate arrays

Breast cancer patient lysate arrays (PMA2-001-L, Protein Biotechnologies) were blotted following the manufacturer's instructions. Colloidal gold staining (170-6527, BioRad) was used to determine total protein content. Signal from 40 of 55 samples was detectable for FASN and 37 of 55 samples for SCD. Dot intensity was measured with ImageJ[39]. "High Phospho-S6" samples had a fold change in P-S6 levels between the tumor and normal tissues greater than $\log_2(0.5)$, whereas "Low Phospho-S6" were those lower than $\log_2(-0.5)$.

Statistical analysis

All data were analyzed with GraphPad Prism. P-values were calculated by an unpaired two-tailed Student's t-test, where appropriate.

2.4 RESULTS

2.4.1 Oncogenic PI3K and K-Ras are sufficient to induce *de novo* lipid synthesis and do so in an mTORC1-dependent manner

Since both the PI3K and Ras pathways are frequently activated in cancer and converge to activate mTORC1 (Figure 2.1A), we asked whether activating mutants commonly found in human cancer ($PIK3CA^{H1047R}$ and $K\text{-}Ras^{G12V}$) were sufficient to stimulate lipogenesis. We generated an isogenic set of cell lines stably expressing either empty vector or one of these two oncogenic mutants in MCF10a cells, a non-transformed human breast epithelium cell line. The oncogene-expressing cells exhibited growth-factor independent activation of mTORC1, as detected by phosphorylation of its downstream targets, S6K1 and 4E-BP1, and the S6K target ribosomal S6, which were sensitive to rapamycin and the mTOR kinase inhibitor Torin1 (Figure 2.1B). Consistent with these oncogenes activating mTORC1 primarily through distinct pathways, the $PIK3CA^{H1047R}$ cells displayed activated Akt but not Erk, whereas the $K\text{-}Ras^{G12V}$ cells had activated Erk with minimal activation of Akt. To measure specific effects on *de novo* lipid synthesis, cells were labeled with ^{14}C-acetate in order to avoid established effects of these oncogenes on glucose uptake. Importantly, both oncogenic PI3K and K-Ras stimulated an increase in the incorporation of acetate into lipid (Figure 2.1C). Rapamycin significantly reduced this oncogene-induced lipogenesis, and treatment with two structurally distinct mTOR kinase inhibitors[23,24], PP242 [23]or Torin1, led to a further reduction.

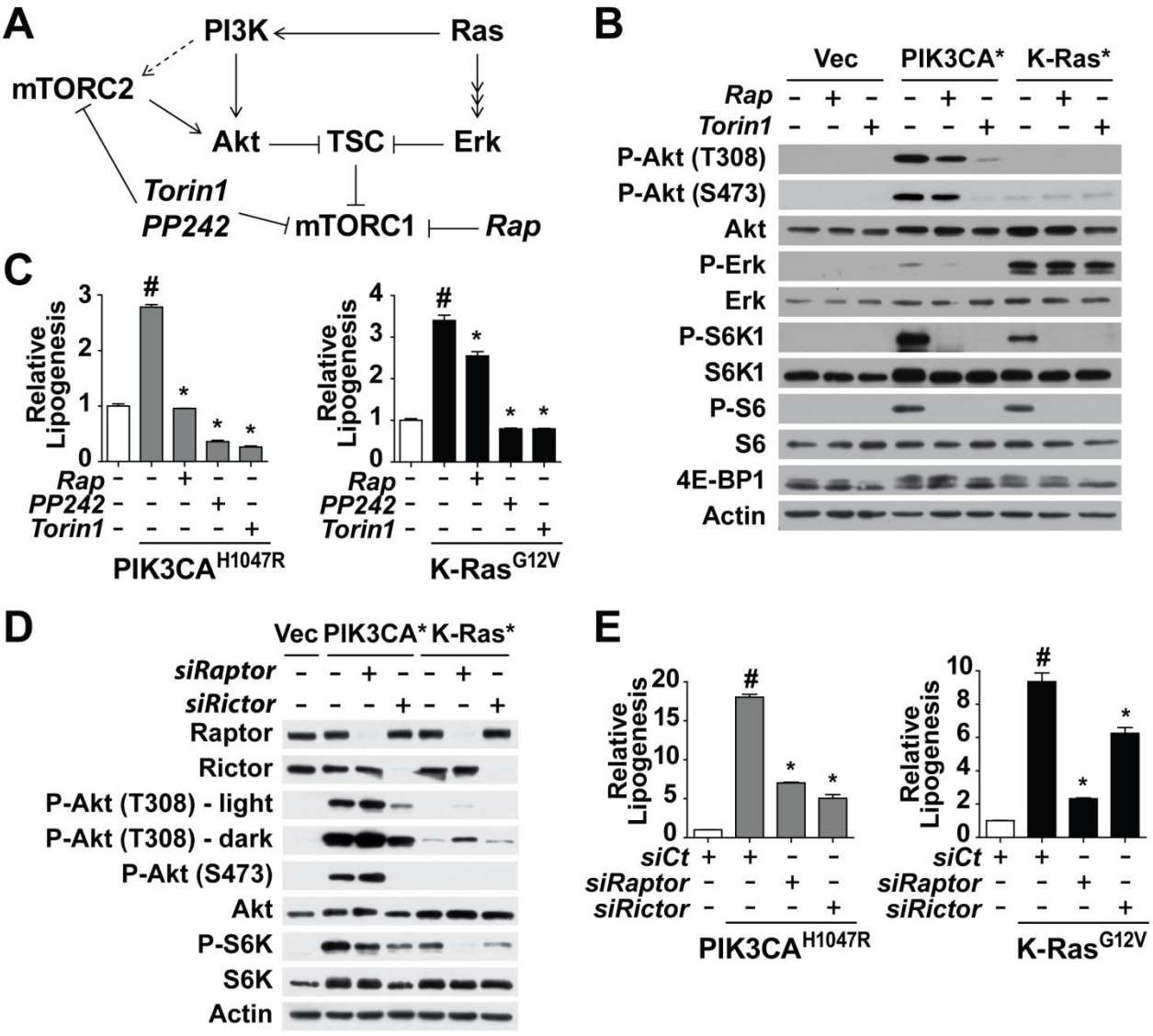

Figure 2.1. Oncogenic PI3K and K-Ras promote *de novo* lipogenesis through mTORC1 activation.

(**A**) Model of the convergent regulation of mTORC1 through the PI3K and K-Ras pathways and the action of different classes of mTOR inhibitors. (**B**) Growth-factor independent activation of mTORC1 signaling by oncogenes. MCF10a cells stably expressing empty vector, PIK3CA^{H1047R}, or K-Ras^{G12V} were serum starved for 16 h in the presence of vehicle, rapamycin (20 nM), or Torin1 (250 nM). Immunoblots are of proteins and phosphorylated (P) proteins in the cytosolic fraction, with phosphorylation of 4E-BP1 detected by mobility shift.

Figure 2.1 (Continued)

(**C**) Oncogene and mTORC1-dependent induction of *de novo* lipid synthesis in MCF10a cells. Incorporation of 1-[14C]-acetate into the lipid fraction was measured in the cells from **B** in the presence of vehicle, rapamycin (20 nM), PP242 (2.5 μM), or Torin1 (250 nM). Representative data are shown as mean ± s.e.m. relative to vector-expressing cells (white bar), n=4. (**D**,**E**) Effects of Raptor and Rictor depletion on signaling and *de novo* lipogenesis. The cells in **B** were transfected with siRNAs targeting Raptor or Rictor. Cells were lysed 72 h post-transfection following 16 h serum starvation, to analyze signaling (**D**) or lipid synthesis, as measured and presented in **C** (**E**). Representative data are shown as mean ± s.e.m. relative to vector-expressing cells (white bar), n=3. (**C,E**) #P-value < 0.05 compared to vector-expressing cells; *P-value < 0.05 compared to vehicle-treated cells expressing the same oncogene.

To determine whether the effects of mTOR inhibitors on the induction of lipid synthesis by oncogenic PI3K and K-Ras were through inhibition of mTORC1 or mTORC2 (Figure 2.1A), siRNAs targeting either mTORC1, through Raptor knockdown, or mTORC2, through Rictor knockdown, were introduced into these cells (Figure 2.1D). In both oncogene-expressing lines, Raptor knockdown decreased S6K1 phosphorylation. Rictor knockdown had the strongest effect on S6K1 phosphorylation in the $PIK3CA^{H1047R}$ cells, where the mTORC2 target Akt lies upstream of mTORC1. Importantly, *de novo* lipogenesis in the oncogene-expressing cells mirrored effects of these siRNAs on mTORC1 signaling, with Raptor knockdown inhibiting in both lines and Rictor knockdown having more pronounced effects in the $PIK3CA^{H1047R}$ cells (Figure 2.1E). Therefore, oncogenic PI3K and K-Ras are sufficient to stimulate *de novo* lipid synthesis and do so through the common downstream activation of mTORC1.

2.4.2 Activation of SREBP downstream of mTORC1 is required for oncogene-induced lipid synthesis

Given that mTORC1 has been found previously to stimulate *de novo* lipid synthesis through activation of the SREBP transcription factors in other settings[13,14], we assessed the effects of oncogenic PI3K and K-Ras on SREBP isoforms and canonical gene targets. Following cellular fractionation to detect the cytosolic, inactive precursor (P) and nuclear, active mature (M) forms of SREBP1 and 2, we found that levels of the SREBP1 precursor were modestly elevated in the oncogene-expressing lines, whereas the SREBP2 precursor was increased only in the oncogenic K-Ras cells (Figure 2.2A). These increases matched closely with differential changes in the transcript levels of the genes encoding these proteins, *SREBF1* and *SREBF2* (Figure 2.2B). Consistent with previous findings suggesting that mTORC1 signaling promotes the processing of SREBP[13,20], the nuclear mature forms of both SREBP1 and 2 were elevated in the oncogene-expressing cells, and treatment with either rapamycin or Torin1 blocked this increase (Figure 2.2A). The oncogene-mediated activation of SREBP was reflected in elevated transcript (Figure 2.2B) and protein (Figure 2.2A) levels of three canonical SREBP targets,

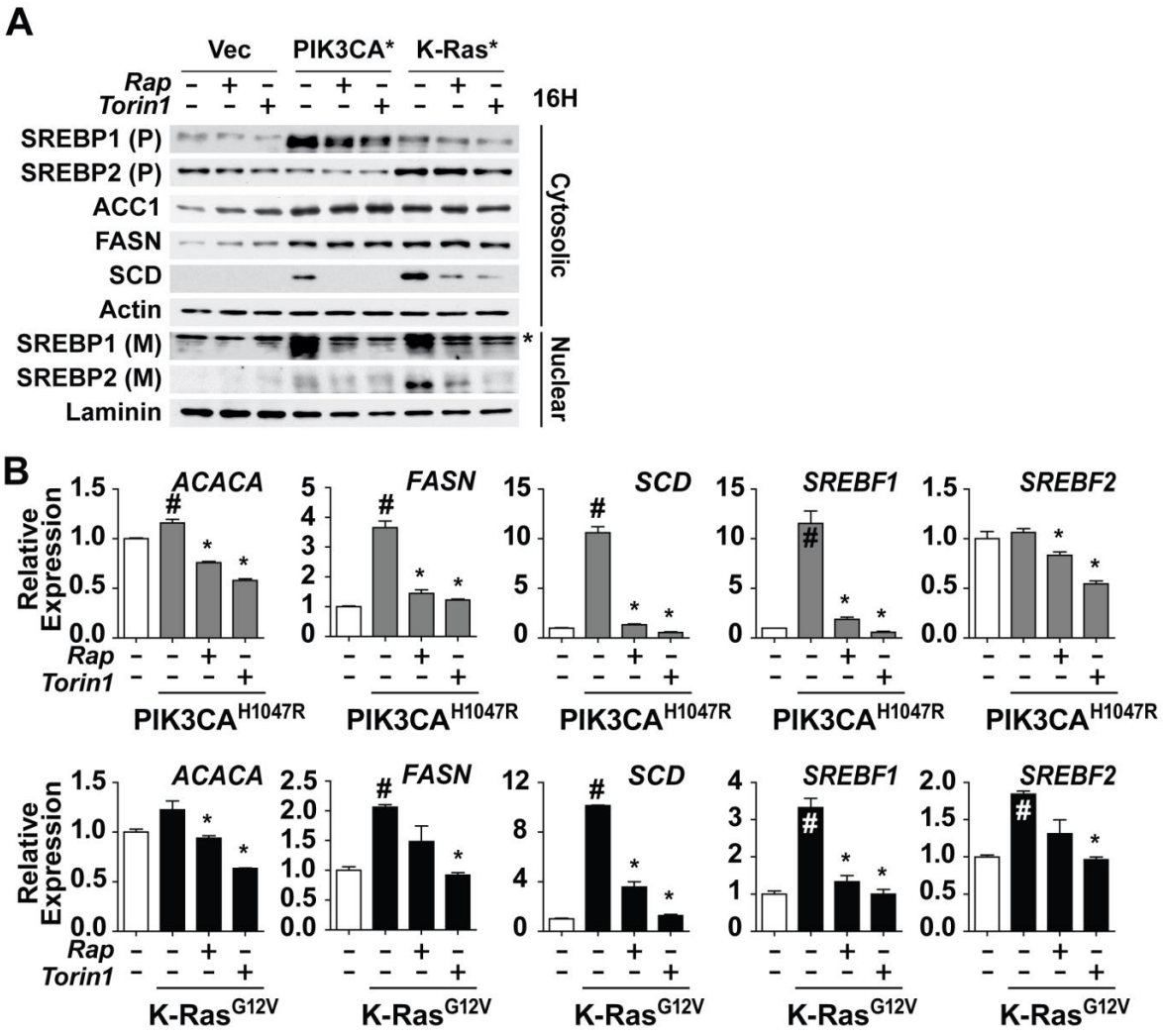

Figure 2.2. mTORC1 is required for activation of SREBP1 and SREBP2 by PI3K and K-Ras.

(**A**) Regulation of SREBP isoforms by oncogenes and mTORC1. MCF10a cells stably expressing empty vector, PIK3CA^{H1047R},or K-Ras^{G12V} were serum starved for 16 h in the presence of vehicle, rapamycin (20 nM), or Torin1 (250 nM). Cytosolic and nuclear fractions were collected to detect the cytosolic precursor (P) and the nuclear mature (M) forms of SREBP1 and 2. * denotes a cross-reacting band. (**B**) Oncogene and mTORC1-dependent induction of *ACACA*, *FASN*, *SCD*, *SREBF1*, and *SREBF2* gene expression. RNA was isolated from cells treated as in **A** for analysis by qRT-PCR. Representative data are shown as mean ± s.e.m. relative to vector-expressing cells (white bar), n=2. # P-value < 0.05 compared to vector-expressing cells; * P-value < 0.05 compared to vehicle-treated cells expressing the same oncogene.

ACC1, FASN and SCD. While the transcript levels of ACC1, FASN and SCD were all sensitive to mTORC1 inhibitors, only SCD was decreased at the protein level following overnight treatment, reflecting the long-lived nature of the ACC1 and FASN proteins[40,41].

To determine whether the oncogene-induced increase in expression of lipogenic genes and stimulation of *de novo* lipid synthesis were through this mTORC1-dependent activation of SREBP isoforms, we used siRNAs to knock down SREBP1, SREBP2, or both. Consistent with redundant regulation of lipogenic gene targets by SREBP1 and 2, the double knockdown resulted in the strongest decrease in FASN and SCD protein (Figure 2.3A) and transcript levels (Figure 2.3B). While the transcript levels of ACC1 were affected by SREBP knockdown, especially in the PIK3CA^{H1047R} cells (Figure 2.3B), ACC1 protein levels were largely unaffected (Figure 2.3A). As observed in previous studies[13,42,43], we found that SREBP2 knockdown, with siRNA sequences that do not directly target SREBP1, decreases *SREBF1* transcript levels (Figure 2.3B), and this is also reflected in SREBP1 protein levels (Figure 2.3A). This cross-regulation likely reflects the presence of functional SREs in the *SREBF1* gene promoter[44]. Importantly, as with mTORC1 inhibitors, oncogene-induced *de novo* lipogenesis was eliminated with siRNA-mediated knockdown of SREBP isoforms, with SREBP2 playing the dominant role in these cells (Figure 2.3C).

Given that treatment with mTOR inhibitors for 16 h is sufficient to block oncogene-driven lipogenesis (Figure 2.1C), but only SCD protein levels, not ACC1 or FASN, are decreased in this time frame (Figure 2.2A), we determined whether inhibition of SCD could explain these inhibitory effects on lipogenesis. Indeed, siRNA-mediated knockdown of SCD significantly reduced *de novo* lipogenesis, with a more pronounced effect in the PI3K^{H1047R} cells, where the decrease mimicked SREBP1/2 knockdown (Figures 2.3D and 2.3E). Therefore, oncogenic PI3K and K-Ras can stimulate lipogenesis through the mTORC1-mediated activation of SREBP and its subsequent induction of SCD, the enzyme responsible for generating the mono-unsaturated fatty acids (MUFAs) prevalent in membrane phospholipids.

Figure 2.3. SREBP and SCD are required for activation of *de novo* lipogenesis by PI3K and K-Ras. (**A**-**C**) Effects of SREBP1 and SREBP2 knockdown on SREBP targets and *de novo* lipogenesis. MCF10a cells stably expressing empty vector, PIK3CA^{H1047R},or K-Ras^{G12V} were transfected with siRNAs targeting SREBP1, SREBP2, or both. Cells were lysed 72 h post-transfection following 20 h serum starvation for immunoblotting of the cytosolic fraction (**A**) or RNA extraction for qRT-PCR analysis (**B**). Representative data are shown as mean ± s.e.m. relative to vector-expressing cells (white bar), n=3. (**C**) Incorporation of 1-[^{14}C]-acetate into the lipid fraction was measured in these cells, with data shown as mean ± s.e.m. relative to vector-expressing cells (white bar), n=2. (**D**,**E**) Effects of SREBP and SCD knockdown on lipogenesis. The cells in **A** were transfected with siRNAs targeting SREBP1 and SREBP2, or SCD. Cells were lysed as in **A** for immunoblotting (**D**). Incorporation of 1-[^{14}C]-acetate into the lipid fraction was measured in these cells (**E**)**.** Data are shown as mean ± s.e.m. relative to vector-expressing cells (white bar), n=2. (**B,C,E**) # P-value < 0.05 compared to vector-expressing cells; * P-value < 0.05 compared to cells expressing the same oncogene transfected with nontargeting siRNA.

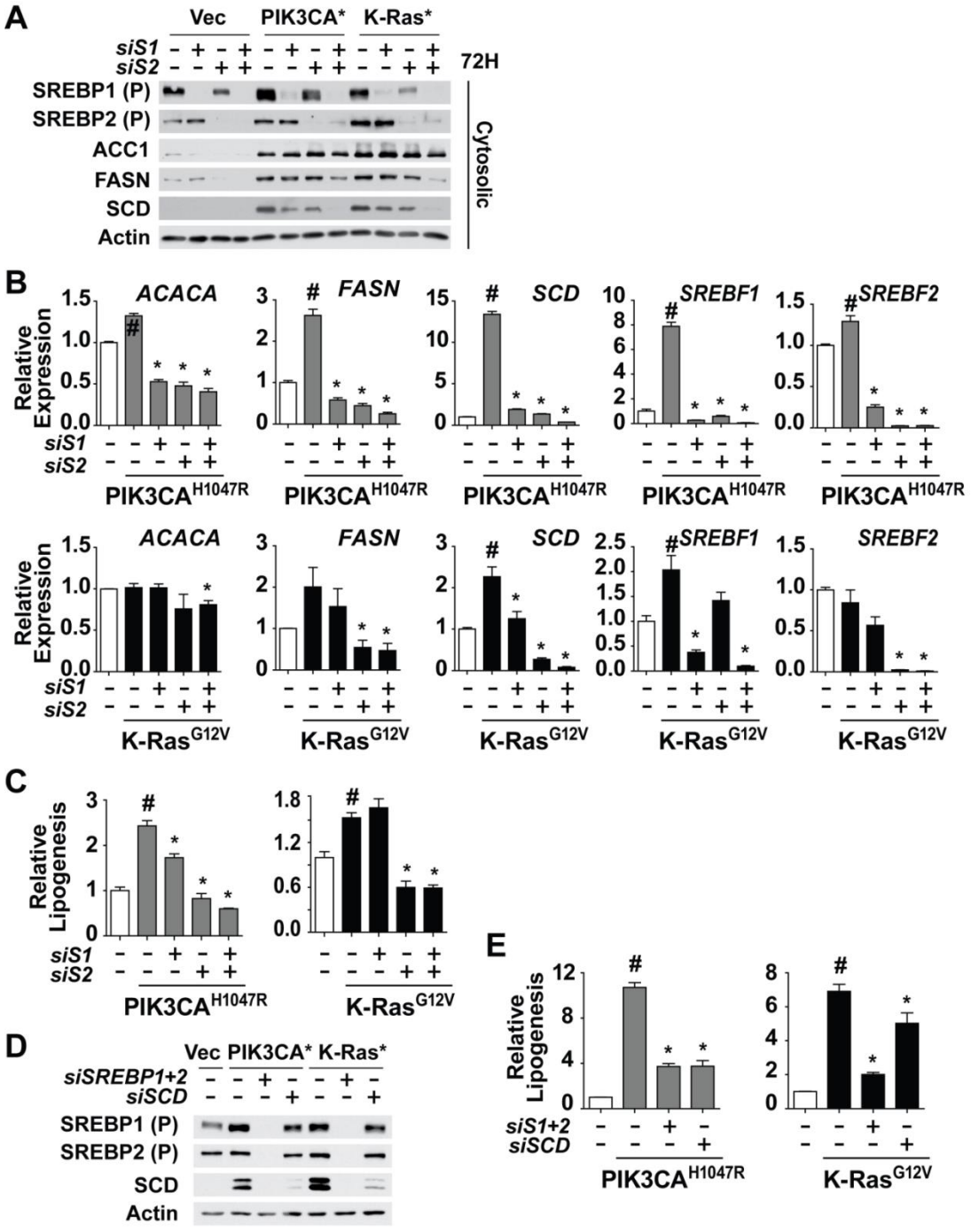

Figure 2.3 (Continued)

2.4.3 mTORC1 and SREBP drive *de novo* lipid synthesis in breast cancer cells

To determine whether mTORC1 signaling also promotes *de novo* lipid synthesis in the more complex genetic setting of cancer cells, we profiled a panel of eight genetically-defined breast cancer cell lines of luminal and basal subtype that, among other mutations, have oncogenic activation of the PI3K or Ras signaling pathways (Table 2.1). Consistent with the presence of these mutations leading to activation of the upstream pathways, all eight cell lines displayed growth-factor independent activation of mTORC1 signaling, which was sensitive to rapamycin, PP242 or Torin1 (Figure 2.4). *De novo* lipogenesis was also constitutively active in these cells, and was significantly reduced by rapamycin in all cases, with mTOR kinase inhibitors leading to a further reduction in some lines (Figure 2.4). Inhibition of mTOR decreased the transcript levels of *SREBF1*, *SREBF2*, *FASN*, and *SCD* in these lines (Figure 2.5A). Similar to the oncogene-expressing MCF10a cells, mTOR inhibitors had little effect on levels of SREBP precursors, but the mature forms of both SREBP1 and 2 were reduced by rapamycin and Torin1 in three representative lines from this panel (Figure 2.5B). As a control, we confirmed that the SREBP precursor and mature forms detected by these antibodies are reduced by siRNA-mediated knockdown of SREBP1 and 2 in these cells (Figure 2.5C). SCD protein levels were also reduced by mTOR inhibitors (Figure 2.5B), whereas a substantial decrease in FASN levels were not observed until 96 h of treatment (Figure 2.5D), despite effects on its transcript levels at 18 h (Figure 2.5A).

To determine the role of SREBP in the induction of lipogenesis in breast cancer cells, SREBP1, SREBP2, or both were knocked-down using siRNAs in these three lines, which we confirmed by measuring *SREBF1*, *SREBF2*, and *SCD* transcript levels (Figure 2.6A). Depletion of SREBP2 alone or in combination with SREBP1 attenuated the ability of these cells to synthesize lipids *de novo* (Figure 2.6B). Therefore, aberrant mTORC1 signaling and its activation of SREBP isoforms underlie the lipogenic property of heterogeneous breast cancer cell lines.

Table 2.1. Breast cancer cell lines used in this study with known mutations upstream of mTORC1.

#	Cell Line	Mutations	Subtype[a]
1	**MDA-MB-468**	PTEN p.V85_splice	Basal
2	**HCC1937**	PTEN del/del	Basal
3	**MCF-7**	PIK3CA E545K	Luminal
4	**BT-483**	PIK3CA E542K	Luminal
5	**T-47D**	PIK3CA H1047R	Luminal
6	**MDA-MB-453**	PIK3CA H1047R (PTEN[b])	Luminal
7	**Hs578T**	HRAS G12D	Basal
8	**MDA-MB-134-VI**	KRAS G12R	Luminal

[a] Subtype is based on the gene expression signature published by Neve *et al.*[45]

[b] PTEN mutation with undefined effect.

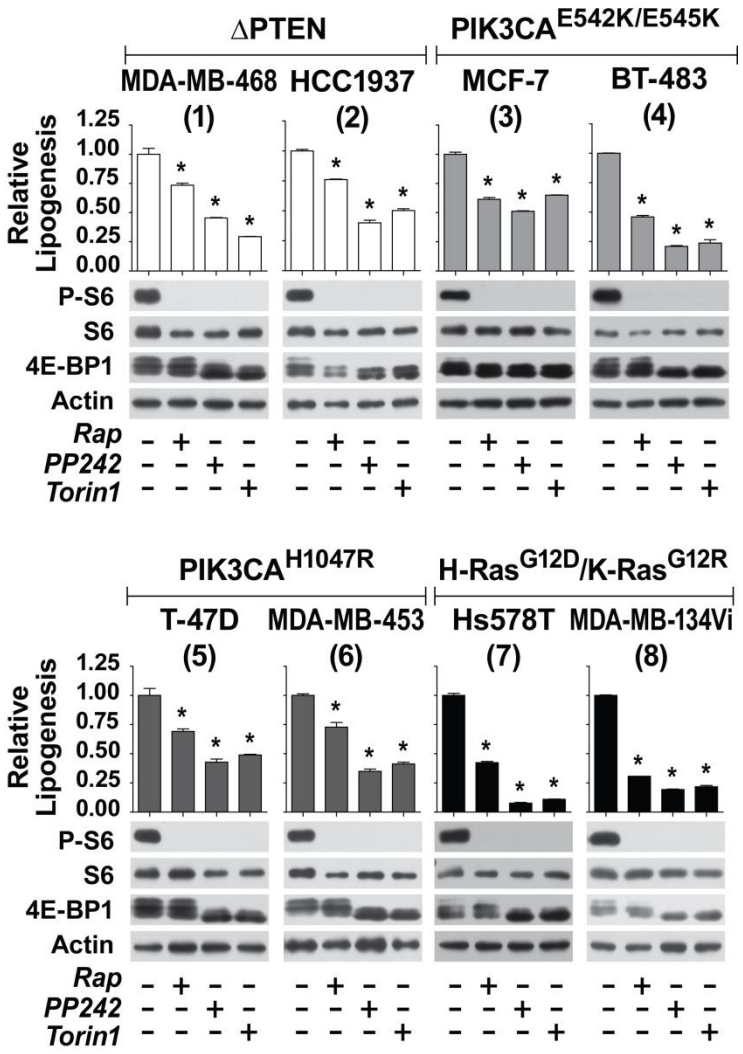

Figure 2.4. Breast cancer lines depend on mTORC1 for *de novo* lipogenesis.

Signaling and *de novo* lipogenesis in response to mTOR inhibition. Eight breast cancer cell lines were serum starved for 18 h in the presence of vehicle, rapamycin (20 nM), PP242 (2.5 μM), or Torin1 (250 nM). Note: phosphorylation of S6 and, via mobility shifts, 4E-BP1 are shown as markers of mTORC1 activation. Incorporation of 1-[^{14}C]-acetate into the lipid fraction was measured. Representative data are shown as mean ± s.e.m. relative to vehicle-treated cells, n=2. * P-value < 0.05 compared to vehicle-treated cells.

Figure 2.5. mTOR inhibitors decreases the expression of SREBP and its target genes in breast cancer cells.

(**A**) mTORC1-dependent *FASN*, *SCD*, *SREBF1*, and *SREBF2* expression in breast cancer cells. The cell lines, numbered as in Table 1**,** were serum starved for 18 h in the presence of vehicle, rapamycin (20 nM), or Torin1 (250 nM). RNA was isolated for analysis by qRT-PCR, with transcript levels shown as mean ± s.e.m. relative to vehicle-treated cells. * P-value < 0.05 compared to vehicle-treated cells. (**B**) Dependence of SREBP processing on mTORC1 in breast cancer cells. MDA-MB-468, MDA-MB-453 and Hs578T were treated as **A** and fractionated into nuclear and cytosolic fractions for immunoblotting. The SREBP full-length precursor (P), processed C-terminus (C) and nuclear mature (M) isoforms were detected. * denotes a cross-reacting band. (**C**) Immunoblots demonstrating the specificity of SREBP1 and SREBP2 antibodies. MDA-MB-468, MDA-MB-453, and Hs578T cells were transfected with siRNAs targeting SREBP1 and SREBP2 for 72 h. Cytosolic and nuclear fractions were collected after 18 h serum starvation to detect the cytosolic precursor (P) and the nuclear mature (M) forms of SREBP1 and 2, and the C-terminal cleaved form of SREBP2 (C). (**D**) Effect of long-term mTOR inhibition on FASN and SCD levels. MDA-MB-453 cells were serum starved for 96 h and rapamycin (20 nM) or Torin1 (250 nM) was added in 24 h increments.

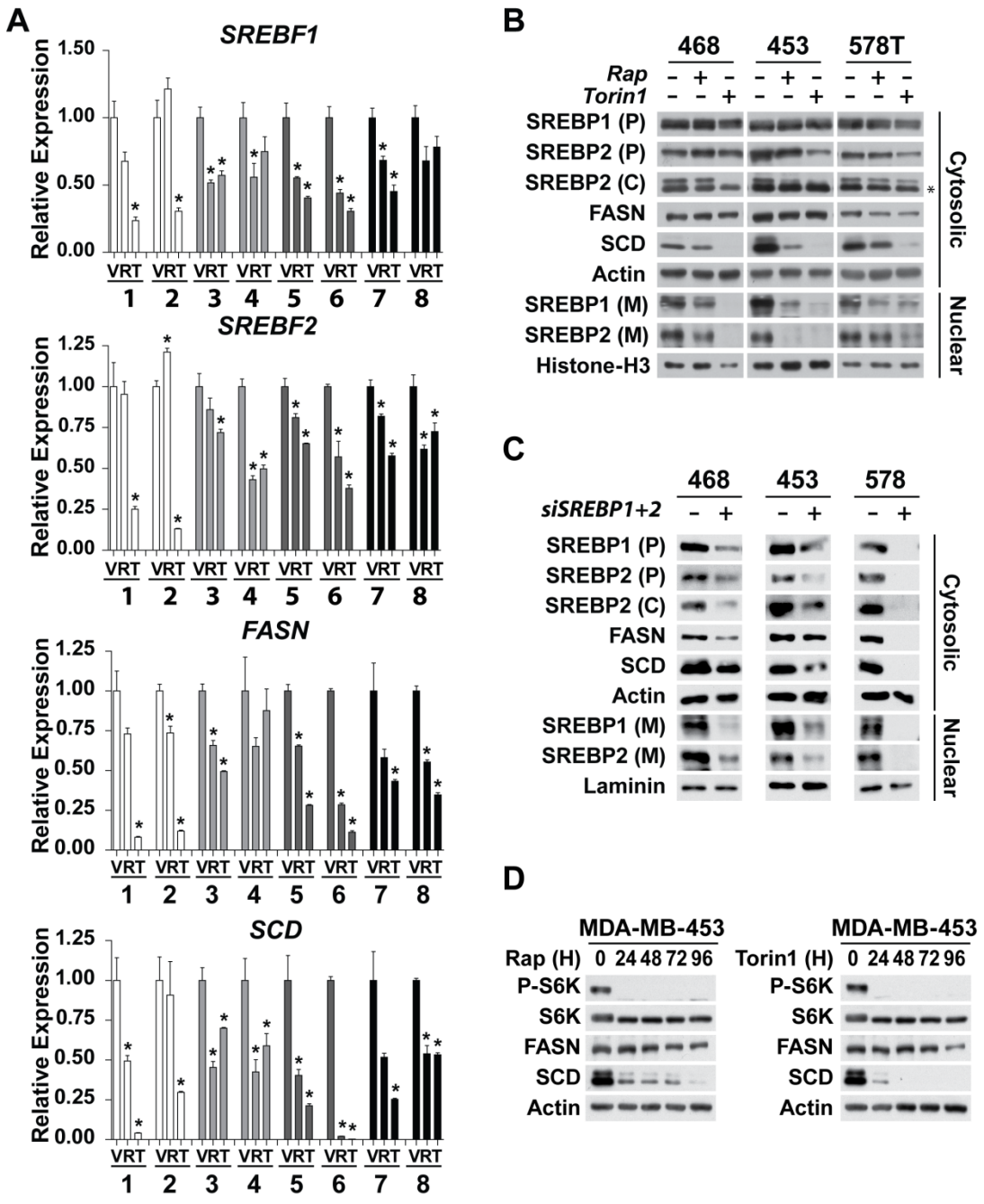

Figure 2.5 (Continued)

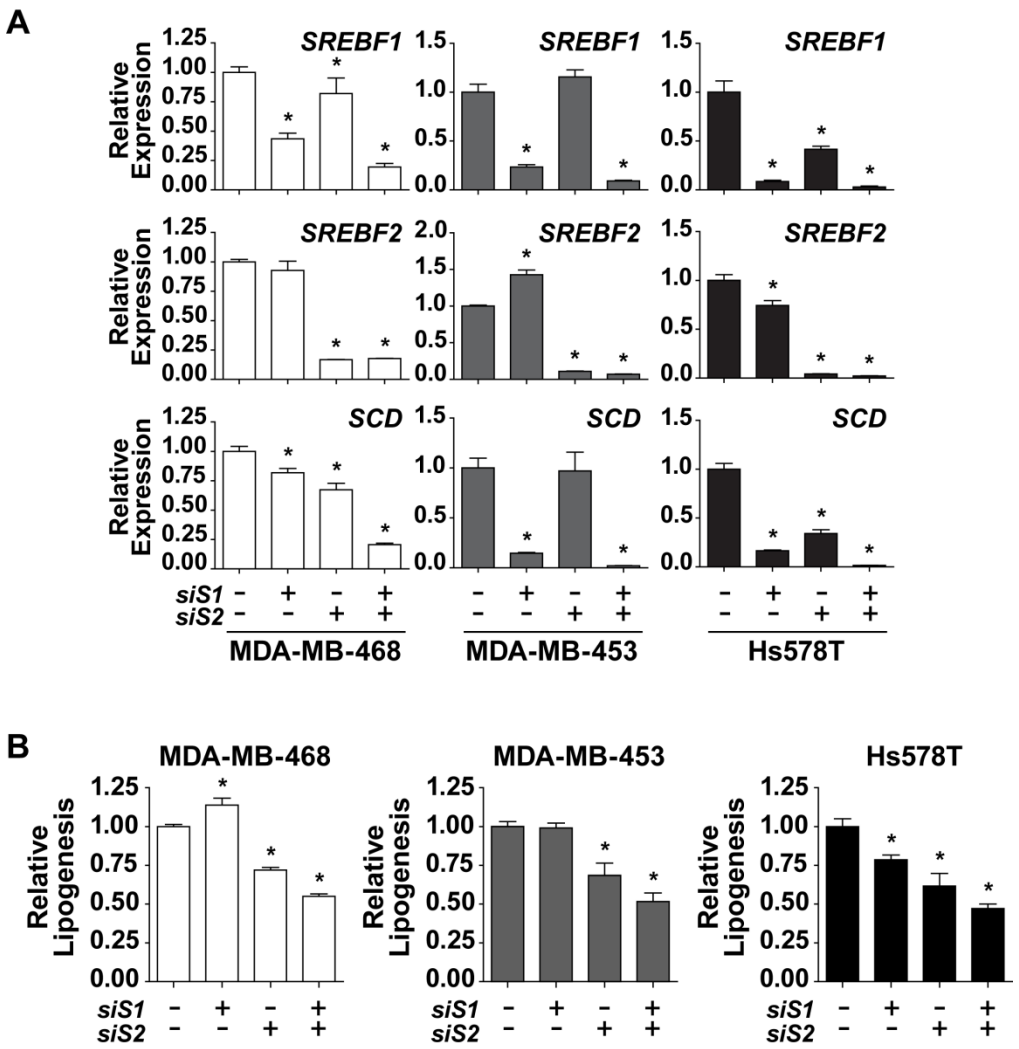

Figure 2.6. Effect of SREBP1 or SREBP2 knockdown on *de novo* lipogenesis in breast cancer cells. (**A**) Effect of SREBP knockdown on expression of *SREBF1*, *SREBF2*, and *SCD*. Breast cancer cells were transfected with siRNAs targeting SREBP1, 2 or both. RNA was extracted for qRT-PCR analysis 72 h after transfection, following 18 h serum starvation. Representative data are shown as mean ± s.e.m. relative to vehicle-treated cells, n=2. * P-value < 0.05 compared to cells with control siRNAs. (**B**) SREBP knockdown attenuates *de novo* lipogenesis in breast cancer cells. The cells were transfected as in **A** with siRNAs targeting SREBP1, SREBP2, or both. Cells were lysed 72 h post-transfection following 16 h serum starvation to analyze lipid synthesis by measuring the incorporation of 1-[^{14}C]-acetate into the lipid fraction. Data are shown as mean ± s.e.m. relative to cells transfected with non-targeting siRNA, n=2. * P-value < 0.05.

2.4.4 The SREBPs support oncogene-induced cell proliferation and growth

We next determined the importance of downstream activation of SREBP on the growth properties of breast cancer cells with activated mTORC1. The proliferation of MDA-MB-468, MDA-MB-453, and Hs578T grown in full serum was significantly reduced by combined knockdown of SREBP1 and 2, with the Hs578T cells being equally sensitive to SREBP2 knockdown alone (Figure 2.7A). To determine the influence of exogenous lipids on these responses, proliferation was also measured in lipid-depleted serum. While the overall responses to SREBP isoform knockdown were similar, reducing serum lipids greatly sensitized the MDA-MB-468 cells to the knockdown of SREBP2 (Figure 2.7B). Exogenous expression of mouse SREBP2, which is resistant to the siRNAs targeting human SREBP2 and, thereby, restores FASN and SCD expression, rescued the inhibitory effects of SREBP2 knockdown on the proliferation of these cells (Figure 2.7C). As further confirmation of the specificity of these effects, four different shRNA sequences targeting SREBP2 were tested. The inhibition of proliferation with these shRNAs closely matched the degree of decrease in FASN and SCD protein levels elicited by the individual shRNAs (Figure 2.7D). The knockdown of SREBP isoforms also led to a reduction in cell size, with the double knockdown having the strongest effect in all three cell lines tested (Figure 2.8A). The differential effects of SREBP1 and SREBP2 depletion on the proliferation and growth of these cell lines were also observed for measurements of cell death, with the double knockdown most strongly decreasing viability (Figure 2.8B). Therefore, SREBP plays a key role in supporting cell growth, proliferation and survival in these breast cancer cells.

To better define the cellular role of SREBP as a downstream effector of oncogenic signaling pathways, we compared the $PIK3CA^{H1047R}$ and $K\text{-}Ras^{G12V}$-expressing MCF10a cells to the isogenic vector-expressing cells. When grown in full serum, the proliferation rate of the vector control cells was comparable to the oncogene-expressing cells (Figure 2.9A), and knocking down SREBP isoforms, particularly SREBP2, only modestly reduced proliferation in the oncogene-expressing lines (Figure 2.9B). To better distinguish between the control cells, which exhibit growth-factor dependent mTORC1

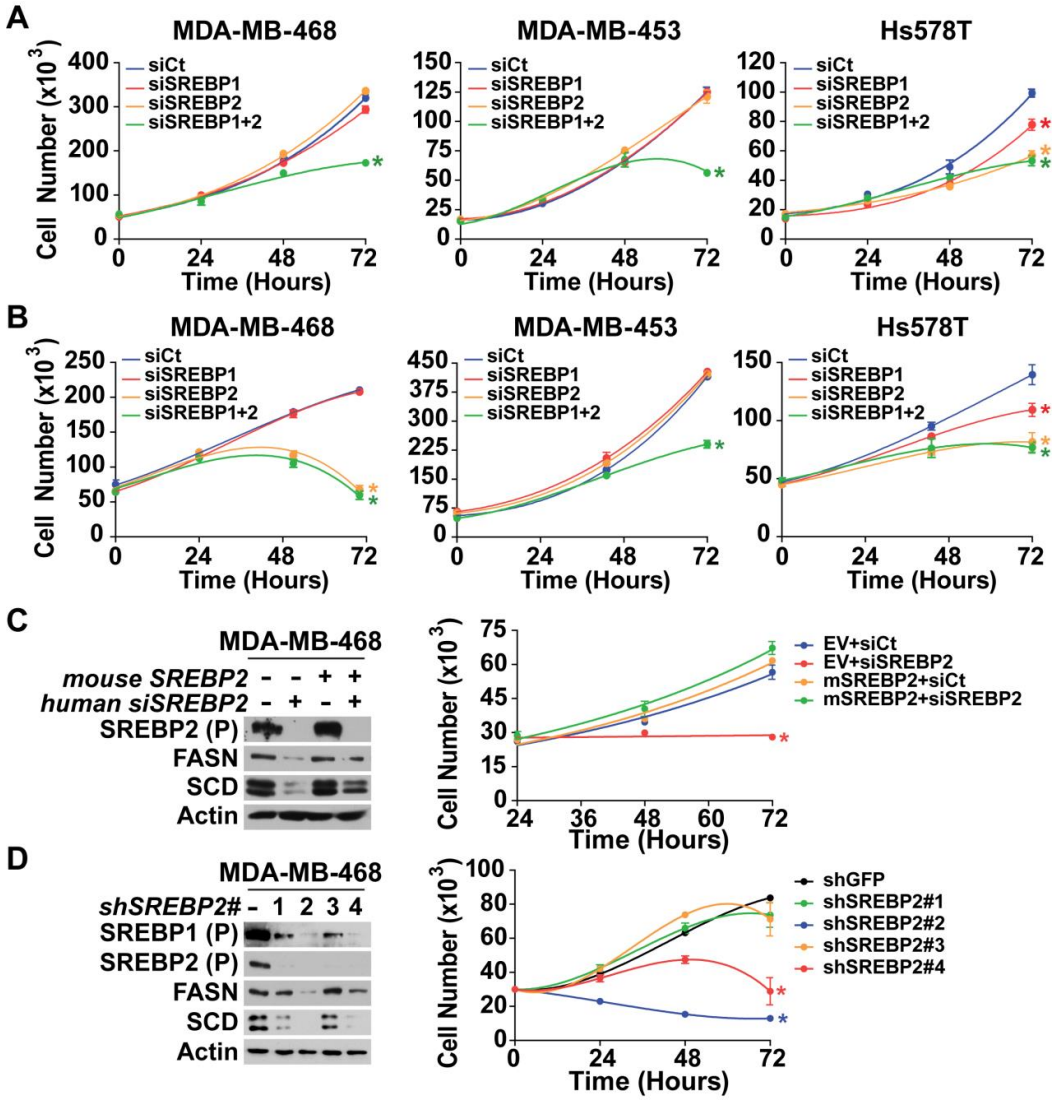

Figure 2.7. Effects of SREBP1 and SREBP2 depletion on the proliferation of breast cancer cells. (**A**,**B**) Effect of SREBP1 and SREBP2 depletion on proliferation in breast cancer cells. MDA-MB-468, MDA-MB-453 and Hs578T cells were transfected with siRNAs targeting SREBP1, SREBP2, or both and were either (**A**) cultured in full serum or (**B**) switched to lipid-reduced serum 24 h after the knockdown (t = 0 h). For all proliferation graphs, data are shown as mean ± s.e.m., n=3. * P-value < 0.05 compared to control cells at the final time point. (**C**) Rescue of human SREBP2 knockdown with mouse SREBP2 expression. MDA-MB-468 cells stably expressing mouse SREBP2 were transfected with siRNA targeting human SREBP2. Cells were lysed for immunoblotting 72 h post-transfection, following 16 h serum starvation. To measure proliferation, cells were cultured in lipid-reduced serum and counted every 24 h.

Figure 2.7 (Continued)

(**D**) Effects of SREBP2 shRNA on SREBP target expression and proliferation. MDA-MB-468 cells stably expressing four different shRNA sequences targeting SREBP2 were either serum starved for 16 h for immunoblot analysis or cultured in lipid-reduced serum to measure proliferation.

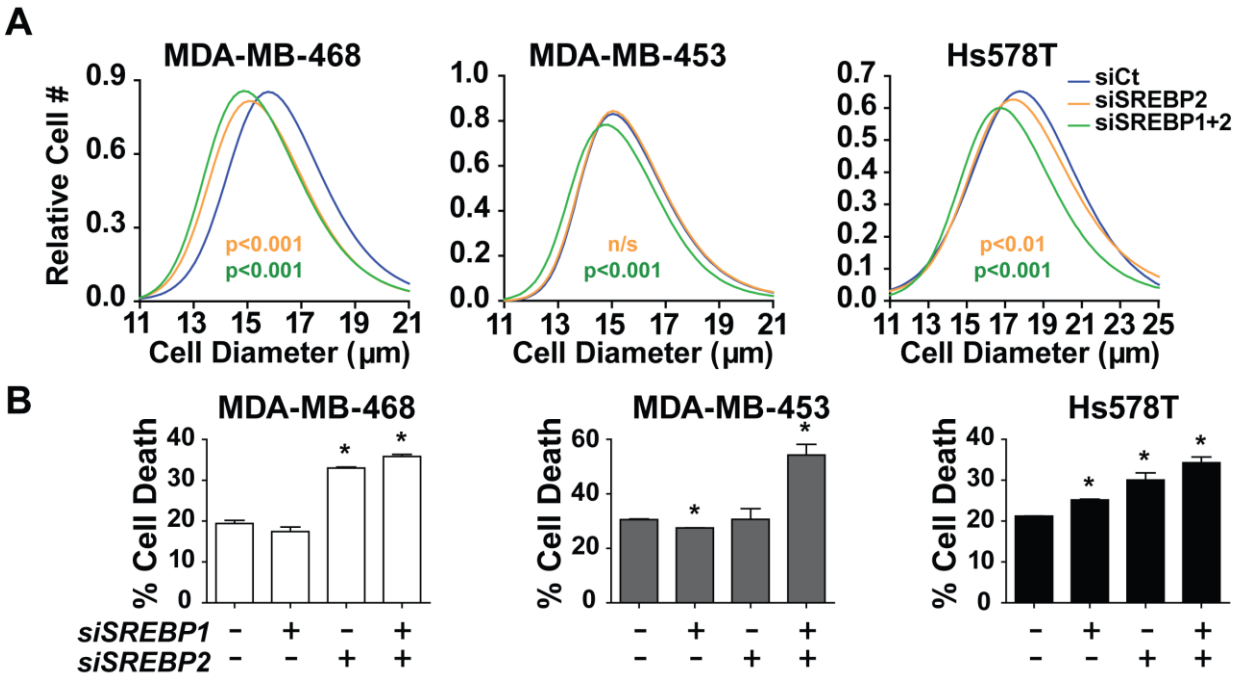

Figure 2.8. The SREBPs support growth and survival in breast cancer cell lines.

(**A**) Effects of SREBP knockdown on cell size. Cell diameter was measured at 48 h in cells from **Figure 2.7B**, in solution. Color-coded P-values, compared to cells with control siRNAs, correspond to the color-coding in the legend (>1000 cells measured for each). (**B**) Effect of SREBP knockdown on breast cancer cell viability. Percent cell death was determined by counting Annexin-V and/or propidium iodide positive cells treated as in **Figure 2.7B** by flow cytometry 72 h after siRNA transfection. Data are shown as mean ± s.e.m. relative to cells transfected with non-targeting siRNA, n=2. * P-value < 0.05.

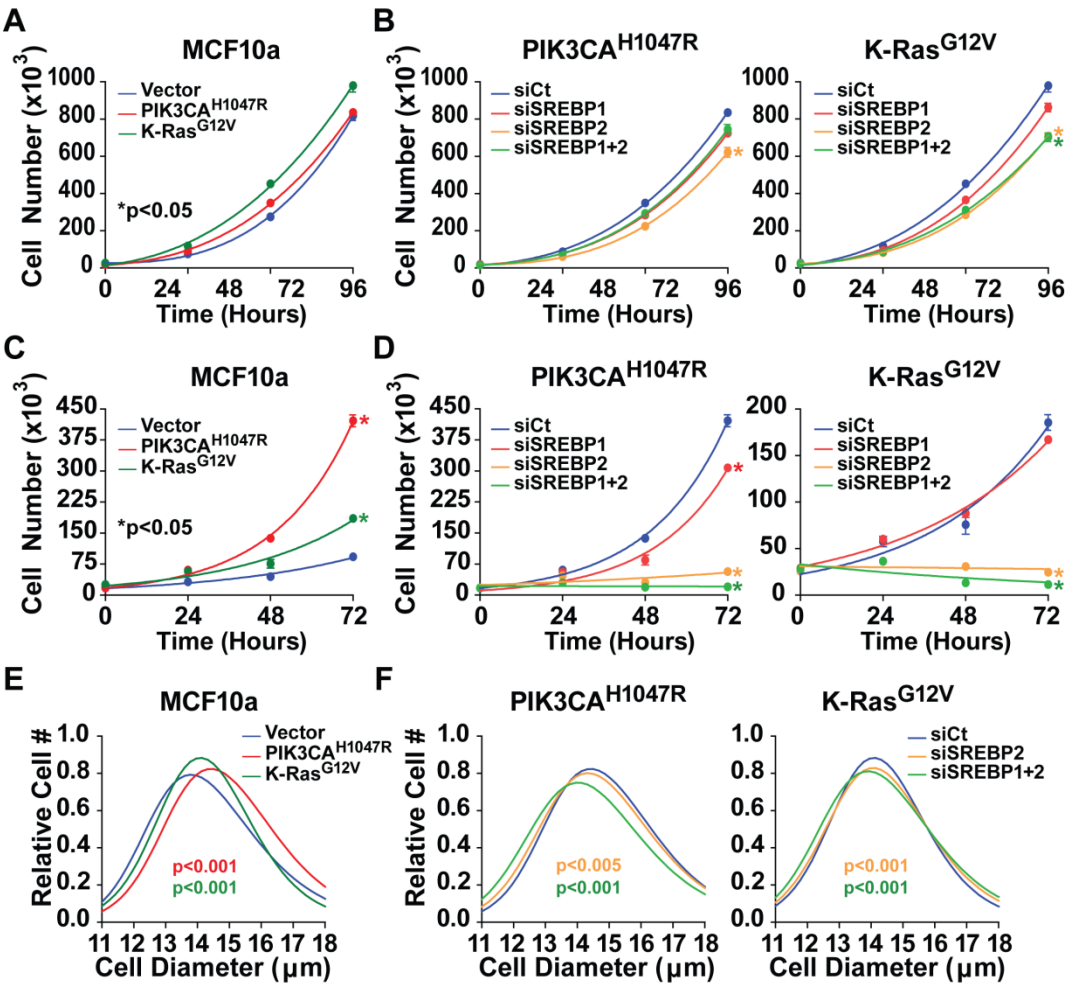

Figure 2.9. Effects of oncogene expression and SREBP depletion on cell growth and proliferation in MCF10a cells.

(**A**,**C**) Proliferation of PIK3CA^{H1047R}- and K-Ras^{G12V}-expressing MCF10a cells compared to vector-expressing cells cultured in full growth medium (**A**) or in low serum conditions (**C**) starting 24 h post-knockdown (t = 0 h). For all proliferation graphs, time points are shown as mean ± s.e.m., n=3. * P-value < 0.05 compared to control cells at the final time point. (**B**,**D**) Effect of SREBP depletion on proliferation of oncogene-expressing MCF10a cells. Cells from **a** and **c** cultured in full serum (**B**) or low serum (**D**) were counted every 24 h following the siRNA-mediated knockdown of SREBP1, SREBP2, or both. (**E**,**F**) Oncogene- and SREBP-dependent effects on cell growth. The diameters of the cells treated as in **C** (**E**) and **D** (**F**) were measured at 48 h, following trypsinization. Color-coded P-values, compared to cells with control siRNAs, correspond to the color-coding in the legend (>1000 cells measured for each).

activation, and the oncogene-expressing lines, with constitutive mTORC1 activation (Figure 2.1B), proliferation was also measured in low serum and growth factor conditions, where both the PI3K and K-Ras cells exhibit a proliferation advantage over the controls (Figure 2.9C). Under these conditions, SREBP2 knockdown arrested the proliferation of both oncogene-expressing lines, an effect enhanced when combined with SREBP1 knockdown (Figure 2.9D). The oncogene-expressing cells also exhibited an increase in cell size relative to the control cells (Figure 2.9E), and their size was significantly reduced upon knockdown of SREBP2 alone or in combination with SREBP1 (Figure 2.9F). Collectively, these findings reveal a requirement for SREBP in the aberrant, growth factor-independent growth and proliferation of oncogene-expressing cells.

2.4.5 Association of mTORC1 activation with the expression of SREBP targets in human breast cancer

To determine whether the mTORC1-SREBP pathway is activated in human breast cancers, we analyzed the coupled gene expression and reverse phase protein array data from the breast invasive carcinoma dataset of The Cancer Genome Atlas (TCGA)[36–38]. Using phosphorylation of ribosomal S6 (P-S6) as an indication of mTORC1 activation, the expression of canonical SREBP targets in cells with low and high mTORC1 signaling was compared. When compared to tumors with low P-S6 (n=116), those with high P-S6 (n=112) displayed increased expression of the SREBP target genes *FASN*, *SCD*, *LDLR*, and *MVK* (Figure 2.10A). To further assess a connection between mTORC1 activation and increased protein levels of SREBP targets, we used arrays of protein extracts from primary breast cancer samples comprised of matched pairs of tumor and adjacent normal breast tissue from each patient (n=40), comparing P-S6 levels to that of FASN and SCD. To validate the antibodies for this assay, we used dot blots of MDA-MB-468 cell lysates and confirmed the decreased signal in lysates from Torin1-treated cells (Figure 2.11). Examples of the array data with triplicate spots of normal and tumor tissue from each of 6 patients are shown in Figure 2.10B. An association between the fold change in P-S6 levels in the

Figure 2.10. Expression of SREBP targets is associated with mTORC1 activation in human breast cancer.

(**A**) Comparison of SREBP target gene expression and P-S6 levels in data from primary breast cancer samples. Expression of *FASN, SCD, LDLR,* and *MVK* in breast carcinoma samples from the TCGA, grouped by high (n=112) or low (n=116) P-S6-S240/244 levels. Data are shown as mean ± s.e.m. relative to low P-S6 samples. (**B**,**C**) Association of FASN and SCD protein levels with P-S6 levels in primary human breast cancers. Dot blots of six different matched pairs of breast cancer and normal tissue are shown, each spotted in triplicate (**B**). The $\log_2$ fold change of P-S6 levels in paired tumor versus normal tissue is graphed with $\log_2$ fold change of either FASN (n=40) or SCD (n=37) (**C**), with the coefficient of determination (R^2) provided. (**D**) The data from **C** was grouped into high and low fold changes of P-S6 levels in tumor versus normal tissue and graphed for the fold-change in FASN and SCD protein levels.

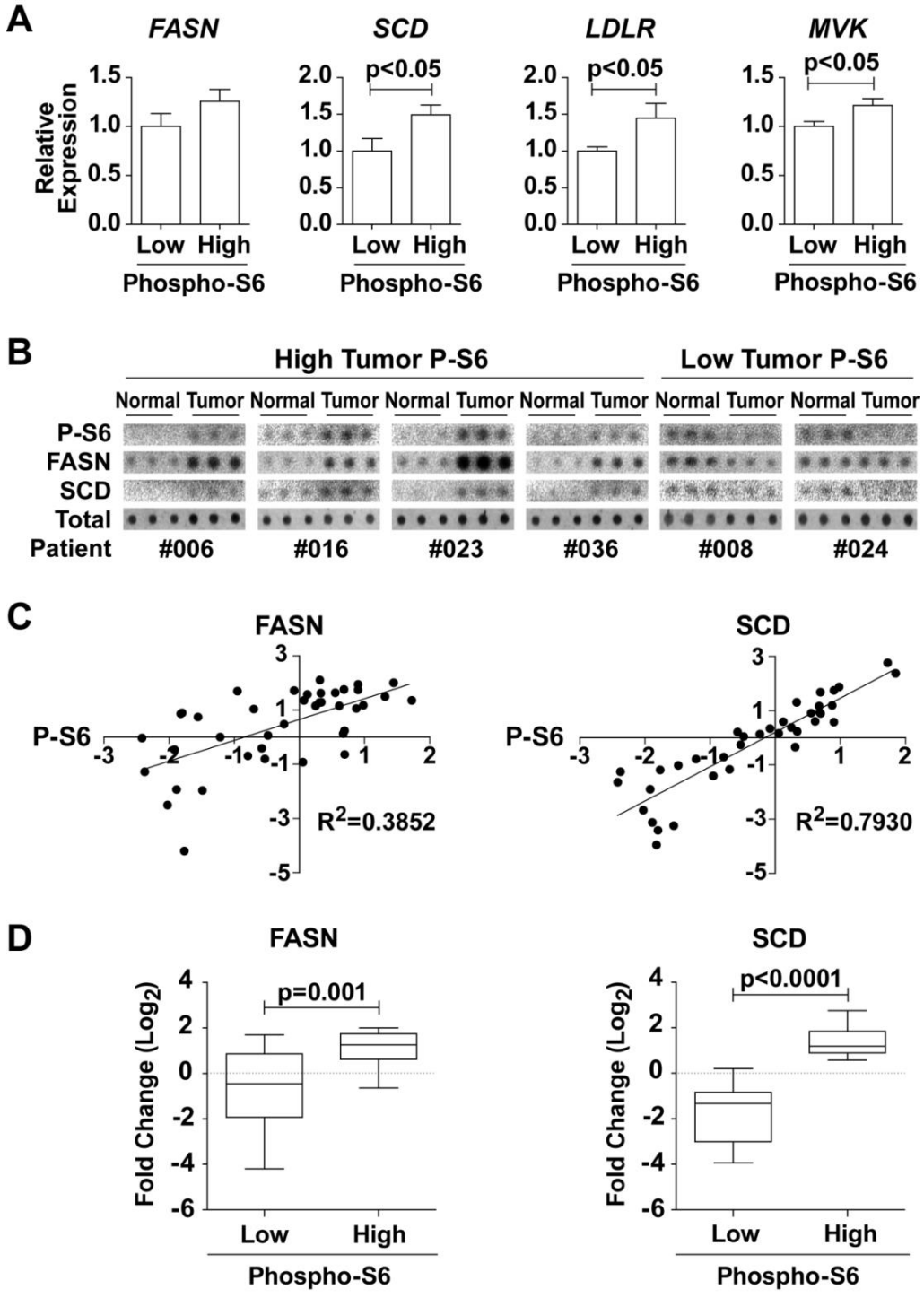

Figure 2.10 (Continued)

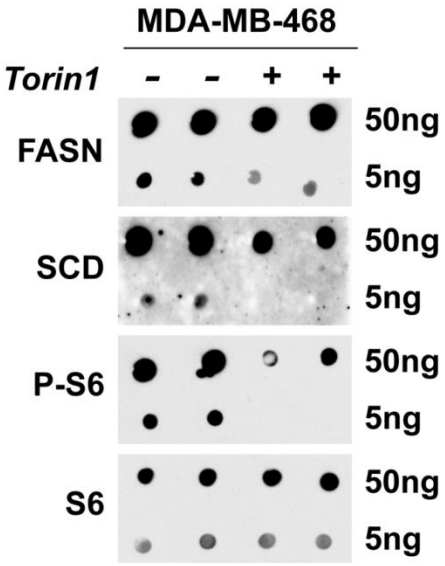

Figure 2.11. Validation of antibodies for use in tissue array dot blots.

MDA-MB-468 cells were serum starved for 20 h in the presence of vehicle or Torin1 (250 nM). Dilutions of protein extract from these cells were spotted onto nitrocellulose membranes and immunoblotted for the indicated proteins.

tumor samples relative to their matched normal tissue and the fold change in FASN and, especially, SCD protein levels was evident in this analysis (Figure 2.10C). FASN and SCD protein levels were significantly increased in tumor samples with elevated P-S6 compared to tumor samples with decreased P-S6 (Figure 2.10D). Taken together with our isogenic and breast cancer cell data, these findings indicate that the aberrant activation of mTORC1 in cancer promotes a lipogenic program through the activation of SREBP and its gene targets.

2.5 DISCUSSION

An important metabolic characteristic of cancer cells that distinguishes them from their cells of origin is their enhanced capacity to synthesize, *de novo*, the major macromolecules needed to make new cells, including proteins, nucleotides, and lipids[46]. While there has been much progress in defining the unique metabolic properties of cancer cells, how these properties are acquired over the course of oncogenic transformation is less well understood. In this study, we demonstrate that mTORC1 activation downstream of oncogenic PI3K and Ras signaling is a major mechanism by which cancer cells stimulate aberrantly elevated rates of *de novo* lipid synthesis. Furthermore, we show that the SREBP family of transcription factors, well-established promoters of lipid synthesis in physiological settings, such as the liver[6], are the key downstream effectors of mTORC1 promoting oncogene-induced lipid synthesis.

SREBP has emerged as a major effector of mTORC1 signaling. Porstmann *et al*. were the first to show that aberrant activation of an oncogene (Akt) could activate SREBP[47], which was later found to be through downstream activation of mTORC1[14]. In a bioinformatics search for common cis-regulatory elements in the promoters of mTORC1-induced genes, we identified SREs, which are recognized by SREBP, to be most prevalent, demonstrating the importance of SREBP as a primary downstream transcriptional effector of mTORC1[13]. How mTORC1 activates SREBP is unknown, although multiple direct downstream targets of mTORC1 have been implicated[12]. These distinct mechanisms are likely to

underlie the differential sensitivity of SREBP1/2 processing and lipid synthesis to rapamycin and TOR kinase inhibitors. It is now clear that the mTORC1-SREBP1c pathway represents a major route by which insulin signaling activates physiological lipid synthesis in the liver[15,16,20,22]. Recent studies have also implicated an important role for the SREBPs in cancer cell viability[42,48–50]. We find that activation of the mTORC1-SREBP pathway underlies the elevated lipid synthesis observed in cancer cells, providing a key link between oncogenic signaling and this metabolic process. Relative to SREBP1, SREBP2 appears to have a stronger effect on *de novo* lipogenesis and proliferation in the cell settings used in this study. It is not clear whether this is due to a specific function of SREBP2, which unlike SREBP1, is embryonic lethal if knocked out in mice[51], or whether it is due to the influence of SREBP2 on SREBP1 expression detected here and in previous studies[13,42,43], resulting in a functional decrease in both isoforms upon SREBP2 knockdown.

Lipogenic enzymes transcriptionally activated by the SREBPs have emerged as potential therapeutic targets in cancer. Chemical inhibition or genetic knockdown of ATP citrate lyase (ACLY)[52,53], FASN[2], and SCD[54–56] have been found to reduce proliferation and survival in a variety of cancer cells and xenograft tumor models[2,53]. Recent studies have suggested that proliferating cells need to coordinate protein synthesis with the synthesis of MUFAs, prevalent in membrane phospholipids, to prevent ER stress[42,57], suggesting a potential selective pressure for the co-regulation of protein and lipid synthesis by mTORC1. SCD is required for the production of MUFAs and is, therefore, particularly important for the proliferation and survival of cancer cells[54–56]. Blocking the mevalonate pathway downstream of SREBP, which is responsible for isoprenoid and cholesterol production, has also been found to reduce cancer cell viability[58,59].

Despite the apparent importance of *de novo* lipogenesis in some cancer settings, it is unclear what role lipid uptake plays and whether exogenous lipids become limiting for cancer cells in the tumor microenvironment. In our study, depletion of serum lipids had little effect on the sensitivity of breast cancer cells to knockdown of SREBP isoforms. However, in the oncogene-expressing MCF10a lines, a

requirement for SREBP was only revealed under conditions of low serum, where oncogenic PI3K and K-Ras exert a proliferation advantage. Interestingly, cancer cells cultured in hypoxic conditions have been shown to be dependent on the uptake of exogenous lipids for sustained growth and survival, and this has been attributed to the oxygen dependence of SCD for its production of endogenous MUFAs[57,60]. Consistent with our findings that SCD is essential for the mTORC1- and SREBP-dependent stimulation of *de novo* lipid synthesis downstream of oncogenes (Figure 2.3E), Kamphorst *et al*[60] have demonstrated that activated Akt stimulates the *de novo* production of MUFAs. In contrast, they found that oncogenic Ras actually decreases cellular MUFA content and enhances the percentage of MUFAs acquired through uptake of exogenous lipids. In addition to increasing lipid uptake[60], we show in a distinct isogenic setting that oncogenic K-Ras can also enhance *de novo* lipid synthesis under conditions where exogenous lipids are not readily available. Interestingly, relative to cells expressing oncogenic PI3K, SCD was found to be less critical for Ras-stimulated lipogenesis in our assays, consistent with these previous findings[60]. It is important that we gain a better understanding of the balance between lipid synthesis and uptake in the tumor microenvironment and how distinct oncogenic lesions influence this in different cancers. It is interesting to note that a major physiological effect of systemic treatment with rapamycin is an increase in circulating lipids[61,62], likely resulting from the stimulation of lipolysis in adipose tissue[63–65]. Such an increase in the availability of exogenous lipids to growing tumors might overcome the suppressive effects of mTORC1 inhibition on *de novo* synthesis within the tumor.

Our data here suggest that oncogenic activation of mTORC1 and its downstream induction of an SREBP-driven lipogenic program are key elements to the transforming capacity of PI3K and K-Ras signaling. Together with established downstream effectors of these pathways that promote cancer cell survival and proliferation, activation of the mTORC1-SREBP pathway serves to enhance cell autonomous growth.

2.6 ACKNOWLEDGEMENTS

This work was supported in part by NSF predoctoral fellowship DGE-1144152 (S.J.H.R.), a postdoctoral fellowship from the LAM Foundation (I.B.S.), a Sanofi Innovation Award (B.D.M.), and NIH grants R01-CA181390 and P01-CA120964 (B.D.M.).

2.7 REFERENCES

1 Medes G, Thomas A, Weinhouse S. Metabolism of neoplastic tissue. IV. A study of lipid synthesis in neoplastic tissue slices in vitro. *Cancer Res* 1953; **13**: 27–29.

2 Menendez JA, Lupu R. Fatty acid synthase and the lipogenic phenotype in cancer pathogenesis. *Nat Rev Cancer* 2007; **7**: 763–777.

3 Santos CR, Schulze A. Lipid metabolism in cancer. *FEBS J* 2012; **279**: 2610–2623.

4 Kuhajda FP, Jennert K, Wood FD, Hennigart RA, Jacobs LB, Dick JD *et al.* Fatty acid synthesis : A potential selective target for antineoplastic therapy. *Proc Natl Acad Sci USA* 1994; **91**: 6379–6383.

5 Li J, Ding S, Habib N, Fermor B, Wood C, Gilmour R. Partial characterization of a cDNA for human stearoyl-CoA desaturase and changes in its mRNA expression in some normal and malignant tissues. *Int J Cancer* 1994; **57**: 348–352.

6 Horton JD, Goldstein JL, Brown MS. SREBPs: activators of the complete program of cholesterol and fatty acid synthesis in the liver. *J Clin Invest* 2002; **109**: 1125–1131.

7 Wang X, Sato R, Brown MS, Hua X, Goldsteln JL. SREBP-1, a membrane-bound transcription factor released by sterol-regulated proteolysis. *Cell* 1994; **77**: 53–62.

8 Hua X, Sakai J, Brown MS, Goldstein JL. Regulated cleavage of sterol regulatory element binding proteins requires sequences on both sides of the endoplasmic reticulum membrane. *J Biol Chem* 1996; **271**: 10379–10384.

9 Sakai J, Duncan EA, Rawson RB, Hua X, Brown MS, Goldstein JL. Sterol-regulated release of SREBP-2 from cell membranes requires two sequential cleavages, one within a transmembrane segment. *Cell* 1996; **85**: 1037–1046.

10 Goldstein JL, DeBose-Boyd RA, Brown MS. Protein sensors for membrane sterols. *Cell* 2006; **124**: 35–46.

11 Jeon T, Osborne TF. SREBPs: metabolic integrators in physiology and metabolism. *Trends Endocrinol Metab* 2011; **23**: 65–72.

12 Ricoult SJH, Manning BD. The multifaceted role of mTORC1 in the control of lipid metabolism. *EMBO Rep* 2013; **14**: 242–251.

13 Düvel K, Yecies JL, Menon S, Raman P, Lipovsky AI, Souza AL *et al.* Activation of a metabolic gene regulatory network downstream of mTOR complex 1. *Mol Cell* 2010; **39**: 171–183.

14 Porstmann T, Santos CR, Griffiths B, Cully M, Wu M, Leevers S *et al.* SREBP activity is regulated by mTORC1 and contributes to Akt-dependent cell growth. *Cell Metab* 2008; **8**: 224–236.

15 Li S, Brown MS, Goldstein JL. Bifurcation of insulin signaling pathway in rat liver: mTORC1 required for stimulation of lipogenesis, but not inhibition of gluconeogenesis. *Proc Natl Acad Sci*

USA 2010; **107**: 3441–3446.

16 Yecies JL, Zhang HH, Menon S, Liu S, Yecies D, Lipovsky AI *et al.* Akt stimulates hepatic SREBP1c and lipogenesis through parallel mTORC1-dependent and independent pathways. *Cell Metab* 2011; **14**: 21–32.

17 Li S, Ogawa W, Emi A, Hayashi K, Senga Y, Nomura K *et al.* Role of S6K1 in regulation of SREBP1c expression in the liver. *Biochem Biophys Res Commun* 2011; **412**: 197–202.

18 Wang BT, Ducker GS, Barczak AJ, Barbeau R, Erle DJ, Shokat KM. The mammalian target of rapamycin regulates cholesterol biosynthetic gene expression and exhibits a rapamycin-resistant transcriptional profile. *Proc Natl Acad Sci USA* 2011; **108**: 15201–15206.

19 Liu X, Yuan H, Niu Y, Niu W, Fu L. The role of AMPK/mTOR/S6K1 signaling axis in mediating the physiological process of exercise-induced insulin sensitization in skeletal muscle of C57BL/6 mice. *Biochim Biophys Acta* 2012; **1822**: 1716–1726.

20 Owen JL, Zhang Y, Bae S-H, Farooqi MS, Liang G, Hammer RE *et al.* Insulin stimulation of SREBP-1c processing in transgenic rat hepatocytes requires p70 S6-kinase. *Proc Natl Acad Sci USA* 2012; **109**: 16184–16189.

21 Luyimbazi D, Akcakanat A, McAuliffe PF, Zhang L, Singh G, Gonzalez-Angulo AM *et al.* Rapamycin regulates stearoyl CoA desaturase 1 expression in breast cancer. *Mol Cancer Ther* 2010; **9**: 2770–2784.

22 Peterson TR, Sengupta SS, Harris TE, Carmack AE, Kang SA, Balderas E *et al.* mTOR complex 1 regulates lipin 1 localization to control the SREBP pathway. *Cell* 2011; **146**: 408–420.

23 Feldman ME, Apsel B, Uotila A, Loewith R, Knight ZA, Ruggero D *et al.* Active-site inhibitors of mTOR target rapamycin-resistant outputs of mTORC1 and mTORC2. *PLoS Biol* 2009; **7**: e1000038.

24 Thoreen CC, Kang SA, Chang JW, Liu Q, Zhang J, Gao Y *et al.* An ATP-competitive mammalian target of rapamycin inhibitor reveals rapamycin-resistant functions of mTORC1. *J Biol Chem* 2009; **284**: 8023–8032.

25 Dibble CC, Elis W, Menon S, Qin W, Klekota J, Asara JM *et al.* TBC1D7 is a third subunit of the TSC1-TSC2 complex upstream of mTORC1. *Mol Cell* 2012; **47**: 535–546.

26 Dibble CC, Manning BD. Signal integration by mTORC1 coordinates nutrient input with biosynthetic output. *Nat Cell Biol* 2013; **15**: 555–564.

27 Huang J, Manning BD. The TSC1–TSC2 complex: a molecular switchboard controlling cell growth. *Biochem J* 2008; **412**: 179–190.

28 Crino PB, Nathanson KL, Henske EP. The tuberous sclerosis complex. *N Engl J Med* 2006; **355**: 1345–1356.

29 Menon S, Manning BD. Common corruption of the mTOR signaling network in human tumors. *Oncogene* 2008; **27**: S43–51.

30 Manning BD, Tee AR, Logsdon MN, Blenis J, Cantley LC. Identification of the tuberous sclerosis complex-2 tumor suppressor gene product tuberin as a target of the phosphoinositide 3-kinase/akt pathway. *Mol Cell* 2002; **10**: 151–162.

31 Inoki K, Li Y, Zhu T, Wu J, Guan K. TSC2 is phosphorylated and inhibited by Akt and suppresses mTOR signalling. *Nat Cell Bio* 2002; **4**: 648–657.

32 Johannessen CM, Reczek EE, James MF, Brems H, Legius E, Cichowski K. The NF1 tumor suppressor critically regulates TSC2 and mTOR. *Proc Natl Acad Sci USA* 2005; **102**: 8573–8578.

33 Ma L, Chen Z, Erdjument-Bromage H, Tempst P, Pandolfi PP. Phosphorylation and functional inactivation of TSC2 by Erk implications for tuberous sclerosis and cancer pathogenesis. *Cell* 2005; **121**: 179–193.

34 Roux PP, Ballif BA, Anjum R, Gygi SP, Blenis J. Tumor-promoting phorbol esters and activated Ras inactivate the tuberous sclerosis tumor suppressor complex via p90 ribosomal S6 kinase. *Proc Natl Acad Sci USA* 2004; **101**: 13489–13494.

35 Zhao JJ, Liu Z, Wang L, Shin E, Loda MF, Roberts TM. The oncogenic properties of mutant p110alpha and p110beta phosphatidylinositol 3-kinases in human mammary epithelial cells. *Proc Natl Acad Sci USA* 2005; **102**: 18443–18448.

36 Gao J, Aksoy BA, Dogrusoz U, Dresdner G, Gross B, Sumer SO *et al.* Integrative analysis of complex cancer genomics and clinical profiles using the cBioPortal. *Sci Signal* 2013; **6**: pl1.

37 Cerami E, Gao J, Dogrusoz U, Gross BE, Sumer SO, Aksoy BA *et al.* The cBio cancer genomics portal: an open platform for exploring multidimensional cancer genomics data. *Cancer Discov* 2012; **2**: 401–404.

38 The Cancer Genome Atlas Network -. Comprehensive molecular portraits of human breast tumours. *Nature* 2012; **490**: 61–70.

39 Schneider CA, Rasband WS, Eliceiri KW. NIH Image to ImageJ: 25 years of image analysis. *Nat Methods* 2012; **9**: 671–675.

40 Tweto J, Liberati M, Larrabee A. Protein turnover and 4'-phosphopantetheine exchange in rat liver fatty acid synthetase. *J Biol Chem* 1971; **246**: 2468–2471.

41 Nakanishi S, Numa S. Purification of rat liver acetyl coenzyme A carboxylase and immunochemical studies on its synthesis and degradation. *Eur J Biochem* 1970; **16**: 161–173.

42 Griffiths B, Lewis CA, Bensaad K, Ros S, Zhang Q, Ferber EC *et al.* Sterol regulatory element binding protein-dependent regulation of lipid synthesis supports cell survival and tumor growth. *Cancer Metab* 2013; **1**: 3.

43 Kidani Y, Elsaesser H, Hock MB, Vergnes L, Williams KJ, Argus JP *et al.* Sterol regulatory element–binding proteins are essential for the metabolic programming of effector T cells and adaptive immunity. *Nat Immunol* 2013; **14**: 489–499.

44 Amemiya-Kudo M, Shimano H, Yoshikawa T, Yahagi N, Hasty AH, Okazaki H *et al.* Promoter analysis of the mouse sterol regulatory element-binding protein-1c gene. *J Biol Chem* 2000; **275**:

31078–31085.

45 Neve RM, Chin K, Fridlyand J, Yeh J, Frederick L, Fevr T *et al.* A collection of breast cancer cell lines for the study of functionally distinct cancer subtypes. *Cancer Cell* 2006; **10**: 515–527.

46 Howell JJ, Ricoult SJH, Ben-Sahra I, Manning BD. A growing role for mTOR in promoting anabolic metabolism. *Biochem Soc Trans* 2013; **41**: 906–912.

47 Porstmann T, Griffiths B, Chung Y-L, Delpuech O, Griffiths JR, Downward J *et al.* PKB/Akt induces transcription of enzymes involved in cholesterol and fatty acid biosynthesis via activation of SREBP. *Oncogene* 2005; **24**: 6465–6481.

48 Guo D, Prins RRM, Dang J, Kuga D, Iwanami A, Soto H *et al.* EGFR signaling through an Akt-SREBP-1-dependent, rapamycin-resistant pathway sensitizes glioblastomas to antilipogenic therapy. *Sci Signal* 2009; **2**: ra82.

49 Krycer JRJ, Phan L, Brown AJA. A key regulator of cholesterol homeostasis, SREBP-2, can be targeted in prostate cancer cells with natural products. *Biochem J* 2012; **446**: 191–201.

50 Williams KJ, Argus JP, Zhu Y, Wilks MQ, Marbois BN, York AG *et al.* An essential requirement for the SCAP/SREBP signaling axis to protect cancer cells from lipotoxicity. *Cancer Res* 2013; **73**: 2850–2862.

51 Shimano H, Shimomura I, Hammer RE, Herz J, Goldstein JL, Brown MS *et al.* Elevated levels of SREBP-2 and cholesterol synthesis in livers of mice homozygous for a targeted disruption of the SREBP-1 gene. *J Clin Invest* 1997; **100**: 2115–2124.

52 Hatzivassiliou G, Zhao F, Bauer DE, Andreadis C, Shaw AN, Dhanak D *et al.* ATP citrate lyase inhibition can suppress tumor cell growth. *Cancer Cell* 2005; **8**: 311–321.

53 Migita T, Narita T, Nomura K, Miyagi E, Inazuka F, Matsuura M *et al.* ATP citrate lyase: activation and therapeutic implications in non-small cell lung cancer. *Cancer Res* 2008; **68**: 8547–8554.

54 Fritz V, Benfodda Z, Rodier G, Henriquet C, Iborra F, Avancès C *et al.* Abrogation of de novo lipogenesis by stearoyl-CoA desaturase 1 inhibition interferes with oncogenic signaling and blocks prostate cancer progression in mice. *Mol Cancer Ther* 2010; **9**: 1740–1754.

55 Roongta U V, Pabalan JG, Wang X, Ryseck R-P, Fargnoli J, Henley BJ *et al.* Cancer cell dependence on unsaturated fatty acids implicates stearoyl-CoA desaturase as a target for cancer therapy. *Mol Cancer Res* 2011; **9**: 1551–1561.

56 Minville-Walz M, Pierre A-S, Pichon L, Bellenger S, Fèvre C, Bellenger J *et al.* Inhibition of stearoyl-CoA desaturase 1 expression induces CHOP-dependent cell death in human cancer cells. *PLoS One* 2010; **5**: e14363.

57 Young RM, Ackerman D, Quinn ZL, Mancuso A, Gruber M, Liu L *et al.* Dysregulated mTORC1 renders cells critically dependent on desaturated lipids for survival under tumor-like stress. *Genes Dev* 2013; **27**: 1115–1131.

58 Freed-Pastor WA, Mizuno H, Zhao X, Langerød A, Moon S-H, Rodriguez-Barrueco R *et al.*

Mutant p53 disrupts mammary tissue architecture via the mevalonate pathway. *Cell* 2012; **148**: 244–258.

59 Clendening JW, Penn LZ. Targeting tumor cell metabolism with statins. *Oncogene* 2012; **31**: 4967–4978.

60 Kamphorst JJ, Cross JR, Fan J, de Stanchina E, Mathew R, White EP *et al.* Hypoxic and Ras-transformed cells support growth by scavenging unsaturated fatty acids from lysophospholipids. *Proc Natl Acad Sci USA* 2013; **110**: 8882–8887.

61 Morrisett JD, Abdel-Fattah G, Hoogeveen R, Mitchell E, Ballantyne CM, Pownall HJ *et al.* Effects of sirolimus on plasma lipids, lipoprotein levels, and fatty acid metabolism in renal transplant patients. *J Lipid Res* 2002; **43**: 1170–1180.

62 Kasiske BL, de Mattos A, Flechner SM, Gallon L, Meier-Kriesche HU, Weir MR *et al.* Mammalian target of rapamycin inhibitor dyslipidemia in kidney transplant recipients. *Am J Transpl* 2008; **8**: 1384–1392.

63 Zhang C, Yoon M-S, Chen J. Amino acid-sensing mTOR signaling is involved in modulation of lipolysis by chronic insulin treatment in adipocytes. *Am J Physiol Endocrinol Metab* 2009; **296**: E862–868.

64 Chakrabarti P, English T, Shi J, Smas CM, Kandror K V. Mammalian target of rapamycin complex 1 suppresses lipolysis, stimulates lipogenesis, and promotes fat storage. *Diabetes* 2010; **59**: 775–781.

65 Soliman GA, Acosta-Jaquez HA, Fingar DC. mTORC1 inhibition via rapamycin promotes triacylglycerol lipolysis and release of free fatty acids in 3T3-L1 adipocytes. *Lipids* 2010; **45**: 1089–1100.

CHAPTER 3:

SREBP REGULATES THE EXPRESSION AND METABOLIC FUNCTIONS OF WILD-TYPE AND ONCOGENIC IDH1

This chapter is adapted from:

Ricoult SJH, Asara JM, Manning BD. SREBP regulates the expression and metabolic functions of wild-type and oncogenic *IDH1*. Under review at *Molecular and Cellular Biology*.

3.1 ABSTRACT

Sterol regulatory element-binding protein (SREBP) is a major transcriptional regulator of the enzymes underlying *de novo* lipid synthesis. However, little is known about the SREBP-mediated control of processes that indirectly support lipogenesis, for instance, by supplying reducing power in the form of NAPDH or directing carbon flux into lipid precursors. Here, we characterize isocitrate dehydrogenase 1 (IDH1) as a transcriptional target of SREBP across a spectrum of cancer cell lines and human cancers. Like SREBP, IDH1 promotes the synthesis of lipids from glutamine-derived carbons. Neomorphic mutations in IDH1 occur frequently in certain cancers, leading to the production of the oncometabolite 2-hydroxyglutarate (2-HG). We find that SREBP induces expression of oncogenic IDH1 and influences its ability to drive glucose flux into 2-HG. Treatment of cells with cholesterol or statins, which respectively inhibit or activate SREBP, further demonstrates that SREBP regulates IDH1 expression and, in cells with oncogenic IDH1, influences carbon flux into 2-HG.

3.2 INTRODUCTION

The SREBP family of transcription factors is activated by sterol depletion, growth factor signaling pathways, and oncogenes to induce the expression of genes encoding the major enzymes of *de novo* lipid synthesis[1–5]. In sterol-replete conditions, inactive SREBP is held in the endoplasmic reticulum (ER). Upon sterol depletion, SREBP traffics from the ER to the Golgi apparatus, where it is proteolytically processed, leading to release of a mature, active SREBP transcription factor[6,7]. The mature SREBP then translocates to the nucleus and binds SRE-containing gene promoters to induce transcription. The three SREBP isoforms are produced from two different genes, *SREBF1*, which encodes SREBP1a and SREBP1c, and *SREBF2*, which encodes SREBP2. While studies of isoform-specific functions of the SREBPs in the liver have pointed to a role for SREBP1c in fatty acid and triglyceride synthesis and

SREBP2 in cholesterol synthesis[8], SREBP targets appear to be more redundantly regulated in other settings[3,4].

The transcriptional activation of *de novo* lipid synthesis genes by SREBP is well-studied, but less is known about the regulation of auxiliary genes that indirectly support lipogenesis by providing NADPH or directing carbon flux into lipids[8]. Overexpression of mature, active SREBP in the liver of mice increases the transcription of genes encoding glucose-6-phosphate dehydrogenase, 6-phosphogluconate dehydrogenase, and malic enzyme 1, which are all major sources of NADPH production[9,10]. Similarly, mature SREBP increases the expression of acetyl-CoA synthetase (ACSS2) and ATP-citrate lyase (ACLY), as well as the mitochondrial citrate transporter (SLC25A1), which facilitate the flux of carbons into lipids from acetate and citrate, respectively[11–14]. IDH1 is another enzyme that can support lipogenesis either through NADPH production or, through reductive carboxylation, facilitating flux of carbon to lipids[15–17]. The *IDH1* promoter has an identifiable consensus SRE, and a previous study using *in vitro* electrophoretic mobility shift and reporter assays found that SREBP could bind directly to this sequence[18]. However, the extent to which SREBP regulates *IDH1* gene expression and the downstream consequences were not determined.

IDH1 catalyzes the reversible NADPH-dependent decarboxylation of cytosolic isocitrate to α-ketoglutarate (α-KG). This reaction is also carried out by IDH2 and IDH3 in the mitochondrial matrix as part of the tricarboxylic acid (TCA) cycle. Unlike IDH3, IDH1 and IDH2 can catalyze the reductive carboxylation of α-KG to isocitrate[16,17,19,20]. By bypassing the oxidative TCA cycle, reductive carboxylation creates a more direct flux of glutamine-derived carbons to produce the cytosolic acetyl-CoA required *de novo* lipogenesis. In addition, *IDH1* and *IDH2* are oncogenes that are frequently mutated in low grade gliomas and leukemias, respectively[21,22]. The oncogenic mutations primarily affect the same catalytic arginine residue in IDH1 (R132) and IDH2 (R172) and are neomorphic in nature. Oncogenic IDH1 and IDH2 lose the ability to produce isocitrate and convert α-KG to 2-HG, the levels of which are greatly elevated in the tumors and plasma of patients harboring these mutations[23,24]. 2-HG is an

oncometabolite that closely resembles α-KG and, therefore, inhibits α-KG-dependent enzymes, which promotes tumor development through epigenetic changes influencing cellular differentiation[25–27]. Here, we present evidence for the transcriptional activation of IDH1 by SREBP in both wild-type and mutant-IDH1 cells and human cancers and report on the metabolic effects of this regulation.

3.3 MATERIALS AND METHODS

Cell culture

Human cell lines derived from different cancer lineages (denoted) were obtained from the American Type Culture Collection (ATCC). 786-O (renal cell adenocarcinoma), A375 (melanoma), HepG2 (hepatocellular carcinoma), HT1080 (fibrosarcoma), PC3 (prostate adenocarcinoma), SKMEL28 (melanoma), SW1353 (chondrosarcoma), U2OS (osteosarcoma), and U87MG (glioblastoma) cells were cultured in DMEM (CellGro), whereas HCT116 (colorectal carcinoma), MDA-MB-468 (breast adenocarcinoma), and MDA-MB-453 (breast carcinoma) cells were cultured in RPMI-1640, both supplemented with 10% fetal bovine serum (FBS), at 37°C and 5% CO_2. The isogenic $IDH1^{+/+}$ and $IDH1^{R132C/+}$ HCT116 cell lines were obtained from Horizon Discovery (HD 104-021, HD PAR-073). Lipid-deficient FBS was made by mixing FBS with 20 mg/ml fumed silica (S5130, Sigma) for 3 h before removing the silica by centrifugation at 1717 g for 15 min. Cells were cultured in 10% lipid-deficient FBS for the duration of each experiment, or starting 24 hours after siRNA transfection for knockdown experiments. All siRNA experiments used ON-TARGETplus SMARTpool siRNAs (30 nM) (GE/Dharmacon) targeting human *SREBF1* (L-006891-00), *SREBF2* (L-009549-00), or *IDH1* (L-008294-01) for reverse transfection into cells using Lipofectamine RNAiMAX (Invitrogen), according to the manufacturer's instructions. 25-hydroxycholesterol (H1015), Atorvastatin (PZ0001), and Simvastatin (S6196) were purchased from Sigma.

Immunoblotting

Cells were lysed in ice-cold NP-40 buffer (40 mM HEPES, pH 7.4; 400 mM NaCl; 1 mM EDTA, pH 8.0; 1% NP-40 (CA-630, Sigma); 5% glycerol; 10 mM pyrophosphate; 10 mM β-glycerophosphate; 50 mM NaF; 0.5 mM orthovanadate) containing Protease Inhibitor Cocktail (P8340, Sigma) and 1 mM DTT. The following antibodies were used for detection of proteins transferred to nitrocellulose membranes after SDS-PAGE: Actin (A5316, Sigma), FASN (3180, Cell Signaling Technologies (CST)), IDH1 (8137, CST), IDH2 (ab55271, Abcam), SCD (2438, CST), SREBP1 (sc-8984, Santa Cruz), SREBP2 (557037, BD Biosciences). SREBP blots are of the full-length precursor (P), unless indicated otherwise as the mature active form (M).

mRNA expression analysis

Complimentary DNA was synthesized with the Superscript III First Strand Synthesis System (Invitrogen) from RNA isolated using the RNeasy Mini Kit (Qiagen). SYBR-Green (Applied Biosystems) was used for qRT-PCR (Applied Biosystems 7300 Real Time PCR System). Each sample was run in technical triplicates and normalized to *RPLP0* expression. The following forward and reverse primer sequences were used:

RPLP0 (F 5′-CAGATTGGC TACCCAACTGTT-3′, R 5′-GGGAAGGTGTAATCCGTCTCC-3′),

FASN (F 5′-AAGGACCTGTCTAGGTTTGATGC-3′, R 5′-TGGCTTCATA GGTGACTTCCA-3′),

IDH1 (F 5’-ATAATGTTGGCGTCAAATGTGC-3’, R 5’-CTTGAACTCCTCAACCCTCTTC-3’),

IDH2 (F 5’-CGCCACTATGCCGACAAAAG-3’, R 5’-ACTGCCAGATAATACGGGTCA-3’),

LDLR (F 5’-TCTGCAACATGGCTAGAGACT-3’, R 5’-TCCAAGCATTCGTTGGTCCC-3’),

SCD (F 5′-CCCAGCTGTCAAAGAGAAGG-3′, R 5′-CAA GAAAGTGGCAACGAACA-3′),

SREBF1 (F 5′-TGCATTTT CTGACACGCTTC-3′, R 5′-CCAAGCTGTACAGGCTCTCC-3′),

SREBF2 (F 5′-TG GCTTCTCTCCCTACTCCA-3′, R 5′-GAGAGGCACAGGAAGGTGAG-3′).

***De novo* lipid synthesis**

Cells were cultured in low glucose (1 mM) DMEM containing 10% lipid-deficient FBS for 48 h prior to extraction of lipids with 2:1 chloroform/methanol using the Folch method, as described previously [3]. Cells were labeled for the final 4 h with 5 μCi/ml [1-^{14}C]-acetate (NEC084H001MC, Perkin Elmer) or [U-^{14}C]-glucose (NEC042V250UC, Perkin Elmer). Cells labeled with [U-^{14}C]-glutamine (NEC451050UC, Perkin Elmer) were cultured similarly but in the absence of cold glutamine during the 4-h labeling. Extracted ^{14}C-labeled lipids were quantified from biological duplicates using a LS6500 scintillation counter (Beckman Coulter) and normalized to protein concentration. Data shown are the composite of 2 independent experiments.

Analysis of TCGA data

TCGA gene expression data from the breast carcinoma (n=1100), prostate adenocarcinoma (n=498), colorectal adenocarcinoma (n=382), hepatocellular carcinoma (n=373), lung adenocarcinoma (n=517), cutaneous melanoma (n=471), and lower grade glioma (n=530) datasets were downloaded from cBioPortal[28–35]. Mutation data from TCGA was used to identify samples in the lower grade glioma dataset with oncogenic mutations in IDH1 (n=221). The SREBP gene signature was calculated using a cumulative average gene expression of *ACACA*, *FASN*, *HMGCR*, *HMGCS1*, and *LDLR*. Samples that were greater than or less than one standard deviation from the mean were considered "High" or "Low", respectively. Average RNA expression for *IDH1*, *SCD*, or *IDH2* was calculated for samples in each category.

Metabolic flux analysis

Intracellular metabolites were extracted for LC-MS/MS analysis with -80°C methanol (80%) as described previously[36,37]. Briefly, cells were harvested from culture dishes after incubation with 80% methanol on dry ice for 20 min. Three extractions were performed in ice-cold 80% methanol, and the supernatants were pooled following each centrifugation. Collected supernatants were dried under a steady stream of nitrogen gas (N-EVAP, Organomation Associates, Inc). Dried pellets were resuspended in

water just prior to injection into a 5500 QTRAP hybrid triple quadrupole mass spectrometer (AB/SCIEX), with selected reaction monitoring (SRM) and polarity switching between positive and negative modes, coupled to a Prominence UFLC HPLC system (Shimadzu) with Amide XBridge HILIC chromatography (Waters). Peak area from the total ion current for each metabolite SRM transition was integrated using MultiQuant v2.0 software (AB/SCIEX). Custom SRMs were created to detect incorporation of ^{13}C into 2-HG using targeted LC-MS/MS [2-HG (m+2): Q1=149.1; Q3=130.7; Collision Energy=-17]. Cells used for glucose flux analysis were washed with PBS prior to incubation for 20 min in media containing 4 mM [U-^{13}C]-glucose (CLM-1396-1, Cambridge Isotope Laboratories).

Statistical analysis

All data were analyzed with GraphPad Prism and shown as mean ± s.e.m. P-values for qRT-PCR were calculated by one-way ANOVA with a Tukey HSD post-hoc test. Significance for all other experiments was calculated by an unpaired two-tailed Student's t-test. In both cases, significance was reached if $p<0.05$. The number of independent experiments (n) is provided in each figure legend, and composite data from these experiments are graphically presented, unless otherwise noted.

3.4 RESULTS

3.4.1 IDH1 expression is regulated by SREBP

To determine whether SREBP regulates IDH1, a panel of 11 cancer cell lines from distinct cancer lineages was cultured in lipid-deficient media to activate SREBP, and the effects of siRNA-mediated depletion of SREBP1, SREBP2, or both on gene expression were measured. The transcripts for canonical SREBP targets, *SCD* and *LDLR*, were significantly decreased upon SREBP isoform depletion, with the relative contributions from SREBP1 and 2 varying between cell lines and the most pronounced decreases arising from knockdown of both isoforms (Figures 3.1A, 3.2, and 3.3A). As we have found in other

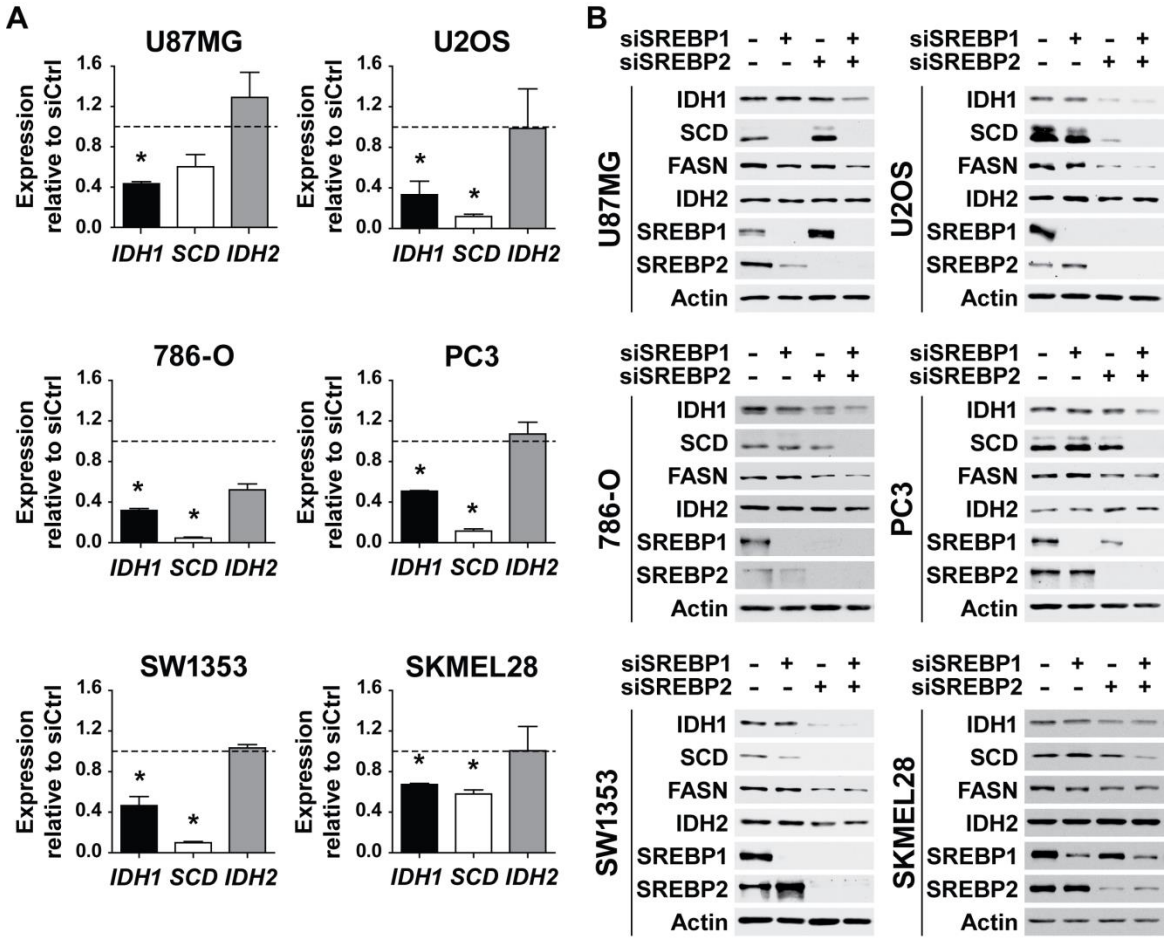

Figure 3.1. SREBP1/2 depletion decreases IDH1 expression in a panel of cancer cell lines.

(**A**) RNA isolated from cell lines 48 h post-transfection with nontargeting siRNAs or siRNAs targeting both SREBP1 and SREBP2 was used for qRT-PCR. Transcript levels for *IDH1*, *IDH2*, and *SCD* following SREBP1/2 knockdown are shown as mean ± s.e.m. relative to cells transfected with nontargeting siRNAs (siCtrl), n=2. *P>0.05. (**B**) Immunoblots of lysates from cells 72 h post-transfection with siRNAs targeting SREBP1, SREBP2, or both are shown compared to control siRNAs (-), and are representative of at least two independent experiments for each cell line.

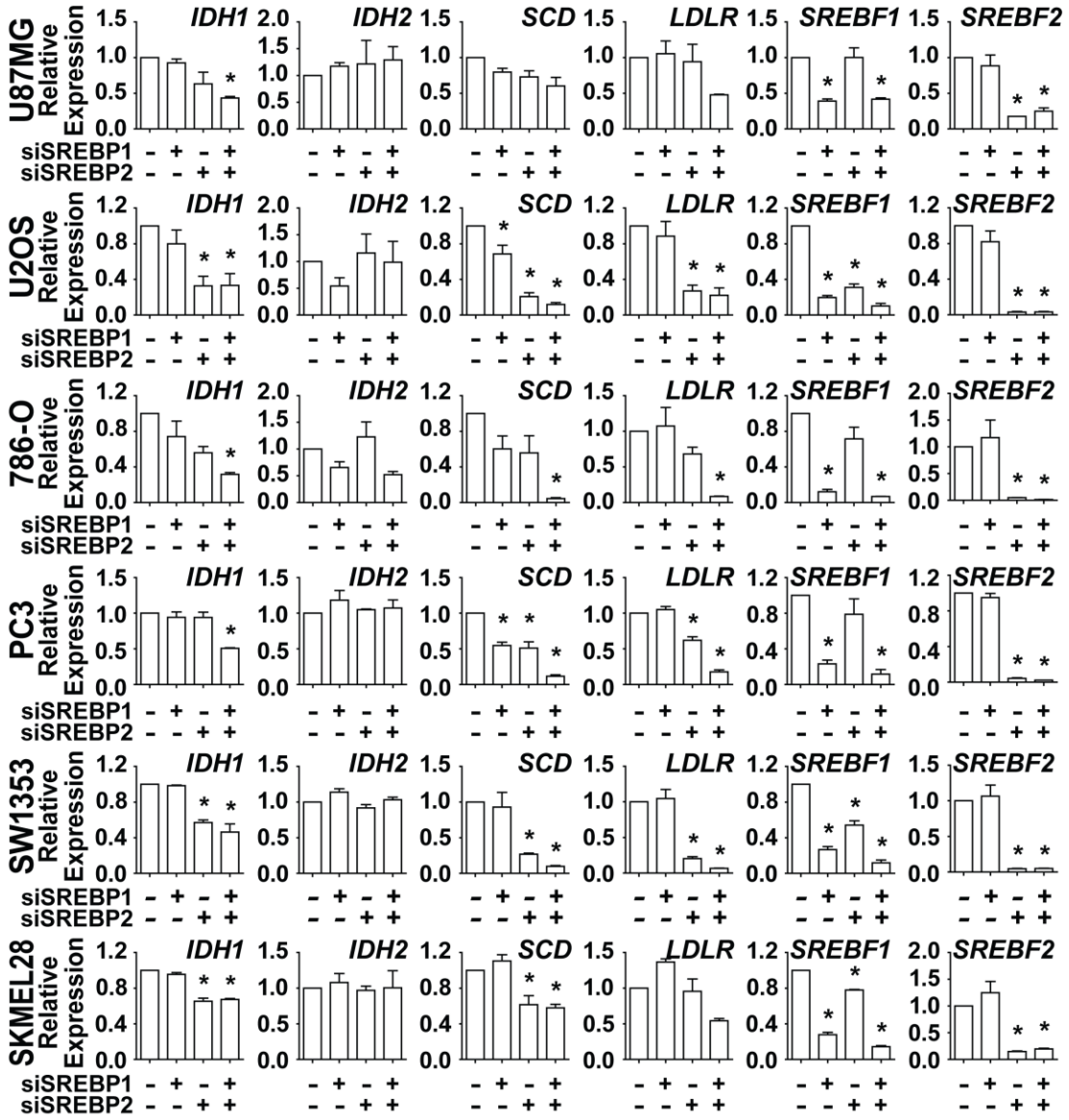

Figure 3.2. Expanded view of the effects of SREBP knockdown in six different cell lines, in support of Figure 3.1A.

RNA from the given cell lines transfected with nontargeting siRNAs or siRNAs targeting SREBP1, SREBP2, or both was subject to qRT-PCR analysis. Transcript levels are shown as mean ± s.e.m. relative to cells transfected with nontargeting siRNA (-), n=2. *P<0.05.

Figure 3.3. Varying effects of SREBP knockdown between cell lines.

(**A**) RNA was isolated from the given cell lines 48 h post-transfection with nontargeting siRNAs (-) or siRNAs targeting SREBP1, SREBP2, or both for analysis by qRT-PCR. Transcript levels are shown as mean ± s.e.m. relative to cells transfected with nontargeting siRNA, n=2. *P<0.05. (**B**) Cells transfected with siRNAs as in (**A**) were lysed 72 h post-transfection for immunoblot analysis. Data shown are representative of at least two independent experiments for each cell line.

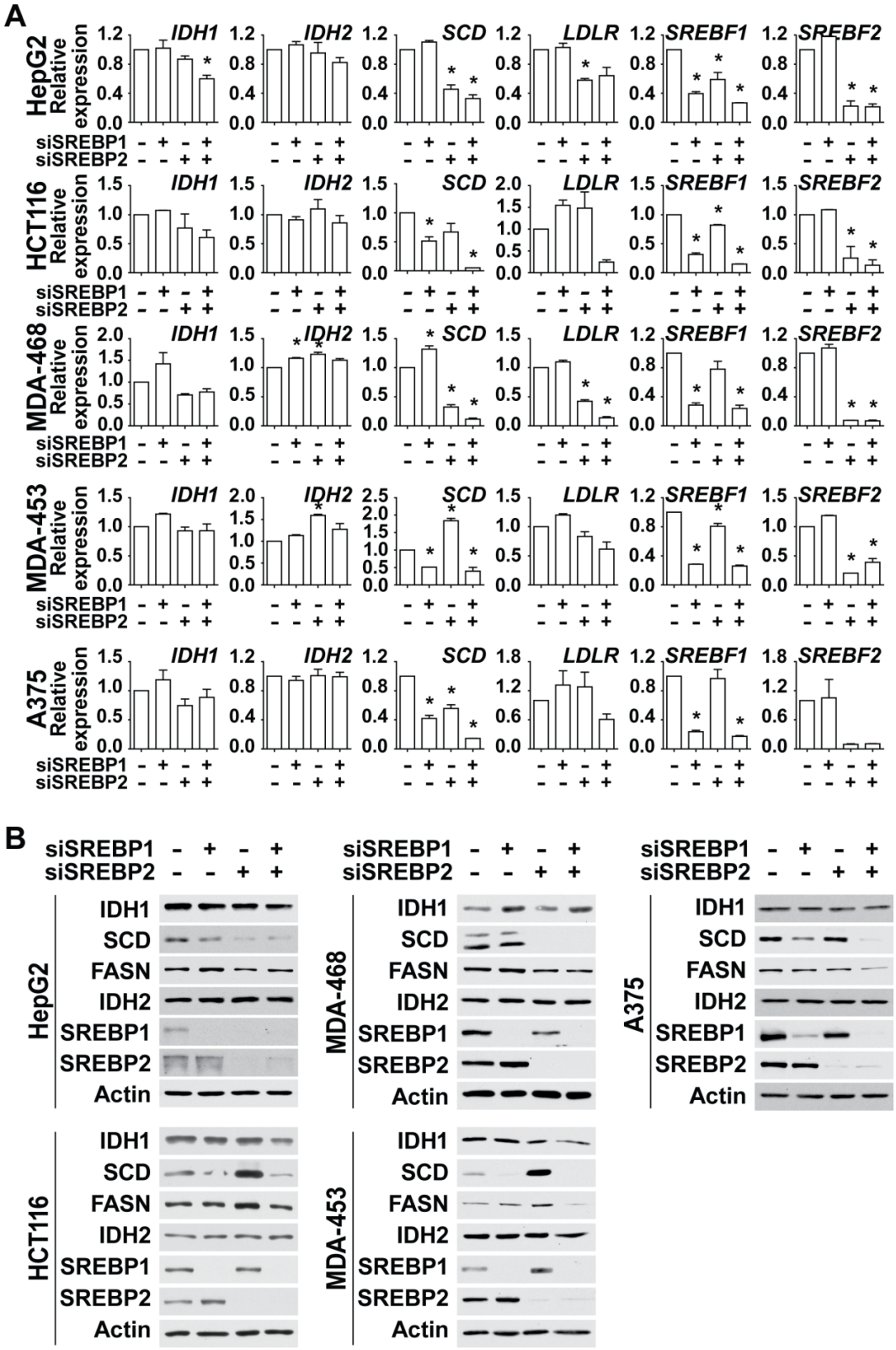

Figure 3.3 (Continued)

cancer cells[3], SREBP2 depletion significantly decreases expression of SREBP1 in a subset of cell lines (Figures 3.1B, 3.2, and 3.3A,B), consistent with the existence of SREs in the promoter of the *SREBF1* gene and cross regulation between these transcription factors[38]. *SCD* expression was significantly decreased by SREBP-depletion in 10 of the 11 cell lines, whereas *LDLR* expression was significantly decreased in only 6 of 11 lines. Consistent with *IDH1* being a shared target of SREBP1 and 2 in these settings, transcript levels of *IDH1* were significantly decreased by the combined knockdown of SREBP isoforms in 7 of the 11 cell lines tested (Figures 3.1A, 3.2, and 3.3A). However, *IDH2* expression was not affected by SREBP depletion in any of these cell lines. Corresponding to these transcriptional changes were decreases in the protein level of IDH1, but not IDH2, following SREBP knockdown (Figures 3.1B and 3.3B). Compared to the SCD protein, which turns over rapidly, the effects of SREBP depletion on IDH1 protein levels were more modest but at least as pronounced as the canonical SREBP target fatty acid synthase (FASN), which is very stable[39].

To assess whether *IDH1* expression is associated with SREBP activation in human cancers, we analyzed publicly available gene expression data from six different cancer lineages (breast, prostate, colorectal, hepatocellular, lung, and melanoma) through The Cancer Genome Atlas (TCGA)[31–35]. For these analyses, we used an SREBP gene signature based on five well-established SREBP1/2 gene targets (*ACACA*, *FASN*, *HMGCR*, *HMGCS1*, and *LDLR*). In 5 of the 6 cancer settings, tumors with high mRNA levels of canonical SREBP targets had significantly elevated expression of *IDH1*, as well as the established SREBP target *SCD*, relative to those with low expression of canonical SREBP targets (Figure 3.4). However, *IDH2* mRNA levels did not correlate with those of SREBP targets. These collective data are consistent with *IDH1* being a transcriptional target of SREBP in the majority of cancer cell lines and human tumors.

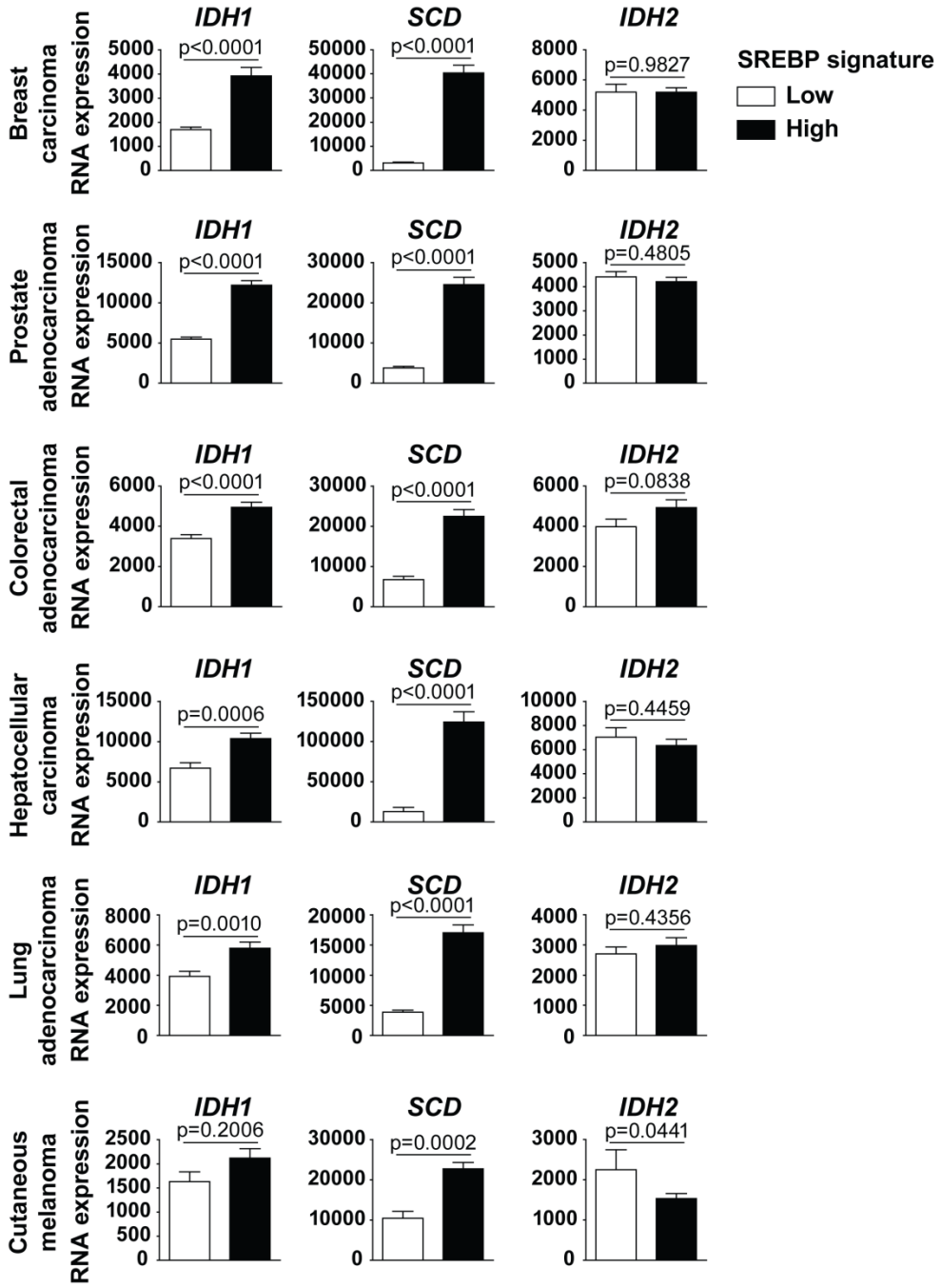

Figure 3.4. Expression of *IDH1* in human cancers is associated with mRNA levels of canonical SREBP targets.

IDH1, *SCD*, and *IDH2* expression in tumors from TCGA datasets for each given cancer, comparing tumors with low and high expression of a defined set of established SREBP targets.

3.4.2 SREBP and IDH1 facilitate carbon flow from glutamine to lipids

We hypothesized that IDH1, as a downstream target of SREBP, might contribute to *de novo* lipid synthesis from different carbon sources. Cells can produce the cytosolic acetyl-CoA required for lipid synthesis using carbons from exogenous acetate, glucose, or glutamine (Figure 3.5A). We compared the effects of siRNA-mediated depletion of SREBP1/2 or IDH1 on *de novo* lipogenesis from these carbon sources by labeling U87MG and U2OS cells with ^{14}C-acetate, ^{14}C-glucose, or ^{14}C-glutamine. As expected, SREBP knockdown significantly decreased incorporation of ^{14}C from all three carbon sources into the lipid fraction, with the most pronounced effects on acetate and glutamine labeling (Figures 3.5B and C). However, IDH1 knockdown only decreased the incorporation of ^{14}C-glutamine into lipids, without decreasing lipid synthesis from acetate or glucose. Interestingly, ^{14}C-glucose-derived lipids were elevated by IDH1 depletion in the U87MG cells (Figure 3.5B). These data suggest that IDH1 is regulated by SREBP, at least in part, due to its role in facilitating carbon flux from glutamine into lipid.

3.4.3 The SREBP-regulating compounds 25-hydroxycholesterol and statins exert reciprocal effects on IDH1 expression

Since SREBP processing and activity are strongly affected by sterol abundance in cells, we tested the effects of exogenous cholesterol and inhibitors of cholesterol synthesis (i.e., statins) on IDH1 expression (Figure 3.6A). 25-Hydroxycholesterol (25-HC) potently inhibits SREBP processing, while statins activate SREBP by reducing intracellular cholesterol through inhibition of 3-hydroxy-3-methylglutaryl (HMG)-CoA reductase (HMGCR), a key enzyme in the sterol synthesis pathway[40]. Culturing three distinct cell lines (U87MG, U2OS, and HCT116) in the presence of 25-HC for two days suppressed expression of the canonical SREBP targets *SCD* and *LDLR* (Figures 3.6B and 3.7A), consistent with the inhibition of SREBP processing (Figure 3.6C). Importantly, 25-HC also suppressed the expression of *IDH1* transcripts, without effects on *IDH2* expression (Figure 3.6B). A time course of 25-HC treatment demonstrated that protein levels of IDH1, but not IDH2, were substantially reduced by

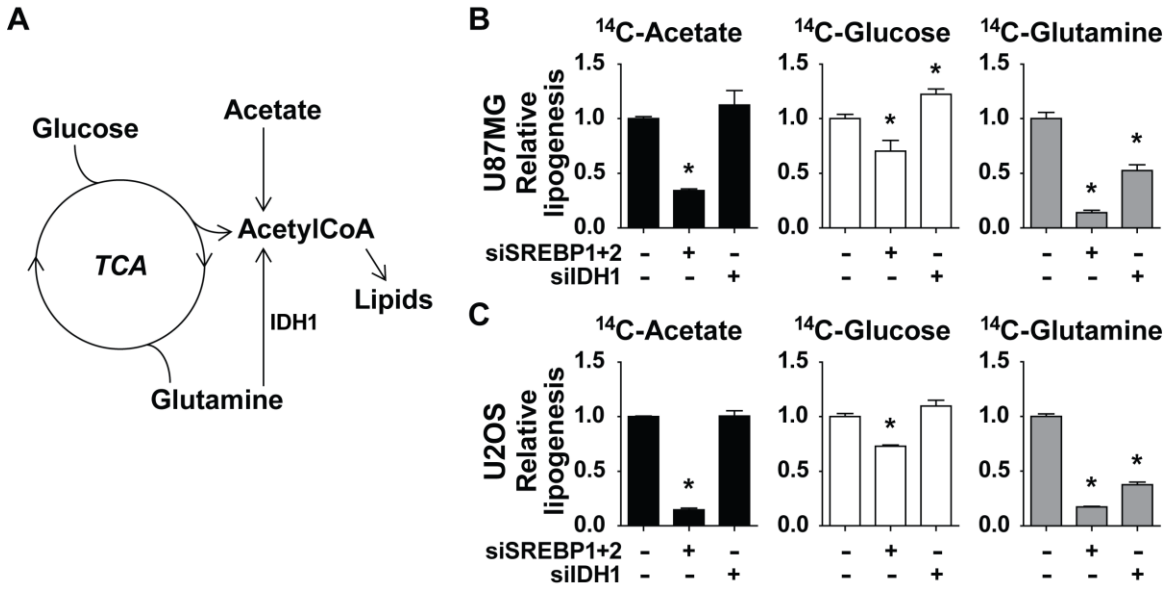

Figure 3.5. Effects of SREBP and IDH1 on *de novo* lipid synthesis from different carbon sources. (**A**) Diagram of the distinct paths of carbon from acetate, glucose, and glutamine to the acetyl-CoA required for lipid synthesis. (**B,C**) Incorporation of [1-^{14}C]-acetate, [U-^{14}C]-glucose, or [U-^{14}C]-glutamine into the lipid fraction was measured in U87MG (**B**) and U2OS (**C**) 72 h post-transfection with siRNAs targeting SREBP1 and 2 or IDH1. Data are shown as mean ± s.e.m. relative to cells transfected with nontargeting control siRNAs (-), n=2. *P>0.05.

Figure 3.6. Reciprocal regulation of SREBP processing by 25-HC or statins respectively inhibits or activates IDH1 expression.

(**A**) Diagram of the effects of cholesterol and statins on SREBP processing. (**B**) qRT-PCR analyses of RNA from the given cells treated with 25-HC (1 μg/ml) for 48 h. (**C**) Cells were treated for 0, 1, 2, or 3 days with 25-HC prior to lysis for immunoblot analysis. (**D**,**E**) Cells were treated with (**D**) atorvastatin (5 μM) or (**E**) simvastatin (5 μM) for 48 h prior to qRT-PCR analysis. (**F**) Cells were treated for 0, 1, or 2 days with atorvastatin or simvastatin prior to lysis immunoblot analysis. (**B**-**E**) All transcript levels are shown as mean ± s.e.m. relative to untreated cells, $n \geq 2$ (*$P < 0.05$), and immunoblots shown are representative of at least two independent experiments. (**C,F**) (P) Precursor, full-length SREBP2; (M) Mature, active SREBP2.

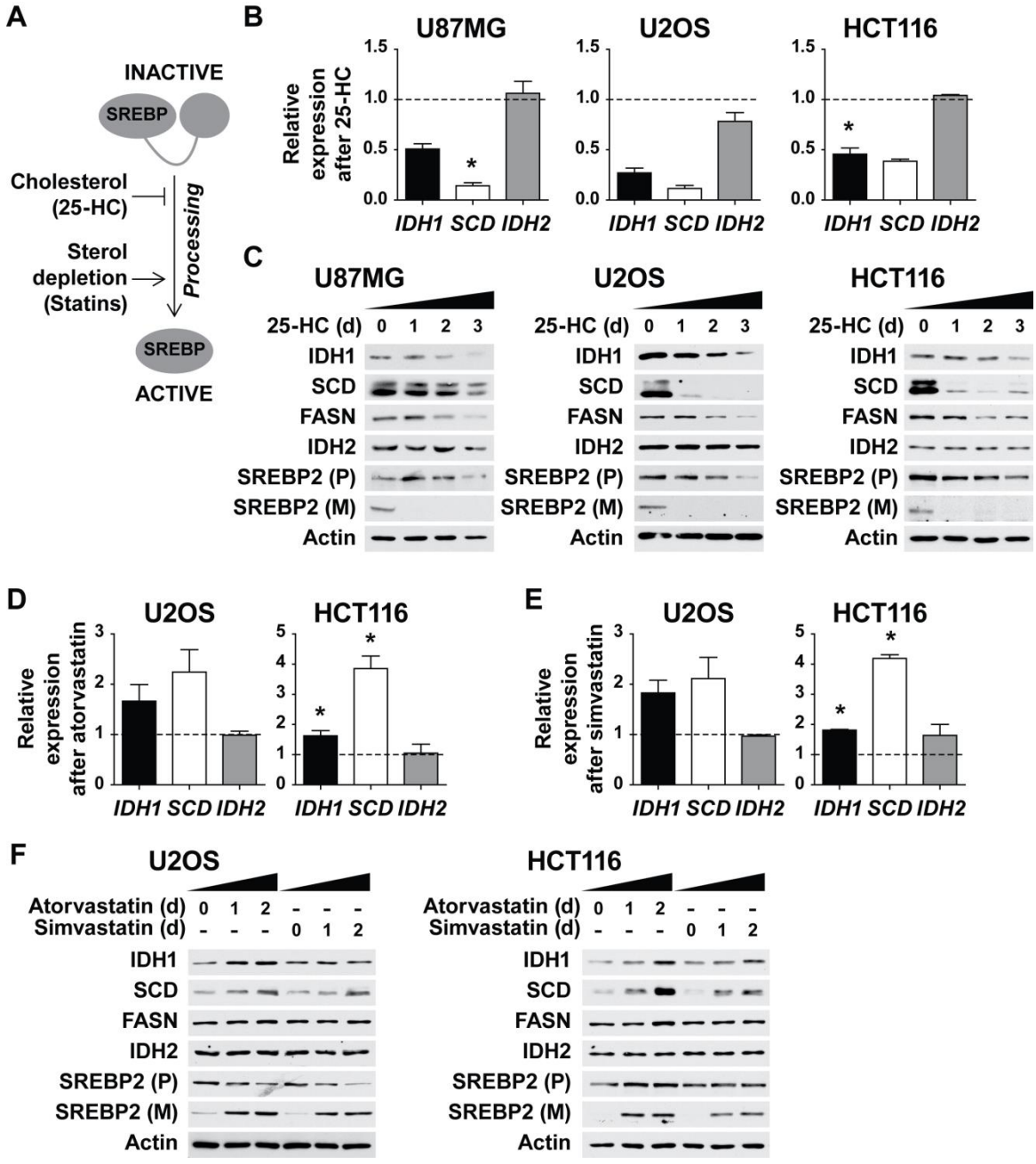

Figure 3.6 (Continued)

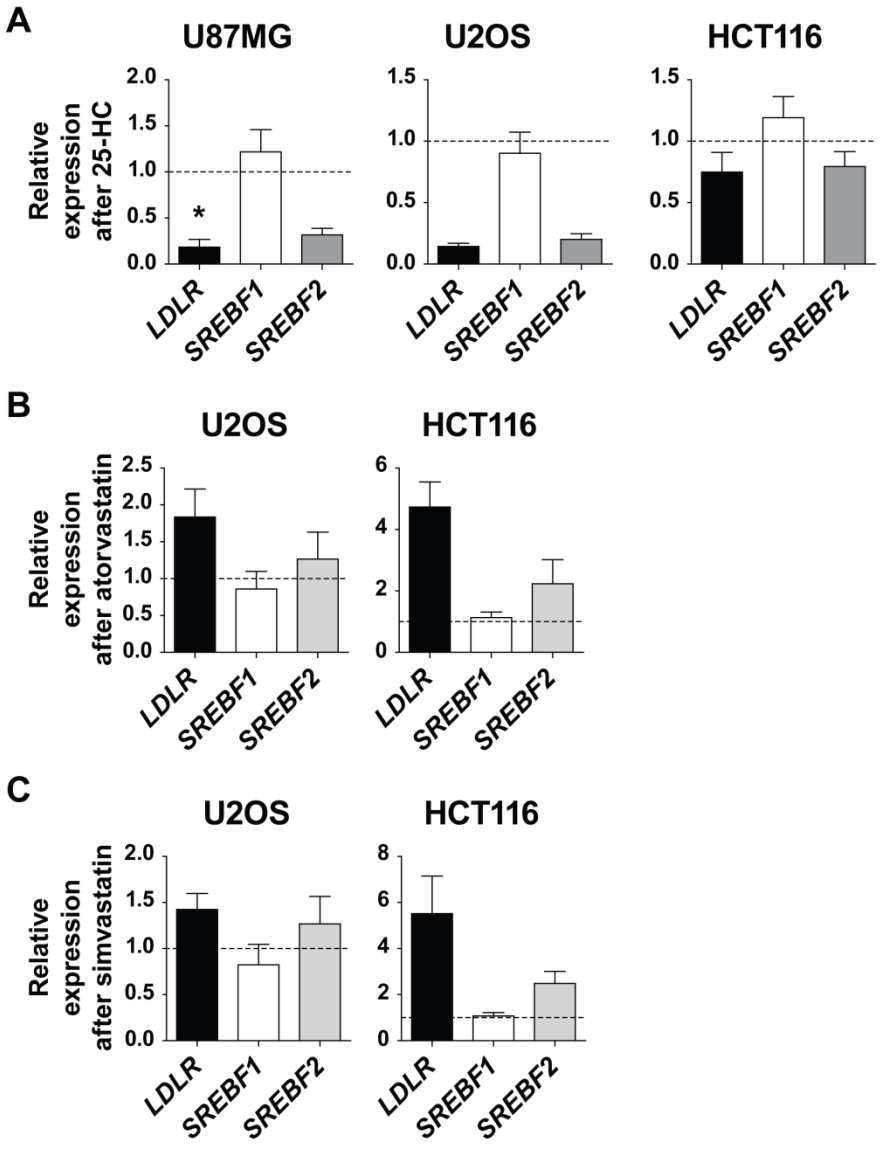

Figure 3.7. Effects of 25-HC and statins on *SREBP* and *LDLR* transcript levels, in support of Figure 3.6.

(**A**) Using the same samples as in Figure 3.6B, qRT-PCR analyses of RNA from the given cells treated with 25-HC (1 μg/ml) for 48 h is shown. (**B**,**C**) Using the same samples as in Figures 3.6D and E, cells were treated with (**B**) atorvastatin (5 μM) or (**C**) simvastatin (5 μM) for 48 h prior to qRT-PCR analysis on isolated RNA. All transcript data are shown as mean ± s.e.m. relative to untreated cells, n≥2. *P<0.05.

2 to 3 days, similar to FASN in these cell lines (Figure 3.6C). While the U87MG cells failed to respond to statins (data not shown), treatment of U2OS and HCT116 cells with either atorvastatin (Figures 3.6D and 3.7B) or simvastatin (Figures 3.6E and 3.7C) induced SREBP processing (Figure 3.6F)and increased expression of *SCD* and *LDLR*. Likewise, *IDH1* transcript levels were increased by both statins (Figures 3.6D and E). This effect was also reflected in increased IDH1 protein abundance starting 24 hours after statin treatment (Figure 3.6F), with atorvastatin more potently inducing increases in both IDH1 and SCD. As seen with 25-HC, neither IDH2 transcript nor protein levels were affected by statin treatment. These findings support the siRNA-depletion data above and further establish a role for SREBP in promoting IDH1 expression.

3.4.4 SREBP regulates oncogenic IDH1

We next wanted to determine whether SREBP also influenced expression of the IDH1 oncogene. Given that *IDH1* mutations occur in more than 70% of low grade glioma, we analyzed publicly available data to determine whether *IDH1* expression correlates with an SREBP activation gene signature in these tumors[30,41]. Consistent with data from other cancers (Figure 3.4), low grade glioma samples with high mRNA levels of canonical SREBP targets had significantly higher *IDH1* and *SCD* expression relative to those with low expression of SREBP targets (Figure 3.8A). Importantly, this association was also observed when analyzing only those low grade glioma samples with known *IDH1* mutations (Figure 3.8B). In both analyses, *IDH2* mRNA levels did not correlate with levels of SREBP targets. These data suggest that the activation state of SREBP might influence expression of the *IDH1* oncogene.

Established glioma cell lines with IDH1 mutations are not readily available. Therefore, to address whether SREBP can influence the expression of oncogenic IDH1, we used both a fibrosarcoma-derived cell line with a naturally occurring $IDH1^{R132C}$ mutation (HT1080) and an engineered HCT116 line with a knock-in of the same mutation. As observed in *IDH1*-wild-type cells, SREBP depletion decreased *SCD* and *LDLR* transcript levels, with the strongest effect resulting from the combined SREBP1/2 double

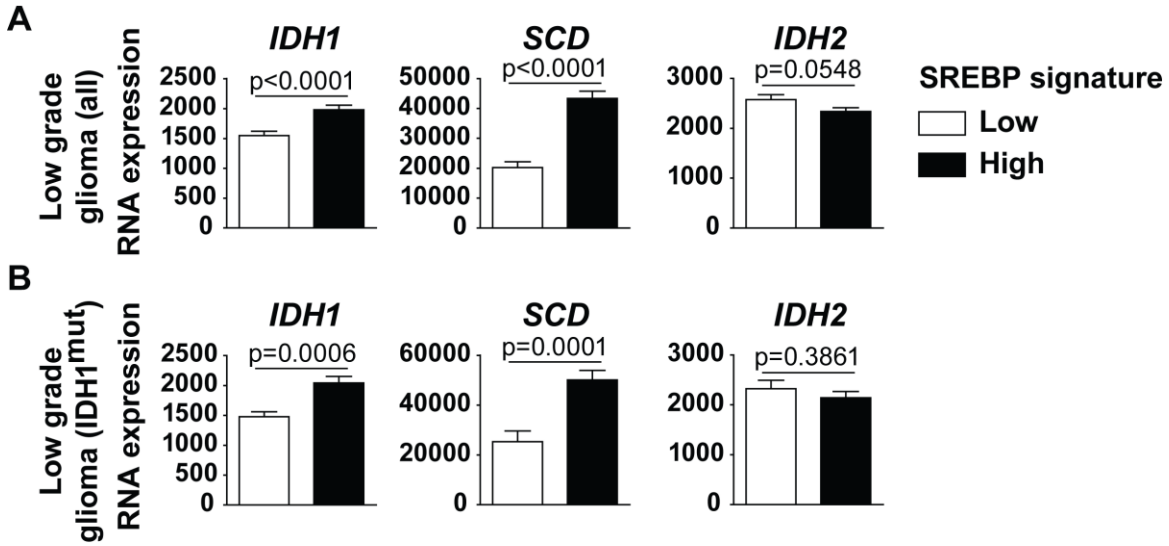

Figure 3.8. Expression of *IDH1* in low grade glioma is associated with mRNA levels of canonical SREBP targets.

(**A**,**B**) *IDH1*, *SCD*, and *IDH2* expression in tumors from either (**A**) the entire lower grade glioma TCGA dataset or (**B**) the subset of these with oncogenic mutations in *IDH1*, comparing tumors with low and high expression of a defined set of established SREBP targets.

knockdown (Figures 3.9A and 3.10A). *IDH1* transcript levels were also decreased by SREBP knockdown in these lines. Consistent with these mRNA changes, SREBP1/2 knockdown decreased IDH1 and SCD protein levels, and to a lesser extent FASN levels (Figure 3.9B), without effects on IDH2. The effects of SREBP depletion on the protein levels of these SREBP targets were more modest in the engineered HCT116-IDH1$^{R132C/+}$ line. IDH2 transcript and protein levels were unchanged in the HCT116-IDH1$^{R132C/+}$ cells and were significantly increased, rather than decreased, by SREBP1 knockdown in the HT1080 cells (Figures 3.9A,B and 3.10A).

To determine whether regulation of SREBP activation by sterols was also able to affect IDH1 expression in *IDH1*-mutant cells, HT1080 and HCT116-IDH1$^{R132C/+}$ cells were cultured in the presence of 25-HC or statins for 2 days. As expected, *SCD* and *LDLR* mRNA expression were decreased by 25-HC treatment (Figures 3.9C and 3.10B). *IDH1* expression was likewise decreased by 25-HC, while *IDH2* expression remained unchanged. As in other cellular settings (Figure 3.6), blocking SREBP processing with 25-HC decreased SCD protein levels by 24 hours, whereas a decrease in FASN protein was only detectable after 2 or 3 days (Figures 3.9D and 3.10C). 25-HC decreased IDH1 protein levels after 1 day, with a more substantial decrease by 2 or 3 days, without effects on IDH2. Conversely, statin-mediated promotion of SREBP activation increased *IDH1* transcript levels, as well as *SCD* and *LDLR*, in the IDH1 mutant cell lines treated with either atorvastatin (Figures 3.9E and 3.10C) or simvastatin (Figures 3.9F and 3.10D). Immunoblots confirmed that statin treatment increased SREBP processing and SCD protein levels and in both cell lines, but FASN protein levels were only increased in the statin-treated HT1080 cells, not the HCT116-IDH1$^{R132C/+}$ cells (Figure 3.9G). Similarly, IDH1 protein levels were increased in both cell lines after 1 day of treatment with statins, with more pronounced changes in the HT1080 cells. Collectively, these data indicate that SREBP can promote IDH1 expression in cells with both wild-type and oncogenic IDH1.

Since the IDH1^{R132C} mutant produces the oncometabolite 2-HG and SREBP can regulate the expression of this oncogene, we tested whether SREBP could affect 2-HG production in *IDH1*-mutant

Figure 3.9. SREBP regulates IDH1 expression in IDH1^{R132C}-mutant cells.

(**A**) qRT-PCR analysis of RNA isolated from the given cells 48 h post-transfection with nontargeting siRNAs or siRNAs targeting both SREBP1 and SREBP2. Transcript levels for *IDH1*, *SCD*, and *IDH2* following SREBP1/2 knockdown are shown as mean ± s.e.m. relative to cells transfected with nontargeting siRNA (siCtrl), n=2. (**B**) Cells transfected with nontargeting control siRNAs (-) or those targeting SREBP1, SREBP2, or both were lysed 72 h post-transfection for immunoblot analysis. (**C**,**D**) Cells were treated with 25-HC (1 μg/ml) for (**C**) 48 h prior to RNA isolation for analysis by qRT-PCR or (**D**) 0, 1, 2, or 3 days prior to lysis for immunoblot analysis. (**E-G**) Cells were cultured in the presence of (**E**) atorvastatin (5 μM) or (**F**) simvastatin (5 μM) for 48 h prior to RNA extraction for qRT-PCR analysis or (**G**) for 0, 1, or 2 days prior to lysis for immunoblot analysis. (**C,E**,**F**) Transcript levels are shown as mean ± s.e.m. relative to untreated cells, n=3. *P<0.05. (**B,D,G**) Immunoblots shown are representative of at least 2 independent experiments. (P) Precursor, full-length SREBP2; (M) Mature, active SREBP2.

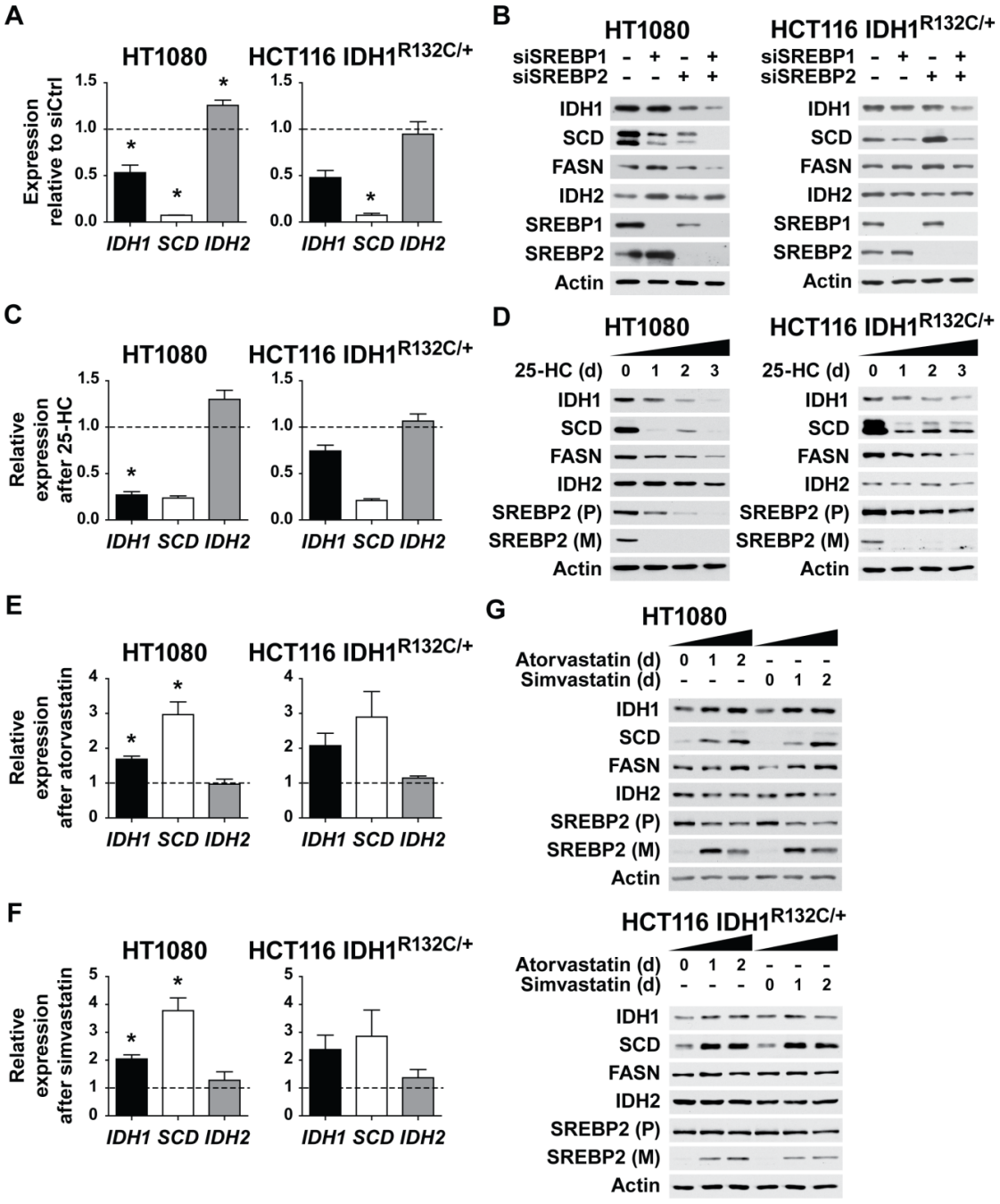

Figure 3.9 (Continued)

Figure 3.10. Expanded view of the effects of SREBP knockdown in *IDH1*-mutant cells lines, in support of Figure 3.9.

(**A**) Using the same samples as in Figure 3.9A, RNA isolated from the given cells was used for qRT-PCR analysis. (**B**) Using the same samples as in Figure 3.9C, qRT-PCR analysis of RNA from given cells treated with 25-HC (1 μg/ml) for 48 h is shown. (**C**,**D**) Using the same samples as in Figures 3.9E and F, RNA from given cells treated with atorvastatin (5 μM) (**C**) or simvastatin (5 μM) (**D**) were used for qRT-PCR analysis. All transcript data are shown as mean ± s.e.m. relative to untreated cells, $n \geq 2$. *$P < 0.05$.

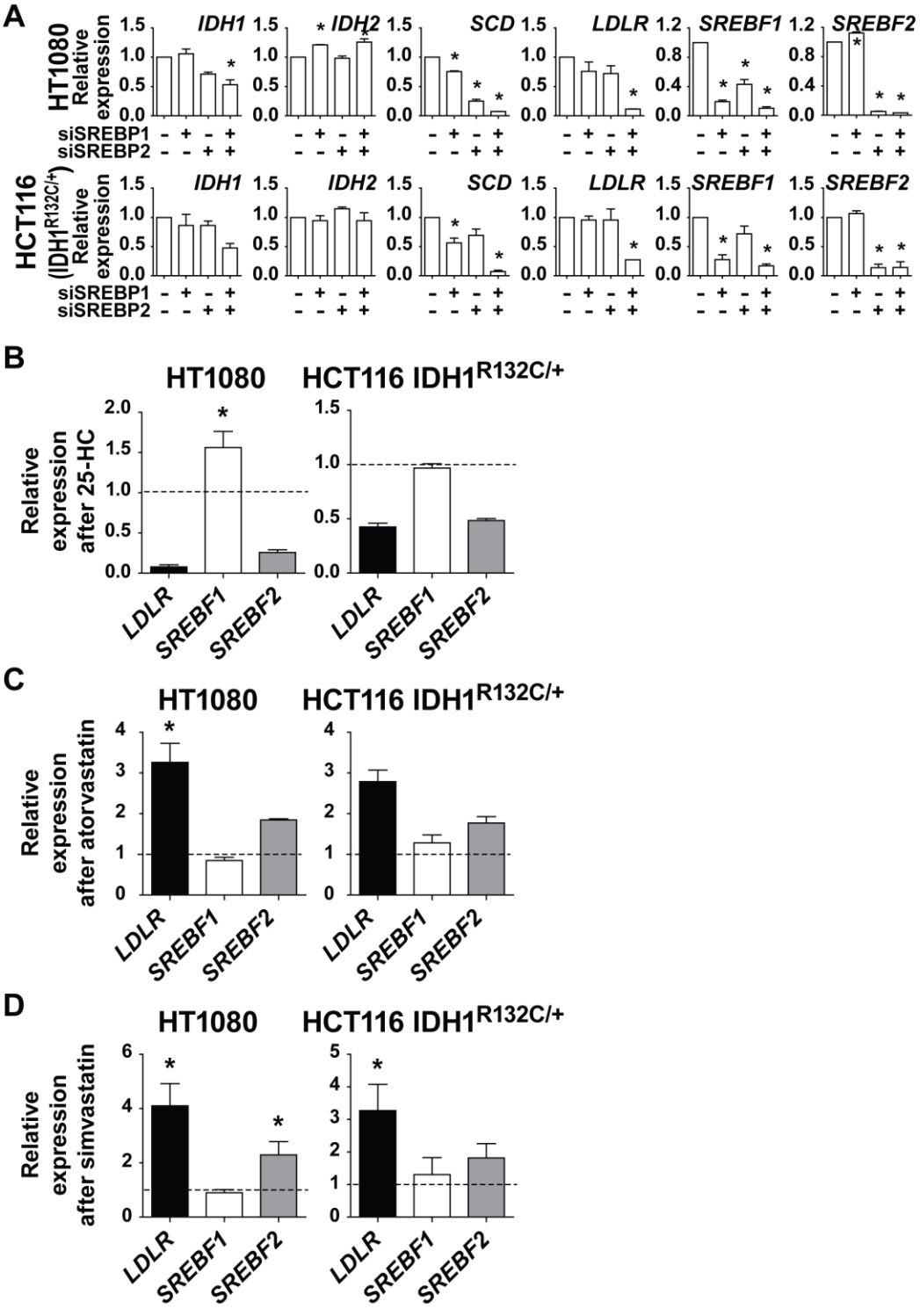

Figure 3.10 (Continued)

cells. We depleted SREBP1/2 or IDH1 using siRNAs in the *IDH1*-mutant HT1080 and HCT116 cells (Figure 3.11A). To detect changes in 2-HG production, we used stable-isotope flux analysis to measure incorporation of carbon from [U-^{13}C]-glucose into 2-HG (Figure 3.11B). 2-HG derived from the labeled glucose contains 2 labeled carbons, and the resulting 2-dalton change in mass can be measured by LC-MS/MS. As confirmation that this approach is measuring oncogenic IDH1 activity, the production of ^{13}C-labeled 2-HG was significantly decreased by IDH1 knockdown in both cell lines, and flux into 2-HG was nearly 30-fold higher in the HCT116-IDH1$^{R132C/+}$ cells than their isogenic wild-type counterparts (Figures 3.11C and D). Depletion of SREBP1/2 in the HT1080 cells led to a significant decrease in glucose flux to 2-HG (Figure 3.11C). In this setting, the level of decrease in labeled 2-HG was proportional to IDH1 protein levels, which are more strongly reduced by knockdown of IDH1 than SREBP (Figure 3.11A). However, despite SREBP knockdown having comparable effects on IDH1 protein levels in HT1080 and HCT116 cells (Figure 3.11A), SREBP knockdown did not decrease 2-HG production in the HCT116-IDH1$^{R132C/+}$ cells. To test whether regulation of SREBP processing by sterols could also influence 2-HG production, we cultured HT1080 cells in the presence of 25-HC or atorvastatin for 2 days, to respectively inhibit or activate SREBP, and measured incorporation of labeled carbon from [U-^{13}C]-glucose into 2-HG. Treatment with 25-HC significantly decreased the flux of glucose into 2-HG, whereas atorvastatin treatment significantly increased it (Figure 3.11E). Taken together, these data suggest that the activation state of SREBP can influence 2-HG production by oncogenic IDH1 in some cellular settings.

3.5 DISCUSSION

The SREBP transcription factors have emerged as major drivers of lipid synthesis in the liver and in cancer[3,8,42,43]. Since *de novo* lipogenesis consumes large quantities of carbon and reducing power in the form of NADPH, cells must adapt their metabolism to provide the necessary substrates. However, little is known about how SREBP coordinates its regulation of lipogenic genes with these auxiliary support

Figure 3.11. SREBP promotes 2-hydroxyglutarate production in IDH1^{R132C}-mutant cells.

(**A**) Cells were lysed for immunoblotting 72 h post-transfection with nontargeting siRNAs (-) or siRNAs targeting SREBP1 and SREBP2 or IDH1. (**B**) Diagram of carbon flux from [U-^{13}C]-glucose into ^{13}C-2-HG (m+2). Filled and empty circles represent ^{13}C and ^{12}C carbons, respectively, with m+6 and m+2 referring to the mass increase from the stable isotope carbons. (**C,D**) Normalized peak areas of ^{13}C-labeled 2-HG (m+2), measured in metabolite extracts by LC-MS/MS, from (**C**) HT1080 and (**D**) isogenic HCT116 cells with wild-type (+/+) or mutant (R132C/+) IDH1 72 h post-transfection with nontargeting control siRNAs (-) or siRNAs targeting SREBP1 and SREBP2 following a pulse label with [U-^{13}C]-glucose for 20 min. (**E**) Normalized peak areas of ^{13}C-labeled 2-HG (m+2) from HT1080 cells cultured for 48 h in the presence of 25-HC (1 μg/ml) or atorvastatin (5 μM) and pulse labeled with [U-^{13}C]-glucose for 20 min. (**C-E**) Data are presented as mean ± s.e.m. of biological triplicates and are representative of at least two independent experiments, *P<0.05 relative to siCtrl (**C,D**) or untreated (**E**) control cells, #P<0.05 relative to wild-type HCT116 cells. (**F**) Model of SREBP-mediated control wild-type and oncogenic IDH1 and *de novo* lipid synthesis.

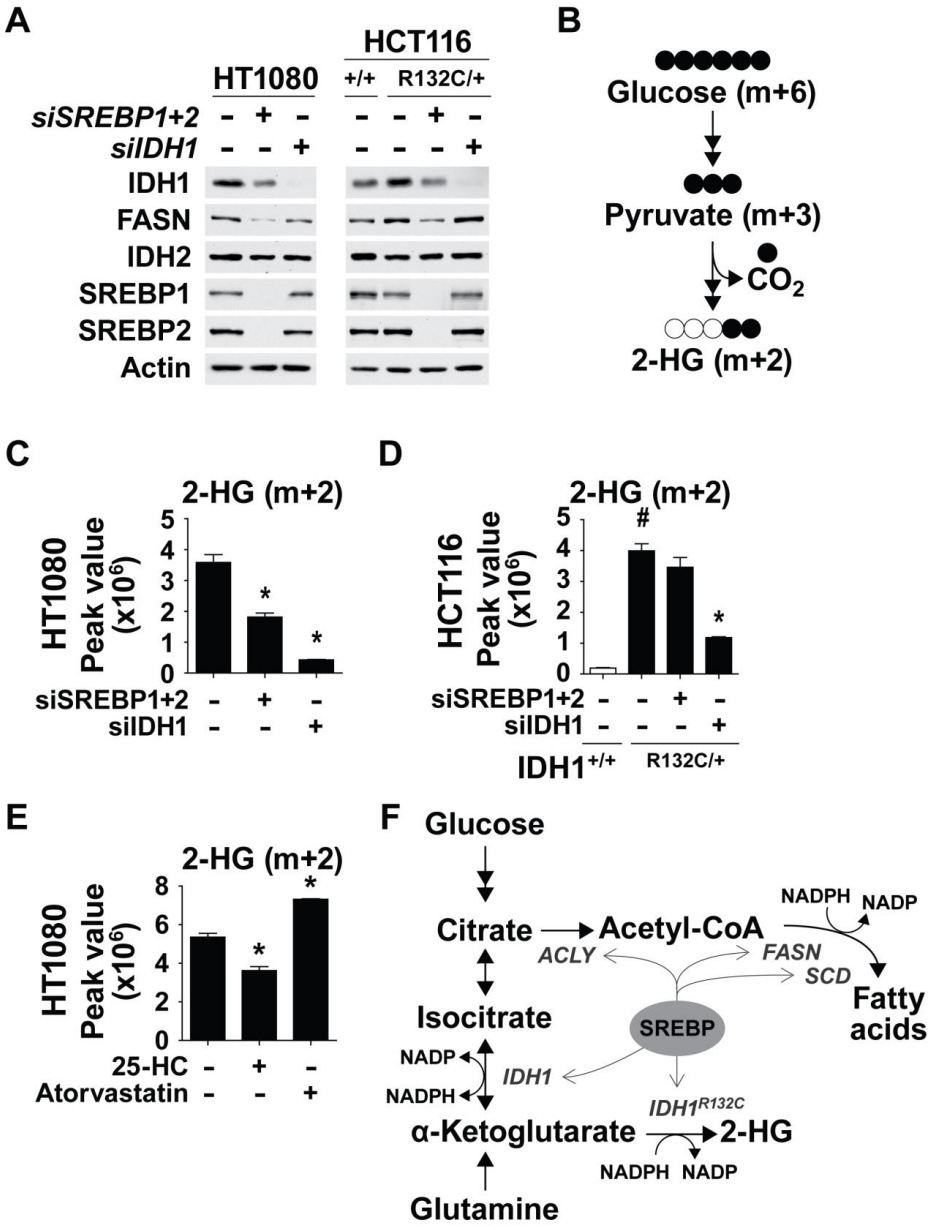

Figure 3.11 (Continued)

processes. In this study, we demonstrate that SREBP activates IDH1 expression in a variety of cell settings. We show that IDH1 supports *de novo* lipogenesis by facilitating the flow of carbons from glutamine to lipids (Figure 3.11F). Furthermore, we reveal that, in *IDH1*-mutant cells, SREBP can activate expression of oncogenic *IDH1* and regulate the production of the oncometabolite 2-HG.

SREBP appears to regulate IDH1 expression in a contextual manner, suggesting other transcription factors also impinging on its regulation in some settings. Consistent with our findings, a review of supplemental data from a transgenic mouse study of SREBP targets in the liver reveals that *IDH1* expression was increased by active versions of either SREBP1 or SREBP2 and was decreased in livers lacking SCAP, which is required for SREBP activation[13]. The transcription factors CHOP and C/EBPβ have been proposed to activate IDH1 expression in response to ER stress, although neither affected basal IDH1 expression [44]. Another study found that the forkhead box O (FOXO) family transcription factors can directly regulate IDH1 expression in certain settings, including the HT1080 cells used in this study [45]. In addition to intracellular sterol levels, reported here, the differential regulation of *IDH1* expression is likely to be dictated by the status of upstream signaling networks in a given setting, as SREBP and FOXO family members are generally activated at opposing times due to their reciprocal regulation by the PI3K-Akt pathway.

The transcriptional control of IDH1 by SREBP is consistent with the central role of SREBP in controlling the expression of enzymes directly and indirectly involved in *de novo* lipogenesis. Under optimal growth conditions, a high ratio of citrate to α-ketoglutarate drives the IDH1 reaction towards production of NADPH[46,47]. However, in conditions of hypoxia or mitochondrial dysfunction, the IDH1 reaction is reversed, favoring the reductive carboxylation of α-ketoglutarate to produce isocitrate[16,17,19]. Here, we find that IDH1 is required for *de novo* lipid synthesis when glutamine is the primary lipogenic carbon source. Consistent with the IDH1 and IDH2 enzymes playing a minor role in cellular NADPH/ NADP+ homeostasis[48], NADPH production by IDH1 does not appear to be a major contributor to

lipogenesis in our experimental settings, given that glucose- and acetate-derived lipogenesis are unaffected by IDH1 knockdown.

Oncogenic hotspot mutations in *IDH1* disrupt its normal homeostatic role, since the mutant enzyme is unable to catalyze the reductive carboxylation reaction and the alternative reaction producing 2-HG consumes NADPH[23,49]. In line with previous work showing that transcriptional regulation of oncogenic $IDH1^{R132C}$ can disrupt 2-HG production[45], we show that SREBP activation and inhibition reciprocally increase and decrease IDH1-dependent 2-HG production in $IDH1^{R132C}$ cells. With multiple transcription factors converging on *IDH1* expression, it will be particularly important to determine its primary mode of regulation in low grade glioma, where it is the major driving oncogene. Our analyses of available gene expression data suggest an association between SREBP activation and IDH1 expression in these tumors. Given that IDH1 mutations only occur in a specific subset of cancers, it is perhaps not surprising that the effects of SREBP on 2-HG production differ between the HT1080 fibrosarcoma cells that have a spontaneous $IDH1^{R132C}$ mutation and the genome-edited HCT116 colorectal cancer cells engineered to express this same mutation. In cells with mutant IDH1, *de novo* lipid synthesis and 2-HG production likely compete for the same pool of carbons, and SREBP controls both of these processes (Figure 3.11F), which perhaps underlies these variable outcomes. As other spontaneous IDH1-mutant cell lines become available, it will be interesting to identify the metabolic factors that account for this variability. Intriguingly, exogenous overexpression of mutant IDH1 in U87MG cells has been reported to activate expression of SREBP and its targets[50,51]. Likewise, in the isogenic HCT116 cells used here, protein levels of SREBP targets, including IDH1 and FASN, were higher in the *IDH1* mutant cells than in the wild-type (Figure 3.11A). These observations suggest that a feed forward loop between mutant IDH1 and SREBP might occur in certain settings, perhaps due to depletion of specific lipid species due to the diversion of carbon flux or consumption of NADPH.

Our collective data show that SREBP can activate IDH1 expression and that this control can influence lipid synthesis in *IDH1*-wild-type cells and 2-HG production in *IDH1*-mutant cells. These

findings add to the functional repertoire of SREBP, which has diverse physiological and pathological roles in the control of cellular metabolism.

3.6 ACKNOWLEDGEMENTS

We thank Min Yuan, Susanne Breitkopf for technical assistance and members of the Manning Lab for thoughtful discussions and advice.

This work was supported by NSF fellowship DGE-1144152 (S.J.H.R.), and NIH grants P01-CA120964 (J.M.A. and B.D.M.) and R35-CA197459 (B.D.M.). All authors declare no competing financial interests.

3.7 REFERENCES

1 Goldstein JL, DeBose-Boyd RA, Brown MS. Protein sensors for membrane sterols. *Cell* 2006; **124**: 35–46.

2 Jeon T, Osborne TF. SREBPs: metabolic integrators in physiology and metabolism. *Trends Endocrinol Metab* 2011; **23**: 65–72.

3 Ricoult SJH, Yecies JL, Ben-Sahra I, Manning BD. Oncogenic PI3K and K-Ras stimulate de novo lipid synthesis through mTORC1 and SREBP. *Oncogene* 2016; **35**: 1250–1260.

4 Düvel K, Yecies JL, Menon S, Raman P, Lipovsky AI, Souza AL *et al.* Activation of a metabolic gene regulatory network downstream of mTOR complex 1. *Mol Cell* 2010; **39**: 171–183.

5 Porstmann T, Santos CR, Griffiths B, Cully M, Wu M, Leevers S *et al.* SREBP activity is regulated by mTORC1 and contributes to Akt-dependent cell growth. *Cell Metab* 2008; **8**: 224–236.

6 Sakai J, Duncan EA, Rawson RB, Hua X, Brown MS, Goldstein JL. Sterol-regulated release of SREBP-2 from cell membranes requires two sequential cleavages, one within a transmembrane segment. *Cell* 1996; **85**: 1037–1046.

7 Wang X, Sato R, Brown MS, Hua X, Goldsteln JL. SREBP-1, a membrane-bound transcription factor released by sterol-regulated proteolysis. *Cell* 1994; **77**: 53–62.

8 Horton JD, Goldstein JL, Brown MS. SREBPs: activators of the complete program of cholesterol and fatty acid synthesis in the liver. *J Clin Invest* 2002; **109**: 1125–1131.

9 Amemiya-kudo M, Shimano H, Hasty AH, Yahagi N, Yoshikawa T, Matsuzaka T *et al.* Transcriptional activities of nuclear SREBP-1a , -1c , and -2 to different target promoters of lipogenic and cholesterogenic genes. *J Lipid Res* 2002; **43**: 1220–1235.

10 Shimomura I, Shimano H, Korn BS, Bashmakov Y, Horton JD. Nuclear sterol regulatory element-binding proteins activate genes responsible for the entire program of unsaturated fatty acid biosynthesis in transgenic mouse liver. *J Biol Chem* 1998; **273**: 35299–35306.

11 Luong A, Hannah VC, Brown MS, Goldstein JL. Molecular characterization of human acetyl-CoA synthetase, an enzyme regulated by sterol regulatory element-binding proteins. *J Biol Chem* 2000; **275**: 26458–26466.

12 Infantino V, Iacobazzi V, De Santis F, Mastrapasqua M, Palmieri F. Transcription of the mitochondrial citrate carrier gene: Role of SREBP-1, upregulation by insulin and downregulation by PUFA. *Biochem Biophys Res Commun* 2007; **356**: 249–254.

13 Horton JD, Shah NA, Warrington JA, Anderson NN, Park SW, Brown MS *et al.* Combined analysis of oligonucleotide microarray data from transgenic and knockout mice identifies direct SREBP target genes. *Proc Natl Acad Sci USA* 2003; **100**: 12027–12032.

14 Sato R, Okamoto A, Inoue J, Miyamoto W, Sakai Y, Emoto N *et al.* Transcriptional regulation of the ATP citrate-lyase gene by sterol regulatory element-binding proteins. *J Biol Chem* 2000; **275**:

12497–12502.

15 Koh H-J, Lee S-M, Son B-G, Lee S-H, Ryoo ZY, Chang K-T *et al.* Cytosolic NADP+-dependent isocitrate dehydrogenase plays a key role in lipid metabolism. *J Biol Chem* 2004; **279**: 39968–39974.

16 Metallo CM, Gameiro PA, Bell EL, Mattaini KR, Yang J, Hiller K *et al.* Reductive glutamine metabolism by IDH1 mediates lipogenesis under hypoxia. *Nature* 2011; **481**: 380–384.

17 Filipp F V, Scott DA, Ronai ZA, Osterman AL, Smith JW. Reverse TCA cycle flux through isocitrate dehydrogenases 1 and 2 is required for lipogenesis in hypoxic melanoma cells. *Pigment Cell Melanoma Res* 2012; **25**: 375–383.

18 Shechter I, Dai P, Huo L, Guan G. IDH1 gene transcription is sterol regulated and activated by SREBP-1a and SREBP-2 in human hepatoma HepG2 cells: evidence that IDH1 may regulate lipogenesis in hepatic cells. *J Lipid Res* 2003; **44**: 2169–2180.

19 Mullen AR, Wheaton WW, Jin ES, Chen P-H, Sullivan LB, Cheng T *et al.* Reductive carboxylation supports growth in tumour cells with defective mitochondria. *Nature* 2011; **481**: 385–388.

20 Wise DR, Ward PS, Shay JES, Cross JR, Gruber JJ, Sachdeva UM *et al.* Hypoxia promotes isocitrate dehydrogenase-dependent carboxylation of α-ketoglutarate to citrate to support cell growth and viability. *Proc Natl Acad Sci USA* 2011; **108**: 19611–19616.

21 Parsons DW, Jones S, Zhang X, Lin JC, Leary RJ, Angenendt P *et al.* An integrated genomic analysis of human glioblastoma multiforme. *Science* 2008; **321**: 1807–1812.

22 Mardis ER, Ding L, Dooling DJ, Larson DE, McLellan MD, Chen K *et al.* Recurring mutations found by sequencing an acute myeloid leukemia genome. *N Engl J Med* 2009; **361**: 1058–1066.

23 Dang L, White DW, Gross S, Bennett BD, Bittinger MA, Driggers EM *et al.* Cancer-associated IDH1 mutations produce 2-hydroxyglutarate. *Nature* 2009; **465**: 739–744.

24 Ward PS, Patel J, Wise DR, Abdel-Wahab O, Bennett BD, Coller HA *et al.* The common feature of leukemia-associated IDH1 and IDH2 mutations is a neomorphic enzyme activity converting a-ketoglutarate to 2-hydroxyglutarate. *Cancer Cell* 2010; **17**: 225–234.

25 Flavahan WA, Drier Y, Liau BB, Gillespie SM, Venteicher AS, Stemmer-Rachamimov AO *et al.* Insulator dysfunction and oncogene activation in IDH mutant gliomas. *Nature* 2015; **529**: 110–114.

26 Xu W, Yang H, Liu Y, Yang Y, Wang PP, Kim S-H *et al.* Oncometabolite 2-hydroxyglutarate is a competitive inhibitor of α-ketoglutarate-dependent dioxygenases. *Cancer Cell* 2011; **19**: 17–30.

27 Koivunen P, Lee S, Duncan CG, Lopez G, Lu G, Ramkissoon S *et al.* Transformation by the (R)-enantiomer of 2-hydroxyglutarate linked to EGLN activation. *Nature* 2012; **483**: 484–488.

28 Cerami E, Gao J, Dogrusoz U, Gross BE, Sumer SO, Aksoy BA *et al.* The cBio cancer genomics portal: an open platform for exploring multidimensional cancer genomics data. *Cancer Discov* 2012; **2**: 401–404.

29 Gao J, Aksoy BA, Dogrusoz U, Dresdner G, Gross B, Sumer SO *et al.* Integrative analysis of complex cancer genomics and clinical profiles using the cBioPortal. *Sci Signal* 2013; **6**: pl1 doi: 10.1126/scisignal.2004088.

30 The Cancer Genome Atlas Network -. Comprehensive, integrative genomic analysis of diffuse lower-grade gliomas. *N Engl J Med* 2015; **372**: 2481–2498.

31 The Cancer Genome Atlas Network -. The molecular taxonomy of primary prostate cancer. *Cell* 2015; **163**: 1011–1025.

32 The Cancer Genome Atlas Network -. Comprehensive molecular characterization of human colon and rectal cancer. *Nature* 2012; **487**: 330–337.

33 The Cancer Genome Atlas Network -. Genomic classification of cutaneous melanoma. *Cell* 2015; **161**: 1681–1696.

34 The Cancer Genome Atlas Network -. Comprehensive molecular portraits of human breast tumours. *Nature* 2012; **490**: 61–70.

35 The Cancer Genome Atlas Network -. Comprehensive molecular profiling of lung adenocarcinoma. *Nature* 2014; **511**: 543–550.

36 Ben-Sahra I, Howell JJ, Asara JM, Manning BD. Stimulation of de novo pyrimidine synthesis by growth signaling through mTOR and S6K1. *Science* 2013; **339**: 1323–1328.

37 Yuan M, Breitkopf SB, Yang X, Asara JM. A positive/negative ion-switching, targeted mass spectrometry-based metabolomics platform for bodily fluids, cells, and fresh and fixed tissue. *Nat Protoc* 2012; **7**: 872–881.

38 Amemiya-Kudo M, Shimano H, Yoshikawa T, Yahagi N, Hasty AH, Okazaki H *et al.* Promoter analysis of the mouse sterol regulatory element-binding protein-1c gene. *J Biol Chem* 2000; **275**: 31078–31085.

39 Tweto J, Liberati M, Larrabee A. Protein turnover and 4'-phosphopantetheine exchange in rat liver fatty acid synthetase. *J Biol Chem* 1971; **246**: 2468–2471.

40 Goldstein JL, Brown MS. Regulation of the mevalonate pathway. *Nature* 1990; **343**: 425–430.

41 Yan H, Parsons W, Jin G, McLendon R, Rasheed A, Yuan W *et al.* IDH1 and IDH2 mutations in gliomas. *N Engl J Med* 2009; **360**: 765–773.

42 Lewis CA, Brault C, Peck B, Bensaad K, Grif B, Mitter R *et al.* SREBP maintains lipid biosynthesis and viability of cancer cells under lipid- and oxygen-deprived conditions and defines a gene signature associated with poor survival in glioblastoma multiforme. *Oncogene* 2015; **34**: 5128–5140.

43 Williams KJ, Argus JP, Zhu Y, Wilks MQ, Marbois BN, York AG *et al.* An essential requirement for the SCAP/SREBP signaling axis to protect cancer cells from lipotoxicity. *Cancer Res* 2013; **73**: 2850–2862.

44 Yang X, Du T, Wang X, Zhang Y, Hu W, Du X *et al.* IDH1, a CHOP and C/EBPβ-responsive

gene under ER stress, sensitizes human melanoma cells to hypoxia-induced apoptosis. *Cancer Lett* 2015; **365**: 201–210.

45 Charitou P, Rodriguez-colman M, Gerrits J, Triest M Van, Groot M, Hornsveld M *et al.* FOXOs support the metabolic requirements of normal and tumor cells by promoting IDH1 expression. *EMBO Rep* 2015; **16**: 456–466.

46 Itsumi M, Inoue S, Elia AJ, Murakami K, Sasaki M, Lind EF *et al.* Idh1 protects murine hepatocytes from endotoxin-induced oxidative stress by regulating the intracellular NADP+/NADPH ratio. *Cell Death Differ* 2015; **22**: 1837–1845.

47 Fendt S-M, Bell EL, Keibler MA, Olenchock BA, Mayers JR, Wasylenko TM *et al.* Reductive glutamine metabolism is a function of the α-ketoglutarate to citrate ratio in cells. *Nat Com* 2013; **4**: 2236.

48 Fan J, Ye J, Kamphorst JJ, Shlomi T, Thompson CB, Rabinowitz JD. Quantitative flux analysis reveals folate-dependent NADPH production. *Nature* 2014; **510**: 298–302.

49 Leonardi R, Subramanian C, Jackowski S, Rock CO. Cancer-associated isocitrate dehydrogenase mutations inactivate NADPH-dependent reductive carboxylation. *J Biol Chem* 2012; **287**: 14615–14620.

50 Miyata S, Urabe M, Gomi A, Nagai M, Yamaguchi T, Tsukahara T *et al.* An R132H mutation in isocitrate dehydrogenase 1 enhances p21 expression and inhibits phosphorylation of retinoblastoma protein in glioma cells. *Neurol Med Chir (Tokyo)* 2013; **53**: 645–654.

51 Zhu J, Cui G, Chen M, Xu Q, Wang X, Zhou D *et al.* Expression of R132H mutational IDH1 in human U87 glioblastoma cells affects the SREBP1a pathway and induces cellular proliferation. *J Mol Neurosci* 2012; **50**: 165–171.

CHAPTER 4:

CONCLUSIONS

Section 4.2.3 of this chapter is adapted from:

Howell JJ, **Ricoult SJH**, Ben-Sahra I, Manning BD. A growing role for mTOR in promoting anabolic metabolism. *Biochem Soc Trans* 2013; **41**: 906–912.

4.1 OVERVIEW

In this dissertation, I investigated the regulation and metabolic functions of SREBP in cancer (Figure 4.1). First, I identified a critical role for mTORC1 and SREBP in activating *de novo* lipid synthesis downstream of oncogenic PI3K and K-Ras, and revealed that the growth-factor independent proliferation of breast cancer cells and breast epithelial cells expressing these oncogenes was dependent on SREBP. Next, I demonstrated that SREBP can activate expression of IDH1, and that this regulation provides a novel mechanism through which cells can coordinate the expression of *de novo* lipid synthesis enzymes with carbon availability. Furthermore, I confirmed that SREBP activates the expression of oncogenic $IDH1^{R132C}$ and the production of the oncometabolite 2-HG in mutant IDH1 cells. Although more experiments will be required to fully understand the complex regulation of cancer metabolism, my data point to important differences in the lipid metabolism of cancer cells that may help identify novel therapeutic targets.

4.2 LIPID METABOLISM IN CANCER

4.2.1 What signals converge on SREBP in cancer?

SREBP has emerged as a major effector of insulin and mTORC1 signaling in non-cancer settings, like the liver, where it promotes the expression of many lipid synthesis genes[1–5]. Disruption of mTORC1 signaling by expression aberrant Akt or deleting either TSC1 or 2[5,6] leads to growth-factor independent activation of mTORC1 signaling and mTORC1-dependent activation of SREBP. Consistent with these findings, I showed that expressing oncogenic PI3K or K-Ras in non-transformed breast epithelial cells increased *de novo* lipogenesis, and that this increase was sensitive to mTORC1 inhibition or SREBP depletion. Expression of these two commonly mutated oncogenes stimulated the processing of both SREBP1 and SREBP2 in an mTORC1-dependent manner, and increased the expression of *de novo*

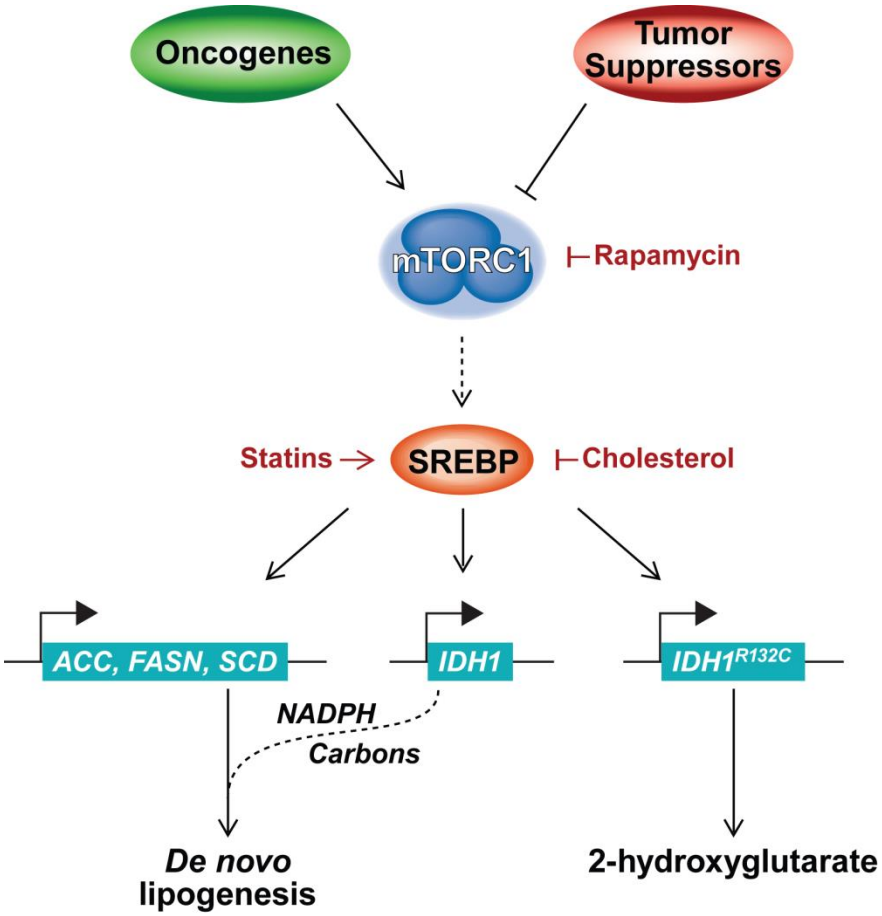

Figure 4.1. Graphical summary of the dissertation.

In cancer cells, activating mutations in oncogenes (e.g. PI3K and K-Ras) and loss-of-function mutations in tumor suppressors (e.g. PTEN) increase mTORC1 signaling and SREBP activity. SREBP promotes *de novo* lipid synthesis through the transcriptional regulation of canonical lipogenic enzymes (e.g. ACC, FASN, and SCD) and of its novel metabolic target, IDH1. IDH1 can either produce NADPH or facilitate the flow of carbons to *de novo* lipid synthesis. SREBP can also regulate the expression of oncogenic mutant IDH1, which produces the oncometabolite, 2-HG. In mutant IDH1 cells, modulating SREBP activity with siRNA, statins, or cholesterol can affect 2-HG production. Since *de novo* lipogenesis is a metabolic hallmark of cancer and 2-HG is an oncometabolite, this work demonstrates important functions of SREBP in cancer.

lipogenesis enzymes, including FASN, which are frequently upregulated in cancer[7]. Using breast cancer patient tumor samples, I demonstrated that mTORC1 signaling is associated with higher expression of *FASN* and *SCD in vivo*. These experiments were the first to show that PI3K and K-Ras converge on mTORC1 and SREBP to increase *de novo* lipid synthesis, a metabolic hallmark of cancer.

Since mTORC1 signaling is activated in at least 50% of cancers[8], it is likely that SREBP will be activated across many cancer types, beyond just breast cancer. Although we do not fully understand how mTORC1 regulates SREBP, several partial mechanisms have been proposed. In particular, the exact mechanisms through which both S6K1 and Lipin1 regulate SREBP downstream of mTORC1 have yet to be determined and could be indirect. The regulation of SREBP by these multiple mechanisms downstream of mTORC1 will likely vary between cancers due to differences in their genetic heterogeneity and local microenvironment. We and others have observed rapamycin-sensitive SREBP regulation in many cellular contexts[9,10]. However, the complexity of this regulation is exemplified by glioblastoma cells expressing an active form of EGFR, which have growth-factor independent mTORC1 signaling and rapamycin-insensitive activation of SREBP processing[11]. The differences in rapamycin-sensitivity of mTORC1 targets could be responsible for some of this variability. In particular, some of the mTORC1 targets involved in SREBP processing are sensitive to rapamycin (i.e., S6K1 and CRTC2), while others are rapamycin-resistant and sensitive only to mTOR kinase inhibitors (i.e., Lipin1 and 4E-BP1) (Figure 1.5B). Future experiments will be needed to fully understand the regulation of SREBP by mTORC1, and to define the role of these regulatory mechanisms in different cancer settings.

In addition to mTORC1 signaling, other pathways regulate SREBP to control the expression of its target genes. For example, Akt-mediated phosphorylation of GSK3β has been shown to prevent ubiquitination of SREBP1 by the Fbw7 ubiquitin ligase, a target of GSK3β, and thus reduce SREBP1 proteasomal degradation[12,13]. Likewise, mutations in the p53 tumor suppressor, which occurs in >50% of cancers, have been shown to promote the expression of canonical SREBP2 targets, possibly through its interaction with SREBP proteins[14]. SREBP1 activity can also be inhibited or activated through poorly

defined mechanisms involving direct phosphorylation by AMPK[15] and cyclin-dependent kinase 1 (CDK1)[16], respectively. It will be important to understand how regulation of SREBP by these independent mechanisms affects the regulation of SREBP by intracellular sterols[17]. Future studies will also need to address how these different mechanisms, including those downstream of mTORC1, are coordinated to regulate SREBP activity in different cancer settings.

4.2.2 What is the role of exogenous lipids in cancer?

Since most of the work on lipid metabolism and cancer used cells in culture, the role and availability of exogenous lipids *in vivo* is still an open question in cancer biology. Nevertheless, several studies have found that cancer cells sometimes depend on exogenous lipids for growth and proliferation. The uptake of unsaturated fatty acids was found to be particularly important for the growth of Ras-transformed cancer cells cultured under hypoxia[18]. This requirement is presumably caused by the inability of these cells to produce unsaturated fatty acids, since oxygen is essential for the SCD-mediated desaturation of saturated fatty acids. In addition, ovarian cancer preferentially metastasizes to the omentum, an abdominal fat pad, where the cancer cells activate lipolysis within the omentum adipocytes and use the released lipids for energy production via β-oxidation[19]. Outside of energy production, the functions of these exogenous lipids are unclear, but fatty acids like palmitate and oleate could contribute to the production of biomass[20]. While these examples suggest that exogenous lipids may be important in certain cancer settings, it remains unclear why the dependency for exogenous versus *de novo* synthesized lipids varies between cancers.

We showed that the proliferation of MDA-MB-468 cells was particularly sensitive to SREBP2 depletion in lipid-reduced conditions and that this sensitivity could be rescued by full FBS, which is rich in lipids (Figures 2.7A,B). To determine whether serum lipids could rescue the anti-proliferative effects of SREBP2 depletion *in vivo*, we tested the effects of SREBP2 knockdown on the growth of breast cancer cells in tumor xenograft models. Stable expression of two different shRNA sequences targeting SREBP2

in MDA-MB-468 cells significantly reduced SREBP2 expression compared to the control cells (Figure 4.2A). We injected these cells into the flank of immunodeficient mice, and measured the size of the ensuing tumors over an 8 week period. The growth of these tumors was slow and there were no significant differences in tumor size between the SREBP2-depleted cells and the control cells after 8 weeks (Figure 4.2B). We then extracted the tumors and purified RNA for qRT-PCR analysis. Interestingly, human SREBP2 expression in the two sets of shSREBP2 tumors was higher than in the shGFP control tumors (Figure 4.2C). The inability of these cells to maintain the SREBP2 knockdown in the presence of serum lipids suggests that SREBP2 expression is important for the proliferation of MDA-MB-468 xenograft tumors *in vivo*. If SREBP2 had not been important to these cells, the knockdown of SREBP2 should have been maintained for the duration of the experiment. Due to the adaptation of these cells to the SREBP2 knockdown, we were unable to determine whether depletion of SREBP2 can reduce tumor growth. Future *in vivo* experiments will be required to fully appreciate the contribution of exogenous serum lipids to cancer cells, particularly in solid tumors, where the diffusion of oxygen and lipids may be limited.

4.2.3 What is the role of SREBP and *de novo* lipogenesis in cancer cells?

We and others have reported that depletion of SREBP1[6,11,21–23] or SREBP2[22] decreases the proliferation and viability of cancer cells in various settings, especially in the absence of exogenous lipids. While the anti-proliferative effects of SREBP depletion in lipid-reduced conditions could be rescued by full serum in certain cell lines, others were equally sensitive to SREBP depletion in lipid-reduced and full serum conditions (Figures 2.7A,B and 2.9B,D). These data suggest that SREBP, and possibly *de novo* synthesized lipids, are important in certain cancer settings regardless of exogenous serum lipid availability. Interestingly, depletion of SREBP2 had a stronger effect on proliferation and survival than SREBP1 in breast cancer cells. This finding is consistent with the embryonic lethality of SREBP2 knock-out mice, but not of SREBP1 knock-out mice[24]. Loss of SREBP2 has been shown to cause a decrease in SREBP1 expression, most likely due to the autoregulation of the SRE in the SREBP1

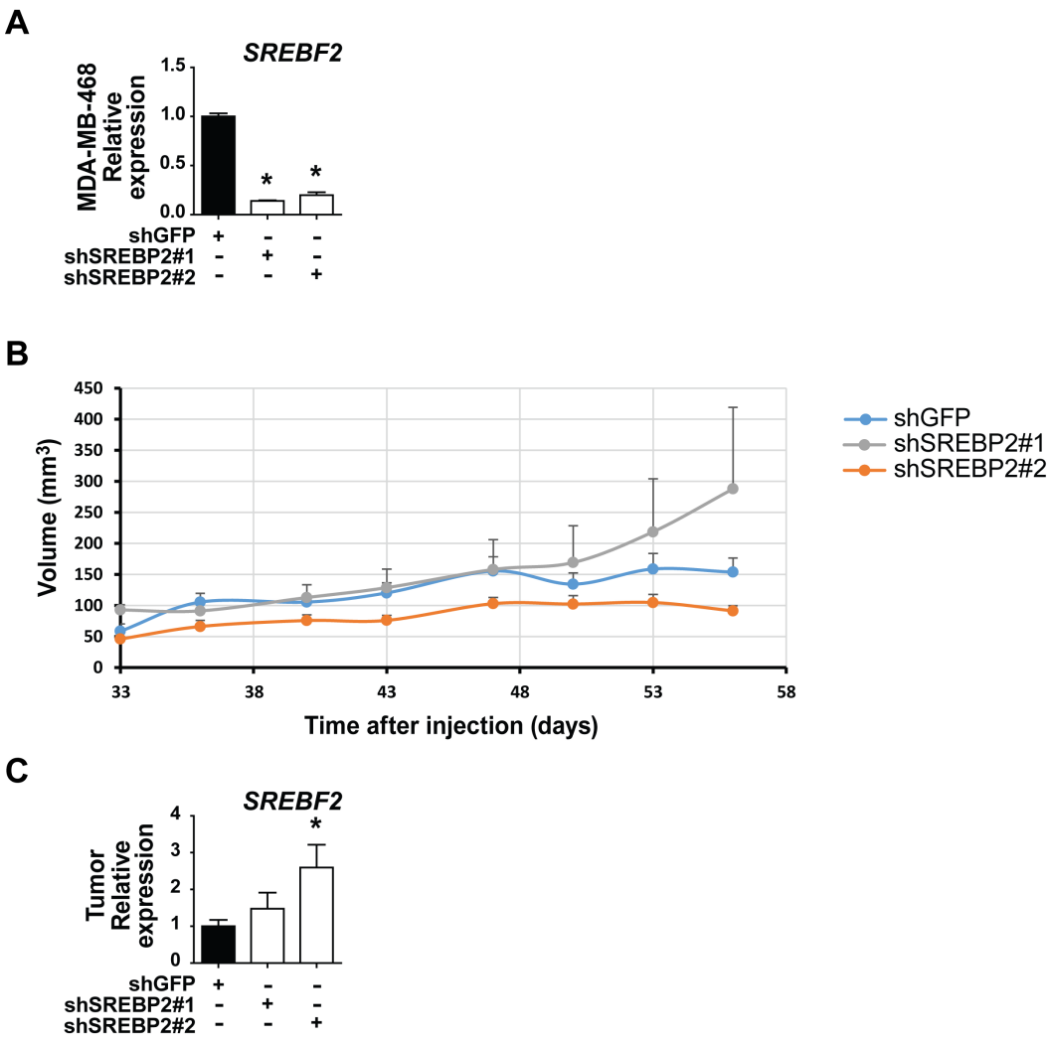

Figure 4.2. Effect of SREBP2 depletion in a xenograft tumor model.

(**A**) MDA-MB-468 cells were transduced with lentiviral shRNA targeting GFP or two different SREBP2 sequences. Following selection of these cells with puromycin, RNA was extracted for qRT-PCR analysis. (**B**) Cells from A were resuspended in Matrigel and $2x10^6$ cells were injected into the flanks of CB17-SCID mice. The size of the tumors was measured twice a week for 8 weeks with a caliper. (**C**) qRT-PCR analysis of RNA extracted from the tumors after 8 weeks. *SREBF2* mRNA levels were measured using primers for the human *SREBF2* gene (F 5′-TGGCTTCTCTCCCTACTCCA-3′, R 5′-GAGAGGCACAGGAAGGTGAG-3′). Transcript levels are shown as mean ± s.e.m. relative to cells transduced with shGFP. *P<0.05

promoter[5,22,25,26]. Since there is overlap in the regulation of targets by SREBP1 and SREBP2, it is possible that the stronger effect of SREBP2 depletion is due to the concurrent decrease in SREBP1 activity.

Alternatively, since SREBP2 was found to preferentially regulate the expression of steroidogenic genes in the liver, the stronger effect of SREBP2 depletion on proliferation could be caused by a dependence of cancer cells on *de novo* sterol synthesis. This idea is supported by the embryonic lethality of HMGCR knock-out mice, which lack the rate limiting enzyme in *de novo* sterol synthesis[27]. Cholesterol plays an important role in influencing membrane fluidity and dynamics, as well as the formation of lipid rafts in the plasma membrane. These lipid rafts are thought to facilitate interactions between signaling molecules by bringing them closer together. In prostate cancer cells, the formation of cholesterol-rich lipid rafts has been shown to be critical for activation of survival pathways[28]. Interestingly, treatment of cancer cells or tumor-bearing mice with mevalonate increases proliferation and tumor growth, while ectopic expression of HMGCR can promote cancer cell transformation[29,30]. In support of this notion, cancer patients taking statins were found to have prolonged survival, but it remains controversial whether statins play a preventative role[31,32]. In addition to cholesterol synthesis, the mevalonate pathway can be used to produce farnesyl and geranyl, which are important for the function of numerous signaling proteins, including Ras and Rheb (Figure 1.4). Farnesyl transferase and geranyl transferase inhibitors have been shown to suppress tumor growth in mouse models, but have had limited success in clinical trials for cancer treatment[33].

In addition to the effects of SREBP2 depletion, we and others have shown that depletion of SREBP1 can also decrease cancer cell proliferation[6,11,21–23]. Consistent with SREBP1 preferentially activating the expression of fatty acid synthesis genes in the liver, inhibition of fatty acid synthesis enzymes, such as ACLY, ACC, ELOVL7, or FASN, had detrimental effects on the proliferation and/or survival of various cancer cells[34–39]. The *de novo* synthesis of saturated fatty acids in cancer cells has been reported to increase the saturation of membrane lipids, making them more resistant to insults, such as DNA damage and reactive oxygen species (ROS)[40]. Proper fatty acid desaturation also appears to be

important, since cancer cells are sensitive to the inhibition of SCD[41,42]. Interestingly, the *de novo* production of mono-unsaturated fatty acids appears to be a strict requirement for proliferating cancer cells[22,23,42]. Maintaining a balance between saturated and unsaturated fatty acids is particularly important in the ER, where excessive amounts of saturated lipids result in ER stress, unfolded protein response (UPR), ROS production, and apoptosis[22,41,43–45]. Consistent with these reports, I showed that PI3K- and K-Ras-induced *de novo* lipogenesis is significantly reduced by SCD depletion. This finding suggests that an overabundance of saturated fatty acids may limit the synthesis of complex lipids or may disrupt ER functions, like lipid synthesis. However, the importance and regulation of other lipid types such as sphingolipids, phosphatidylethanolamines, and phosphatidylcholines remain a mystery. Given that fatty acids are incorporated into a variety of lipid types, including membrane and signaling lipids, it is likely that the synthesis of these complex lipids is also altered in cancer. Together, the dependence on different fatty acids and mevalonate-derived lipids suggests that cancer cells depend on *de novo* lipid synthesis to maintain a complex balance of lipids required for proliferation and survival. Due to the likely variation in lipid composition of different cell types, it seems probable that different cancers would respond differently to the disruption of specific lipid synthesis pathways.

To further investigate the role of SREBP in cancer cells, we tested the importance of the *de novo* cholesterol synthesis pathway in MDA-MB-468 cells, which are particularly sensitive to SREBP2 knockdown in proliferation and cell death assays (Figures 2.7, 2.8). Using siRNA, we knocked down SREBP2 in MDA-MB-468 cells and measured proliferation in media containing full serum or lipid-reduced serum. Interestingly, the anti-proliferative effects of SREBP2 knockdown only occurred in lipid-reduced conditions (Figure 4.3A). Since SREBP1 knockdown had little effect on the proliferation of the MDA-MB-468 cells, we hypothesized that an exclusive SREBP2 target must be important for the proliferation of these cells in lipid-reduced conditions. Unlike SCD mRNA levels, which were redundantly regulated by SREBP1 and 2 in the MDA-MB-468 cells, levels of HMGCR transcript were regulated by SREBP2 and not SREBP1 in these conditions (Figure 4.3B). Depleting HMGCR using

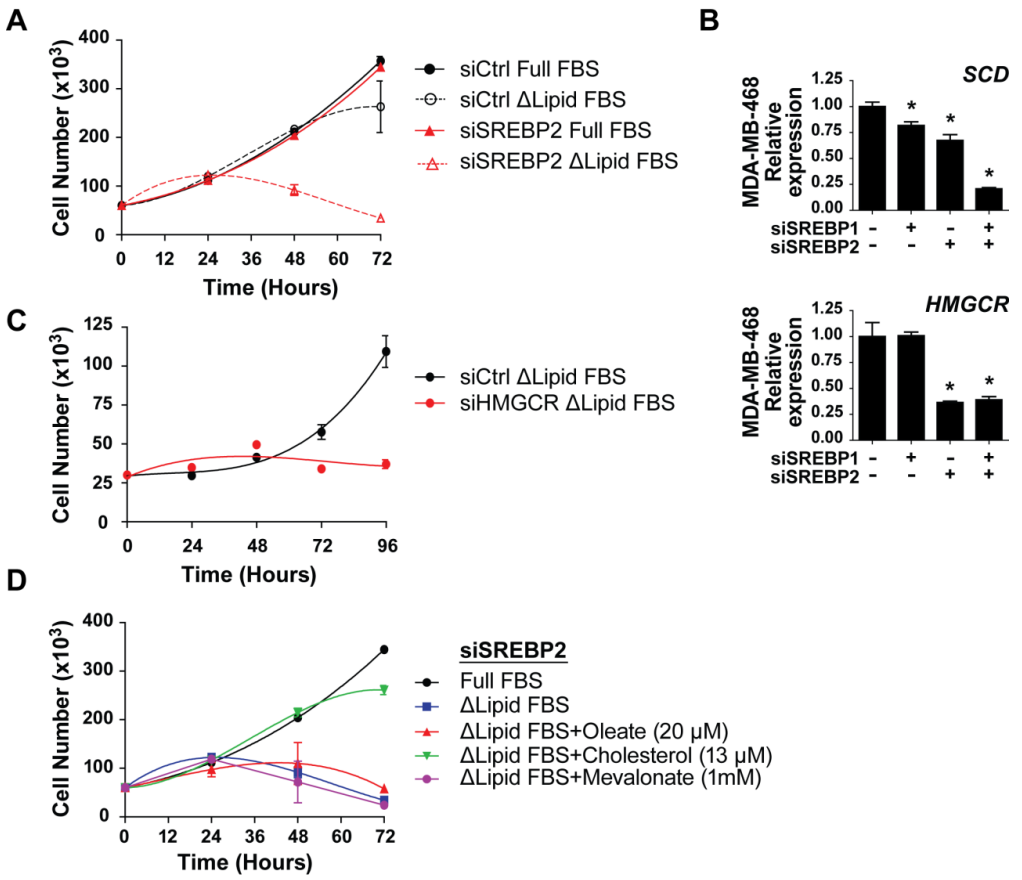

Figure 4.3. MDA-MB-468 cells need cholesterol to proliferate.

(**A**) MDA-MB-468 cells were transfected with siRNAs targeting SREBP2 and were switched to media containing full serum or lipid-reduced serum (Δlipid FBS) after the knockdown (t=0 h). (**B**) RNA was isolated from MDA-MB-468 cells transfected with siRNA targeting SREBP1, SREBP2, or both for analysis by qRT-PCR. Primers targeting the human *SCD* (F 5′- CCCAGCTGTCAAAGAGAAGG-3', R 5'- CAAGAAAGTGGCAACGAACA-3') and *HMGCR* (F 5′-TGATTGACCTTTCCAGAGCAAG-3', R 5'-CTAAAATTGCCATTCCACGAGC-3') genes were used. * $p<0.05$ (**C**) MDA-MB-468 cells were transfected with siRNAs targeting HMGCR and were switched to media containing 10% lipid-reduced serum after the knockdown (t=0 h). (**C**) MDA-MB-468 cells were transfected with siRNAs targeting SREBP2. After the knockdown (t=0 h), the cells were switched to media containing full serum, lipid-reduced serum, or lipid-reduced serum supplemented with oleate (20 μM), cholesterol (13 μM), or mevalonate (1 mM). Data are shown as mean ± s.e.m.

siRNA also reduced the proliferation of MDA-MB-468 cells, almost to the same extent as the SREBP2 knockdown (Figure 4.3C). Since HMGCR is the rate-limiting enzyme in the sterol synthesis pathway, we attempted to rescue the cells with exogenous lipids. Addition of cholesterol to lipid-reduced media rescued the proliferative defect of cells with SREBP2 knockdown (Figure 4.3D). However, addition of exogenous mevalonate or oleate was unable to rescue the proliferation of these cells. Consistent with our data, Guo, *et al.* reported that the combined disruption of exogenous cholesterol uptake by LDLR and of *de novo* cholesterol synthesis decreased the viability of glioblastoma cells[46]. These preliminary results suggest that *de novo* cholesterol synthesis can be important for proliferation when exogenous lipids are limiting. However, the reduced proliferation following the combined knockdown of SREBP1 and SREBP2 in MDA-MB-468 cells was not rescued by full serum (Figure 2.7A,B). Likewise, exogenous cholesterol (data not shown) or full serum (Figure 2.7A,B) was not able to rescue the reduced proliferation of other breast cancer cell lines following the knockdown of SREBP1, SREBP2, or both. This approach lays the groundwork for future experiments, which can use a combination of siRNA-mediated knockdowns and complementation with different lipid species to explore the variable lipid requirement and contribution of SREBP in different cell lines.

4.2.4 What other processes may SREBP control to promote cancer progression?

Although *de novo* lipogenesis has been shown to be important in cancer, it is possible that cancer cells depend on SREBP for the activation of processes that are not directly related to lipid synthesis. Early work on identifying novel SREBP targets found that three NADPH-producing enzymes, G6PD, PGD, and ME1, could be activated by SREBP[5,47,48]. The regulation of these enzymes by SREBP is consistent with its role as a major regulator of lipid synthesis, since NADPH is required for several key steps in *de novo* lipid synthesis. NADPH is also required for the activation of antioxidants, like glutathione[49]. Changes in the NADPH/$NADP^+$ ratio can affect intracellular ROS levels and the redox state of the cell. De Raedt, *et al*. reported that treatment of Ras-driven tumors with rapamycin sensitized them to ROS due to glutathione depletion, which was caused by suppression of SREBP1 and decreased G6PD expression in

response to rapamycin[50]. In Chapter 3, I showed that SREBP could regulate the expression of IDH1, which could further affect intracellular NADPH levels in some settings. IDH1 produces cytosolic NADPH by converting isocitrate to α-KG. The IDH1-mediated reductive carboxylation of α-KG has also been reported to decrease mitochondrial ROS, even though it consumes NADPH. In tumor spheroids, IDH1-mediated reductive carboxylation was shown to be critical for providing citrate to IDH2, which reduces mitochondrial ROS by producing mitochondrial NADPH[51]. Since SREBP regulates both NADPH producing and consuming enzymes, it is unclear what the effects of SREBP activation and inhibition are on the intracellular NADPH/$NADP^+$ ratio in various cancer settings.

Additionally, four separate genome-wide chromatin immunoprecipitation (ChIP) experiments found that SREBP bound to the promoters of genes involved in lipid synthesis, but also to those of many non-lipid related genes[52–55]. One of these studies found that SREBP bound the promoter of several autophagy genes, and that knockdown of SREBP2 in serum starvation conditions prevented autophagosome formation[53]. Consistent with the role of SREBP in regulating lipid synthesis genes, autophagy can be used for the breakdown of lipid droplets[56,57]. ATG7 deletion, which inhibits autophagy, led to the accumulation of lipids in K-Ras-mutant p53-null lung tumor derived cells[58]. Importantly, autophagy has been shown to facilitate tumor progression in certain settings[56,57]. We also showed that SREBP could bind to the promoter of Nrf1 (nuclear factor, erythroid 2-like 1), a transcription factor that induces expression of all the subunits of the proteasome, and that SREBP was required for an increase in proteasome levels in response to mTORC1 activation[59]. This work is interesting given that proteasome levels are elevated in a number of cancer settings[60–62]. Future experiments will likely reveal new targets and cellular processes controlled by SREBP that might contribute to tumor development and progression. Given the heterogeneity of tumors, in terms of their genetic makeup, anatomical location, and microenvironment, it is likely that the role of SREBP and the regulation of these target genes will differ between cancers.

4.3 METABOLIC EFFECTS OF IDH1 TRANSCRIPTIONAL REGULATION BY SREBP

4.3.1 What are the effects of wild-type IDH1 transcriptional activation?

In Chapter 3, I demonstrated that IDH1 is transcriptionally activated by SREBP in a variety of cancer cell lines from different lineages. My findings were consistent with previous data from Shechter, *et al.* identifying an SRE in the proximal promoter of IDH1, and finding that SREBP could bind this region of the promoter *in vitro* and activate its expression in luciferase assays[63]. However, I found that the degree of IDH1 regulation by SREBP varied between cancer cell lines. While we do not understand the reason for this variability, it is possible that regulation of IDH1 by other factors may be dominant over SREBP in certain settings. For example, FOXO transcription factors can directly regulate IDH1 transcription[64], and ER stress has been reported to increase IDH1 expression through CHOP and C/EBPβ[65]. Interestingly, SREBP knockdown has been shown to induce ER stress in certain settings[22], which could actually reduce the effects of SREBP depletion on IDH1 expression. Since mTORC1 signaling can activate SREBP, it is also possible that mTORC1 activation or inhibition may affect IDH1 expression in certain settings. Future experiments will need to address how these different inputs are coordinated.

IDH1 is a versatile enzyme that adapts to cellular needs by changing the direction of the IDH1 reaction. When the ratio of intracellular citrate to α-KG is high, IDH1 catalyzes the conversion of isocitrate to α-KG, which produces NADPH[66]. However, when citrate levels drop, IDH1 catalyzes the reductive carboxylation of α-KG to isocitrate[67–70]. In addition to NADPH, *de novo* lipogenesis also requires acetyl-CoA as a fundamental building block. Through the transcriptional regulation of ACSS2, SLC25A1, and ACLY, SREBP can facilitate the synthesis of acetyl-CoA from acetate and citrate[52,71–73]. The regulation of IDH1 by SREBP is consistent with its role in promoting lipid synthesis, since IDH1 can produce either NADPH or acetyl-CoA, depending on the direction of the reaction (Figures 1.8A,B). We found that IDH1 knockdown decreased lipid production from glutamine, but not glucose and acetate. This result suggests that NADPH production by IDH1 is less important for *de novo* lipogenesis than its role in

facilitating flux from glutamine to lipids in this setting. Enzymes that increase the flux of different carbon sources into lipid synthesis could be important points of regulation and potential therapeutic targets. Future experiments should also explore the function of IDH1 in various settings, since IDH1 was shown to have different roles in cells cultured in monolayer versus cells cultured in spheroids[51].

4.3.2 What are the effects of mutant-IDH1 transcriptional regulation?

Mutations in IDH1 and IDH2 occur frequently in certain cancer types, including gliomas and leukemias, and result in the production of the oncometabolite 2-HG by the mutant enzymes[74,75]. However, little is known about the regulation of mutant IDH1-mediated production of 2-HG. Consistent with the regulation of 2-HG levels by FOXO-mediated transcriptional activation of mutant IDH1[64], I showed that SREBP could also regulate mutant IDH1 levels and influence 2-HG production in mutant-IDH1 cells. Interestingly, 2-HG production in these mutant IDH1 cells was increased by statins, which deplete intracellular sterols and induce SREBP activation. Given the wide use of statins as preventative agents for cardiovascular disease, it remains to be determined whether statins could have a similar effect in patients with mutant IDH1-driven cancers, perhaps exacerbating the tumor phenotype through enhanced 2-HG production. In addition, the regulation of *de novo* lipogenesis by SREBP may also indirectly affect 2-HG synthesis, since *de novo* lipogenesis enzymes and 2-HG-producing mutant IDH1 likely compete for sources of cytosolic carbon and NADPH. The proliferation of mutant IDH1 cells is hindered by the inhibition of glutaminolysis without affecting 2-HG levels[76,77]. This finding could be explained by the mutant IDH1 enzyme depriving growth-promoting cellular processes of carbons.

While I have shown that the flux of glucose into 2-HG is reduced by SREBP knockdown in the HT1080 mutant IDH1 cell line, there are still several unanswered questions that I have begun to address. To determine whether SREBP also affected 2-HG production from glutamine, I used stable-isotope flux analysis to measure incorporation of carbons from [U-^{13}C]-glutamine into 2-HG (Figure 4.4A). 2-HG derived from the labeled glutamine contains 5 labeled carbons, a change in mass that can be measured by

LC-MS/MS. In both the HT1080 and the HCT116-IDH1$^{R132C/+}$ cells, knockdown of IDH1 with siRNAs significantly decreased the production of glutamine-derived 2-HG (m+5) (Figures 4.4B,C). As expected, the HCT116-IDH1$^{R132C/+}$ cells produced much more 2-HG from glutamine than the wild-type HCT116 cells. Consistent with our glucose flux data, depleting SREBP1/2 in the HT1080 cells decreased glutamine flux into 2-HG, albeit not significantly, whereas it had no effect on 2-HG production from glutamine in the HCT116-IDH1$^{R132C/+}$ cells. 2-HG can also be produced from glutamine through a more indirect route involving the oxidative TCA cycle, which produces 2-HG with 3 labeled carbons (m+3). Since IDH1^{R132C} is responsible for nearly all of the 2-HG production in these cells, the IDH1 knockdown served as an internal control. Neither the (m+3) nor (m+4) 2-HG were decreased by IDH1 knockdown, suggesting that these isotopomers are likely masked by another metabolite peak of nearly the same mass in our LC-MS/MS analysis (Figure 4.4D). An analysis of the raw data confirmed the presence of another peak masking the (m+3) 2-HG (data not shown). Interestingly, the (m+1) and (m+2) forms were much more abundant than the (m+5) form, and were significantly reduced by both SREBP1/2 and IDH1 knockdown. However, it is not clear how these 2-HG isotopomers are produced from glutamine. One possible path involves the entry of (m+5) glutamine into the TCA cycle as α-KG to produce (m+4) citrate. The (m+4) citrate can produce (m+3) pyruvate through ACLY and ME1, which can re-enter the mitochondria to produce (m+2) acetyl-CoA, and (m+2) 2-HG by means of citrate and α-KG. However, it is unclear how the (m+1) 2-HG is produced. Future experiments will be needed to confirm whether this convoluted path is correct, and, if so, why the (m+1) and (m+2) forms are more abundant than (m+5) 2-HG produced through a much more direct path.

Since IDH1 functions as a dimer, mutant IDH1 cells contain wild-type homodimers, mutant-homodimers, and wild-type/mutant heterodimers. Wild-type IDH1 has been suggested to be required for maximal 2-HG production by mutant-IDH1[78]. Consistent with this idea, the heterodimer is believed to facilitate 2-HG production by funneling α-KG and NADPH produced by the wild-type IDH1 enzyme

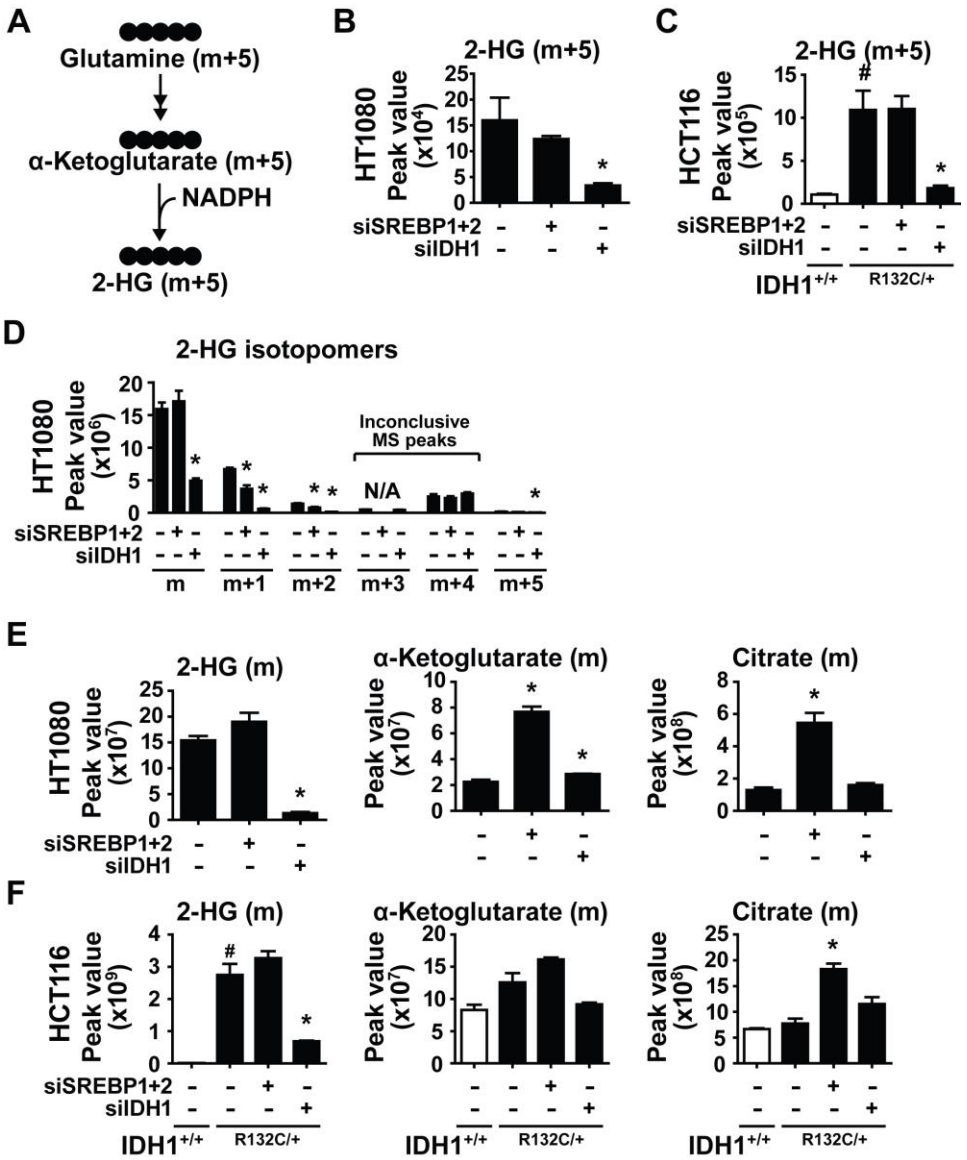

Figure 4.4. Regulation of 2-HG production and steady state levels by SREBP.

(**A**) Diagram of carbon flux from [U-^{13}C]-glutamine into 2-HG (m+5). Filled circles represent ^{13}C carbons, with m+5 referring to the mass increase from the stable isotope carbons. (**B,C**) Normalized peak areas of ^{13}C-labeled 2-HG (m+5), measured in metabolite extracts by LC-MS/MS, from (**B**) HT1080 and (**C**) isogenic HCT116 cells with wild-type (+/+) or mutant (R132C/+) IDH1 following a pulse label with [U-^{13}C]-glutamine for 20 min. Cells were transfected with nontargeting control siRNAs (-) or siRNAs targeting SREBP1+2 or IDH1 72 h prior to metabolite extraction.

Figure 4.4 (Continued)

(**D**) Normalized peak areas of ^{13}C-labeled 2-HG isotopomers from HT1080 cells in **B**. (**E,F**) Normalized steady state peak areas, measured in metabolite extracts by LC-MS/MS, from (**E**) HT1080 and (**F**) isogenic HCT116 cells 72 h post-transfection with nontargeting control siRNAs (-) or siRNAs targeting SREBP1/2 or IDH1. * $p<0.05$

directly into the mutant IDH1 enzyme. These properties of IDH1 could explain the low (m+5) 2-HG production measured in our experiments, relative to the other isotopomers (Figure 4.4D). The substrate funneling in the heterodimer could hinder the entry of glutamine-derived α-KG into the enzyme complex, thus reducing the production of (m+5) 2-HG by the heterodimer. Additionally, the decreased efficiency of the mutant IDH1 homodimer, compared to the heterodimer[78], could further limit the 2-HG (m+5) produced from glutamine-derived α-KG.

Another unanswered question concerns the effect of SREBP on total levels of 2-HG in mutant IDH1 cells. To measure steady state 2-HG levels, I knocked down SREBP1/2 or IDH1 in HT1080 or HCT116-IDH1$^{R132C/+}$ cells and extracted polar metabolites for analysis by LC-MS/MS. As expected, depletion of IDH1 decreased steady state 2-HG levels in both cell lines (Figures 4.4E,F). However, despite IDH1 protein levels being reduced, SREBP1/2 knockdown led to a small, yet insignificant, increase in 2-HG levels in both cell lines. This result suggests that, even though 2-HG production from glucose can be regulated by SREBP, other factors affect steady state 2-HG levels in response to SREBP depletion. It is possible that depleting SREBP, which blocks *de novo* lipogenesis, increases the availability of citrate-derived carbons and NADPH for the mutant IDH1 enzyme. These increased substrate concentrations could overcome the reduced enzyme levels caused by SREBP1/2 knockdown. Consistent with this idea, α-KG and citrate levels are elevated by SREBP1/2 knockdown (Figures 4.4E,F). These preliminary data reveal that we do not fully understand the relationship between SREBP, lipid synthesis, and mutant IDH1-mediated production of 2-HG, and that further studies are required.

Even though the oncogenic role of 2-HG has been widely studied in the context of mutant IDH1/2, IDH1/2-independent 2-HG production has also been found to be associated with other diseases. Familial mutations in either D2HGDH or L2HGDH cause D- or L-2-hydroxyglutaric aciduria, which results in cognitive deficiency, developmental delay, epilepsy, and dysmorphic features[79,80]. Interestingly, there are no reports of cancer in these patients, possibly due to early morbidity. Mutations in the mitochondrial citrate transporter (SLC25A1), which is an SREBP target, have also been linked to

combined D- and L-2-hydroxyglutaric aciduria, although the mechanism is unknown and may be indirect[81,82]. In breast cancer, the promiscuous activity of phosphoglycerate dehydrogenase (PHGDH), which is often amplified in this cancer type, leads to the conversion of α-KG to D-2-HG[83]. Similarly, Intlekofer, *et al.* found that cancer cell lines cultured in hypoxia had elevated levels of L-2-HG, which was dependent on LDHA and, to a lesser extent, malate dehydrogenase (MDH)[84]. Like PHGDH, the promiscuous binding of α-KG to LDHA is believed to be responsible for this increase. The development of more sensitive techniques to study cellular metabolism will likely continue to expand the role of metabolic enzymes and of the two isoforms of 2-HG in different cancers.

4.4 DEVELOPMENT OF NOVEL CANCER THERAPIES TARGETING LIPID METABOLISM

Inhibition of *de novo* lipid synthesis has proved effective in killing cancer cells in a variety of settings, but the therapeutic potential of targeting the enzymes of *de novo* lipogenesis in patients remains an open question, particularly since hepatic *de novo* lipogenesis is thought to provide lipids to most differentiated cells in the body. Knocking out *ACLY*[85], *ACACA*[86], *FASN*[87], *HMGCR*[27], or *SREBF2*[24] in mice proved to be unsuccessful due to the embryonic lethality of these homozygous deletions. Although *HMGCR* deletion was lethal, HMGCR inhibitors (statins) are used in adults as preventative agents for cardiovascular disease with limited side effects. This difference suggests that adults are more resistant to inhibition of cholesterol synthesis, or that statin accumulation in the liver limits its harmful effects on other organs. In addition, SCD-null asebia mice are viable and develop alopecia[88]. Consistent with the mouse phenotype, SCD inhibitors, developed for the treatment of diabetes and dyslipidemia, caused skin lesions and dry eyes in patients[89]. With the limited side effects of statins and SCD inhibitors, it seems possible that a therapeutic window could be found for inhibitors of certain steps in the *de novo* lipogenesis pathway in cancer.

Cancers driven by mutations in IDH1 provide a unique setting to target SREBP or lipid synthesis. Initial results using inhibitors of the mutant IDH1 protein have been successful in blocking 2-HG production and cancer growth[90], although the inhibitors do not kill the cancers cells. These inhibitors sometimes have no effect on, or may even improve, the proliferation of mutant-IDH1 cells in certain settings[91,92], most likely due to the presence of other driving mutations. As mentioned previously, both 2-HG production and lipid synthesis consume NADPH. Consistent with this idea and the important role of NADPH in the antioxidant response, cells overexpressing mutant IDH1 had lower levels of NADPH and of reduced glutathione, and were more sensitive to hydrogen peroxide[93]. Similarly, cells containing mutant IDH1 had decreased proliferation in response to complex I inhibitors[94], and decreased viability following treatment with ionizing radiation[95] or glutathione reductase inhibition[77], compared to wild-type IDH1 cells. Interestingly, all three of these conditions are known to increase intracellular ROS. The sensitivity of mutant IDH1 cells to radiation was rescued by antioxidants[77]. These findings suggest that mutant IDH1 cells are more sensitive to ROS, and that activating both 2-HG and lipid synthesis could further sensitize these cells to oxidative stress. The efficacy of SREBP in achieving this result will depend on the amount of NADPH produced by G6PD, PGD, and ME1, three SREBP targets. Mutant IDH1 cells have also been found to be particularly sensitive to NAD^+ depletion although the mechanism is still unclear[91]. Therefore, the combination of SREBP activators (e.g. statins) with glutaminase inhibitors or ROS producing agents might be an effective therapy for the treatment of mutant IDH1 cancers.

4.5 FUTURE DIRECTIONS

The work in this dissertation provides a major mechanism through which commonly mutated oncogenes induce *de novo* lipid synthesis. In cultured breast cancer cells and oncogene-expressing breast epithelial cells, mTORC1 and SREBP were required for the increase in lipid synthesis driven by oncogenic PI3K and K-Ras. Although several models have been proposed, the mechanism through which

mTORC1 activates SREBP is still poorly understood. Future studies are required to improve our understanding of this key point of regulation in different cancer settings. My work also adds to the growing evidence that cancer cells in various settings are dependent on *de novo* lipogenesis for proliferation and survival. Given the complicated balance between uptake of exogenous lipids and *de novo* lipid synthesis, mouse tumor models will be required to determine the extent to which tumors depend on *de novo* synthesized lipids *in vivo*.

In addition, understanding how SREBP1 and SREBP2 activate the transcription of their unique and redundant targets will be crucial in populating a complete list of SREBP targets. As a starting point, many of the putative SREBP targets identified in genome wide ChIP screens have not yet been verified. In this dissertation, I have characterized the regulation of IDH1 by SREBP and have identified a novel mechanism through which SREBP supports *de novo* lipid synthesis. This new regulatory mechanism also affected expression of oncogenic $IDH1^{R132C}$ and the production of the oncometabolite 2-HG in mutant IDH1 cells.

The development of more sensitive techniques to study metabolism will be important to explore new areas of tumor metabolism. I have been working with John Asara (Beth Israel Deaconess Medical Center) to develop an unbiased LC-MS/MS lipidomics platform, which will measure the relative levels of thousands of different lipids across different conditions. This new technique will provide a more complete picture of the lipidome of a cancer cell, and will allow us to identify changes in specific lipid species that are unique to cancer.

This dissertation has established SREBP as an important regulator of cancer metabolism in a variety of cancer settings and has improved our understanding of how transcription can affect tumor metabolism. We hope that this knowledge, together with the future studies proposed herein, will lead to the development of novel and effective therapies to treat cancer.

4.6 REFERENCES

1 Brown NF, Stefanovic-Racic M, Sipula IJ, Perdomo G. The mammalian target of rapamycin regulates lipid metabolism in primary cultures of rat hepatocytes. *Metabolism* 2007; **56**: 1500–1507.

2 Yecies JL, Zhang HH, Menon S, Liu S, Yecies D, Lipovsky AI *et al.* Akt stimulates hepatic SREBP1c and lipogenesis through parallel mTORC1-dependent and independent pathways. *Cell Metab* 2011; **14**: 21–32.

3 Li S, Brown MS, Goldstein JL. Bifurcation of insulin signaling pathway in rat liver: mTORC1 required for stimulation of lipogenesis, but not inhibition of gluconeogenesis. *Proc Natl Acad Sci USA* 2010; **107**: 3441–3446.

4 Owen JL, Zhang Y, Bae S-H, Farooqi MS, Liang G, Hammer RE *et al.* Insulin stimulation of SREBP-1c processing in transgenic rat hepatocytes requires p70 S6-kinase. *Proc Natl Acad Sci USA* 2012; **109**: 16184–16189.

5 Düvel K, Yecies JL, Menon S, Raman P, Lipovsky AI, Souza AL *et al.* Activation of a metabolic gene regulatory network downstream of mTOR complex 1. *Mol Cell* 2010; **39**: 171–183.

6 Porstmann T, Santos CR, Griffiths B, Cully M, Wu M, Leevers S *et al.* SREBP activity is regulated by mTORC1 and contributes to Akt-dependent cell growth. *Cell Metab* 2008; **8**: 224–236.

7 Kuhajda FP. Fatty-acid synthase and human cancer: new perspectives on its role in tumor biology. *Nutrition* 2000; **16**: 202–208.

8 Menon S, Manning BD. Common corruption of the mTOR signaling network in human tumors. *Oncogene* 2008; **27**: S43–51.

9 Ricoult SJH, Yecies JL, Ben-Sahra I, Manning BD. Oncogenic PI3K and K-Ras stimulate de novo lipid synthesis through mTORC1 and SREBP. *Oncogene* 2016; **35**: 1250–1260.

10 Ricoult SJH, Manning BD. The multifaceted role of mTORC1 in the control of lipid metabolism. *EMBO Rep* 2013; **14**: 242–251.

11 Guo D, Prins RRM, Dang J, Kuga D, Iwanami A, Soto H *et al.* EGFR signaling through an Akt-SREBP-1-dependent, rapamycin-resistant pathway sensitizes glioblastomas to antilipogenic therapy. *Sci Signal* 2009; **2**: ra82.

12 Punga T, Bengoechea-Alonso MT, Ericsson J. Phosphorylation and ubiquitination of the transcription factor sterol regulatory element-binding protein-1 in response to DNA binding. *J Biol Chem* 2006; **281**: 25278–25286.

13 Sundqvist A, Bengoechea-Alonso MT, Ye X, Lukiyanchuk V, Jin J, Harper JW *et al.* Control of lipid metabolism by phosphorylation-dependent degradation of the SREBP family of transcription factors by SCFFbw7. *Cell Metab* 2005; **1**: 379–391.

14 Freed-Pastor WA, Mizuno H, Zhao X, Langerød A, Moon S-H, Rodriguez-Barrueco R *et al.*

Mutant p53 disrupts mammary tissue architecture via the mevalonate pathway. *Cell* 2012; **148**: 244–258.

15 Li Y, Xu S, Mihaylova MM, Zheng B, Hou X, Jiang B *et al.* AMPK phosphorylates and inhibits SREBP activity to attenuate hepatic steatosis and atherosclerosis in diet-induced insulin-resistant mice. *Cell Metab* 2011; **13**: 376–388.

16 Bengoechea-Alonso MT, Ericsson J. Cdk1/cyclin B-mediated phosphorylation stabilizes SREBP1 during mitosis. *Cell Cycle* 2006; **5**: 1708–1718.

17 Jeon T, Osborne TF. SREBPs: metabolic integrators in physiology and metabolism. *Trends Endocrinol Metab* 2011; **23**: 65–72.

18 Kamphorst JJ, Cross JR, Fan J, de Stanchina E, Mathew R, White EP *et al.* Hypoxic and Ras-transformed cells support growth by scavenging unsaturated fatty acids from lysophospholipids. *Proc Natl Acad Sci USA* 2013; **110**: 8882–8887.

19 Nieman KM, Kenny H a, Penicka C V, Ladanyi A, Buell-Gutbrod R, Zillhardt MR *et al.* Adipocytes promote ovarian cancer metastasis and provide energy for rapid tumor growth. *Nat Med* 2011; **17**: 1498–503.

20 Hosios AM, Hecht VC, Danai L V., Johnson MO, Rathmell JC, Steinhauser ML *et al.* Amino acids rather than glucose account for the majority of cell mass in proliferating mammalian cells. *Dev Cell* 2016; **36**: 540–549.

21 Lewis CA, Brault C, Peck B, Bensaad K, Grif B, Mitter R *et al.* SREBP maintains lipid biosynthesis and viability of cancer cells under lipid- and oxygen-deprived conditions and defines a gene signature associated with poor survival in glioblastoma multiforme. *Oncogene* 2015; **34**: 5128–5140.

22 Griffiths B, Lewis CA, Bensaad K, Ros S, Zhang Q, Ferber EC *et al.* Sterol regulatory element binding protein-dependent regulation of lipid synthesis supports cell survival and tumor growth. *Cancer Metab* 2013; **1**: 3.

23 Williams KJ, Argus JP, Zhu Y, Wilks MQ, Marbois BN, York AG *et al.* An essential requirement for the SCAP/SREBP signaling axis to protect cancer cells from lipotoxicity. *Cancer Res* 2013; **73**: 2850–2862.

24 Shimano H, Shimomura I, Hammer RE, Herz J, Goldstein JL, Brown MS *et al.* Elevated levels of SREBP-2 and cholesterol synthesis in livers of mice homozygous for a targeted disruption of the SREBP-1 gene. *J Clin Invest* 1997; **100**: 2115–2124.

25 Kidani Y, Elsaesser H, Hock MB, Vergnes L, Williams KJ, Argus JP *et al.* Sterol regulatory element–binding proteins are essential for the metabolic programming of effector T cells and adaptive immunity. *Nat Immunol* 2013; **14**: 489–499.

26 Amemiya-Kudo M, Shimano H, Yoshikawa T, Yahagi N, Hasty AH, Okazaki H *et al.* Promoter analysis of the mouse sterol regulatory element-binding protein-1c gene. *J Biol Chem* 2000; **275**: 31078–31085.

27 Ohashi K, Osuga JI, Tozawa R, Kitamine T, Yagyu H, Sekiya M *et al.* Early embryonic lethality

caused by targeted disruption of the 3-hydroxy-3-methylglutaryl-CoA reductase gene. *J Biol Chem* 2003; **278**: 42936–42941.

28 Zhuang L, Kim J, Adam R, Solomon K. Cholesterol targeting alters lipid raft composition and cell survival in prostate cancer cells and xenografts. *J Clin Invest* 2005; **115**: 959–968.

29 Clendening JW, Pandyra A, Boutros PC, El Ghamrasni S, Khosravi F, Trentin GA *et al.* Dysregulation of the mevalonate pathway promotes transformation. *Proc Natl Acad Sci U S A* 2010; **107**: 15051–15056.

30 Duncan RE, El-Sohemy A, Archer MC. Mevalonate promotes the growth of tumors derived from human cancer cells in vivo and stimulates proliferation in vitro with enhanced cyclin-dependent kinase-2 activity. *J Biol Chem* 2004; **279**: 33079–33084.

31 Nielsen SF, Nordestgaard BG, Bojesen SE. Statin use and reduced cancer-related mortality. *N Engl J Med* 2012; **367**: 1792–1802.

32 Brown AJ. Cholesterol, statins and cancer. *Clin Exp Pharmacol Physiol* 2007; **34**: 135–141.

33 Sebti SM, Hamilton AD. Farnesyltransferase and geranylgeranyltransferase I inhibitors and cancer therapy: lessons from mechanism and bench-to-bedside translational studies. *Oncogene* 2000; **19**: 6584–6593.

34 Swinnen J V, Brusselmans K, Verhoeven G. Increased lipogenesis in cancer cells: new players, novel targets. *Curr Opin Clin Nutr Metab Care* 2006; **9**: 358–365.

35 Li Y, He K, Huang Y, Zheng D, Gao C, Cui L *et al.* Betulin induces mitochondrial cytochrome c release associated apoptosis in human cancer cells. *Mol Carcinog* 2010; **49**: 630–640.

36 Fritz V, Benfodda Z, Rodier G, Henriquet C, Iborra F, Avancès C *et al.* Abrogation of de novo lipogenesis by stearoyl-CoA desaturase 1 inhibition interferes with oncogenic signaling and blocks prostate cancer progression in mice. *Mol Cancer Ther* 2010; **9**: 1740–1754.

37 Zaidi N, Royaux I, Swinnen J V, Smans K. ATP-citrate lyase (ACLY)-knockdown induces growth arrest and apoptosis through different cell- and environment-dependent mechanisms. *Mol Cancer Ther* 2012; **11**: 1925–1935.

38 Menendez JA, Lupu R. Fatty acid synthase and the lipogenic phenotype in cancer pathogenesis. *Nat Rev Cancer* 2007; **7**: 763–777.

39 Tamura K, Makino A, Hullin-Matsuda F, Kobayashi T, Furihata M, Chung S *et al.* Novel lipogenic enzyme ELOVL7 is involved in prostate cancer growth through saturated long-chain fatty acid metabolism. *Cancer Res* 2009; **69**: 8133–8140.

40 Rysman E, Brusselmans K, Scheys K, Timmermans L, Derua R, Munck S *et al.* De novo lipogenesis protects cancer cells from free radicals and chemotherapeutics by promoting membrane lipid saturation. *Cancer Res* 2010; **70**: 8117–8126.

41 Minville-Walz M, Pierre A-S, Pichon L, Bellenger S, Fèvre C, Bellenger J *et al.* Inhibition of stearoyl-CoA desaturase 1 expression induces CHOP-dependent cell death in human cancer cells. *PLoS One* 2010; **5**: e14363.

42 Mason P, Liang B, Li L, Fremgen T, Murphy E, Quinn A *et al.* SCD1 inhibition causes cancer cell death by depleting mono-unsaturated fatty acids. *PLoS One* 2012; **7**: e33823.

43 Borradaile NM, Han X, Harp JD, Gale SE, Ory DS, Schaffer JE. Disruption of endoplasmic reticulum structure and integrity in lipotoxic cell death. *J Lipid Res* 2006; **47**: 2726–2737.

44 Wei Y, Wang D, Topczewski F, Pagliassotti MJ. Saturated fatty acids induce endoplasmic reticulum stress and apoptosis independently of ceramide in liver cells. *Am J Physiol Endocrinol Metab* 2006; **291**: E275–281.

45 Ariyama H, Kono N, Matsuda S, Inoue T, Arai H. Decrease in membrane phospholipid unsaturation induces unfolded protein response. *J Biol Chem* 2010; **285**: 22027–22035.

46 Guo D, Reinitz F, Youssef M, Hong C, Nathanson D, Akhavan D *et al.* An LXR agonist promotes glioblastoma cell death through inhibition of an EGFR/AKT/SREBP-1/LDLR-dependent pathway. *Cancer Discov* 2011; **1**: 442–456.

47 Amemiya-kudo M, Shimano H, Hasty AH, Yahagi N, Yoshikawa T, Matsuzaka T *et al.* Transcriptional activities of nuclear SREBP-1a , -1c , and -2 to different target promoters of lipogenic and cholesterogenic genes. *J Lipid Res* 2002; **43**: 1220–1235.

48 Shimomura I, Shimano H, Korn BS, Bashmakov Y, Horton JD. Nuclear sterol regulatory element-binding proteins activate genes responsible for the entire program of unsaturated fatty acid biosynthesis in transgenic mouse liver. *J Biol Chem* 1998; **273**: 35299–35306.

49 Reed DJ, Fariss MW. Glutathione depletion and susceptibility. *Pharmacol Rev* 1984; **36**: 25S–33S.

50 De Raedt T, Walton Z, Yecies JL, Li D, Chen Y, Malone CF *et al.* Exploiting Cancer Cell Vulnerabilities to Develop a Combination Therapy for Ras-Driven Tumors. *Cancer Cell* 2011; **20**: 400–413.

51 Jiang L, Shestov AA, Swain P, Yang C, Parker SJ, Wang QA *et al.* Reductive carboxylation supports redox homeostasis during anchorage-independent growth. *Nature* 2016; : 1–16.

52 Horton JD, Shah NA, Warrington JA, Anderson NN, Park SW, Brown MS *et al.* Combined analysis of oligonucleotide microarray data from transgenic and knockout mice identifies direct SREBP target genes. *Proc Natl Acad Sci USA* 2003; **100**: 12027–12032.

53 Seo Y-K, Jeon T-I, Chong HK, Biesinger J, Xie X, Osborne TF. Genome-wide localization of SREBP-2 in hepatic chromatin predicts a role in autophagy. *Cell Metab* 2011; **13**: 367–375.

54 Reed BD, Charos AE, Szekely AM, Weissman SM, Snyder M. Genome-wide occupancy of SREBP1 and its partners NFY and SP1 reveals novel functional roles and combinatorial regulation of distinct classes of genes. *PLoS Genet* 2008; **4**: e1000133.

55 Seo Y-K, Chong HK, Infante AM, Im S-S, Xie X, Osborne TF. Genome-wide analysis of SREBP-1 binding in mouse liver chromatin reveals a preference for promoter proximal binding to a new motif. *Proc Natl Acad Sci U S A* 2009; **106**: 13765–9.

56 White E. Deconvoluting the context-dependent role for autophagy in cancer. *Nat Rev Cancer*

2012; **12**: 401–410.

57 Singh R, Kaushik S, Wang Y, Xiang Y, Novak I, Komatsu M *et al.* Autophagy regulates lipid metabolism. *Nature* 2009; **458**: 1131–1135.

58 Guo JY, Karsli-Uzunbas G, Mathew R, Aisner SC, Kamphorst JJ, Strohecker a. M *et al.* Autophagy suppresses progression of K-ras-induced lung tumors to oncocytomas and maintains lipid homeostasis. *Genes Dev* 2013; **27**: 1447–1461.

59 Zhang Y, Nicholatos J, Dreier JR, Ricoult SJH, Widenmaier SB, Hotamisligil GS *et al.* Coordinated regulation of protein synthesis and degradation by mTORC1. *Nature* 2014; **513**: 440–443.

60 Chen L, Madura K. Increased proteasome activity, ubiquitin-conjugating enzymes, and eEF1A translation factor detected in breast cancer tissue. *Cancer Res* 2005; **65**: 5599–5606.

61 Pilarsky C, Wenzig M, Specht T, Saeger HD, Grützmann R. Identification and validation of commonly overexpressed genes in solid tumors by comparison of microarray data. *Neoplasia* 2004; **6**: 744–750.

62 Kumatori A, Tanaka K, Inamura N, Sone S, Ogura T, Matsumoto T *et al.* Abnormally high expression of proteasomes in human leukemic cells. *Proc Natl Acad Sci U S A* 1990; **87**: 7071–7075.

63 Shechter I, Dai P, Huo L, Guan G. IDH1 gene transcription is sterol regulated and activated by SREBP-1a and SREBP-2 in human hepatoma HepG2 cells: evidence that IDH1 may regulate lipogenesis in hepatic cells. *J Lipid Res* 2003; **44**: 2169–2180.

64 Charitou P, Rodriguez-colman M, Gerrits J, Triest M Van, Groot M, Hornsveld M *et al.* FOXOs support the metabolic requirements of normal and tumor cells by promoting IDH1 expression. *EMBO Rep* 2015; **16**: 456–466.

65 Yang X, Du T, Wang X, Zhang Y, Hu W, Du X *et al.* IDH1, a CHOP and C/EBPβ-responsive gene under ER stress, sensitizes human melanoma cells to hypoxia-induced apoptosis. *Cancer Lett* 2015; **365**: 201–210.

66 Fendt S-M, Bell EL, Keibler MA, Olenchock BA, Mayers JR, Wasylenko TM *et al.* Reductive glutamine metabolism is a function of the α-ketoglutarate to citrate ratio in cells. *Nat Com* 2013; **4**: 2236.

67 Mullen AR, Wheaton WW, Jin ES, Chen P-H, Sullivan LB, Cheng T *et al.* Reductive carboxylation supports growth in tumour cells with defective mitochondria. *Nature* 2011; **481**: 385–388.

68 Wise DR, Ward PS, Shay JES, Cross JR, Gruber JJ, Sachdeva UM *et al.* Hypoxia promotes isocitrate dehydrogenase-dependent carboxylation of α-ketoglutarate to citrate to support cell growth and viability. *Proc Natl Acad Sci USA* 2011; **108**: 19611–19616.

69 Filipp F V, Scott DA, Ronai ZA, Osterman AL, Smith JW. Reverse TCA cycle flux through isocitrate dehydrogenases 1 and 2 is required for lipogenesis in hypoxic melanoma cells. *Pigment Cell Melanoma Res* 2012; **25**: 375–383.

70 Metallo CM, Gameiro PA, Bell EL, Mattaini KR, Yang J, Hiller K *et al.* Reductive glutamine metabolism by IDH1 mediates lipogenesis under hypoxia. *Nature* 2011; **481**: 380–384.

71 Luong A, Hannah VC, Brown MS, Goldstein JL. Molecular characterization of human acetyl-CoA synthetase, an enzyme regulated by sterol regulatory element-binding proteins. *J Biol Chem* 2000; **275**: 26458–26466.

72 Infantino V, Iacobazzi V, De Santis F, Mastrapasqua M, Palmieri F. Transcription of the mitochondrial citrate carrier gene: Role of SREBP-1, upregulation by insulin and downregulation by PUFA. *Biochem Biophys Res Commun* 2007; **356**: 249–254.

73 Sato R, Okamoto A, Inoue J, Miyamoto W, Sakai Y, Emoto N *et al.* Transcriptional regulation of the ATP citrate-lyase gene by sterol regulatory element-binding proteins. *J Biol Chem* 2000; **275**: 12497–12502.

74 The Cancer Genome Atlas Network -. Genomic and epigenomic landscapes of adult de novo acute myeloid leukemia. *N Engl J Med* 2013; **368**: 2059–2074.

75 Yan H, Parsons W, Jin G, McLendon R, Rasheed A, Yuan W *et al.* IDH1 and IDH2 mutations in gliomas. *N Engl J Med* 2009; **360**: 765–773.

76 Seltzer MJ, Bennett BD, Joshi AD, Gao P, Thomas AG, Ferraris D V. *et al.* Inhibition of glutaminase preferentially slows growth of glioma cells with mutant IDH1. *Cancer Res* 2010; **70**: 8981–8987.

77 Mohrenz IV, Antonietti P, Pusch S, Capper D, Balss J, Voigt S *et al.* Isocitrate dehydrogenase 1 mutant R132H sensitizes glioma cells to BCNU-induced oxidative stress and cell death. *Apoptosis* 2013; **18**: 1416–1425.

78 Jin G, Reitman ZJ, Duncan CG, Spasojevic I, Gooden DM, Rasheed BA *et al.* Disruption of wild-type IDH1 suppresses D-2-hydroxyglutarate production in IDH1-mutated gliomas. *Cancer Res* 2013; **73**: 496–501.

79 Rzem R, Veiga-da-Cunha M, Noël G, Goffette S, Nassogne M-C, Tabarki B *et al.* A gene encoding a putative FAD-dependent L-2-hydroxyglutarate dehydrogenase is mutated in L-2-hydroxyglutaric aciduria. *Proc Natl Acad Sci U S A* 2004; **101**: 16849–16854.

80 Struys EA, Salomons GS, Achouri Y, Van Schaftingen E, Grosso S, Craigen WJ *et al.* Mutations in the D-2-hydroxyglutarate dehydrogenase gene cause D-2-hydroxyglutaric aciduria. *Am J Hum Genet* 2005; **76**: 358–360.

81 Nota B, Struys E a, Pop A, Jansen EE, Fernandez Ojeda MR, Kanhai W a *et al.* Deficiency in SLC25A1, encoding the mitochondrial citrate carrier, causes combined D-2- and L-2-hydroxyglutaric aciduria. *Am J Hum Genet* 2013; **92**: 627–631.

82 Edvardson S, Porcelli V, Jalas C, Soiferman D, Kellner Y, Shaag A *et al.* Agenesis of corpus callosum and optic nerve hypoplasia due to mutations in SLC25A1 encoding the mitochondrial citrate transporter. *J Med Genet* 2013; **50**: 240–245.

83 Fan J, Teng X, Liu L, Mattaini K, Looper R, Vander Heiden MG *et al.* Human phosphoglycerate dehydrogenase produces the oncometabolite D-2-hydroxyglutarate. *ACS Chem Biol* 2014; **10**:

510–516.

84 Intlekofer AM, Dematteo RG, Venneti S, Finley LWS, Lu C, Judkins AR *et al.* Hypoxia induces production of L-2-hydroxyglutarate. *Cell Metab* 2015; : 1–8.

85 Beigneux AP, Kosinski C, Gavino B, Horton JD, Skarnes WC, Young SG. ATP-citrate lyase deficiency in the mouse. *J Biol Chem* 2004; **279**: 9557–9564.

86 Abu-Elheiga L, Matzuk MM, Kordari P, Oh W, Shaikenov T, Gu Z *et al.* Mutant mice lacking acetyl-CoA carboxylase 1 are embryonically lethal. *Proc Natl Acad Sci U S A* 2005; **102**: 12011–12016.

87 Chirala SS, Chang H, Matzuk M, Abu-Elheiga L, Mao J, Mahon K *et al.* Fatty acid synthesis is essential in embryonic development: fatty acid synthase null mutants and most of the heterozygotes die in utero. *Proc Natl Acad Sci U S A* 2003; **100**: 6358–6363.

88 Zheng Y, Eilertsen KJ, Ge L, Zhang L, Sundberg JP, Prouty SM *et al.* SCD1 is expressed in sebaceous glands and is disrupted in the asebia mouse. *Nat Genet* 1999; **23**: 268–270.

89 Oballa RM, Belair L, Black WC, Bleasby K, Chan CC, Desroches C *et al.* Development of a liver-targeted stearoyl-CoA desaturase (SCD) inhibitor (MK-8245) to establish a therapeutic window for the treatment of diabetes and dyslipidemia. *J Med Chem* 2011; **54**: 5082–5096.

90 Rohle D, Popovici-Muller J, Palaskas N, Turcan S, Grommes C, Campos C *et al.* An inhibitor of mutant IDH1 delays growth and promotes differentiation of glioma cells. *Science* 2013; **340**: 626–630.

91 Tateishi K, Wakimoto H, Iafrate AJ, Tanaka S, Loebel F, Lelic N *et al.* Extreme vulnerability of IDH1 mutant cancers to NAD+ depletion. *Cancer Cell* 2015; **28**: 773–784.

92 Suijker J, Oosting J, Koornneef A, Struys EA, Gajja S, Schaap FG *et al.* Inhibition of mutant IDH1 decreases D-2-HG levels without affecting tumorigenic properties of chondrosarcoma cell lines. *Oncotarget* 2015; **6**: 12505–12519.

93 Shi J, Zuo H, Ni L, Xia L, Zhao L, Gong M *et al.* An IDH1 mutation inhibits growth of glioma cells via GSH depletion and ROS generation. *Neurol Sci* 2014; **35**: 839–845.

94 Grassian AR, Parker SJ, Davidson SM, Divakaruni AS, Green CR, Zhang X *et al.* IDH1 mutations alter citric acid cycle metabolism and increase dependence on oxidative mitochondrial metabolism. *Cancer Res* 2014; **74**: 3317–3331.

95 Li S, Chou AP, Chen W, Chen R, Deng Y, Phillips HS *et al.* Overexpression of isocitrate dehydrogenase mutant proteins renders glioma cells more sensitive to radiation. *Neuro Oncol* 2013; **15**: 57–68.